MODIFICATION OF POLY(VINYL ALCOHOL) FILM TO MAXIMIZE BARRIER PROPERTIES

Gianmarco Colace

Modification of Poly(vinyl alcohol) film to maximize barrier properties

by

Gianmarco Colace

Doctoral Thesis

Supervisor:

Dr. José Antonio Reina

UNIVERSITAT ROVIRA i VIRGILI

Tarragona

2019

UNIVERSITAT ROVIRA I VIRGILI
MODIFICATION OF POLY(VINYL ALCOHOL) FILM TO MAXIMIZE BARRIER PROPERTIES
Gianmarco Colace

UNIVERSITAT ROVIRA I VIRGILI

Department of Analytical Chemistry and Organic Chemistry

C/ Marcel·lí Domingo, 1
Campus Sescelades
43007, Tarragona
Tel: 977 559 769
Fax: 977 558 446

José Antonio Reina Lozano, Associate Professor at the University Rovira i Virgili, Department of Analytical Chemistry and Organic Chemistry.

I state that the present study, entitled "Modification of Poly(vinyl alcohol) film to maximize barrier properties", presented by Gianmaro Colace for the award of the degree of Doctor, has been carried out under our supervision at the Department of Analytical Chemistry and Organic Chemistry at the University Rovira i Virgili, and that it fulfils all the requirements to be eligible for the Doctor European Mention.

Tarragona, 11 October 2019

Supervisor of the doctoral thesis

Dr. José Antonio Reina Lozano

UNIVERSITAT ROVIRA I VIRGILI
MODIFICATION OF POLY(VINYL ALCOHOL) FILM TO MAXIMIZE BARRIER PROPERTIES
Gianmarco Colace

Acknowledgements

Firstly I would thank to whom has been my thesis director and supervisors: the Dr. José Antonio Reina, Miguel Brandt and Alberto Martinez for giving me a wonderful opportunity to join this program and for the regular support of my Ph.D. study, for their immense knowledge, patience and their guidance in both professional and personal life.

My sincere thanks also go to Dr. Marta Giamberini for her advices and constant availability and the MEMTEC group, full of qualified people. Thank you all: Dr. Ricard Garcia Valls, Dr. Tània Gumí, Dr. Bartosz Tylkowski, Josefa Lázaro, Domenico, Rita, Mario, Jie, Kamila and Adrianna.

Secondly, I would like to thank all professors of Departments of Organic Chemistry and Chemical Engineering of University Rovira i Virgili of Tarragona for their help. My appreciation also goes to Dr. Ángels Serra, Dr. Silvia De la Flor and Dr. Francesc Ferrando for sharing their expertise.

Thanks to all the guys of lab 330 and the others I met in Tarragona:

Claudio, Francesco, Michele, Dailyn, Alberto, Rubén, Lorenza, Ulpiano, Isaac, Mario A., Chiara, Antonio, Luca and Stefano.

My stay in Tarragona was great also because of you.

Next, I would like to thank all the people I met during my amazing experience in Bruxelles at Procter & Gamble and all the Soluble Unit Dose department. Firstly, all the group of SMARTMEM program: Regine Labeque, Florence Courchay, Susana Fernandez Prieto, Raul Rodrigo Gomez, Emily Boswell, Johan Smets and Fabienne De Decker. It was a pleasure and an honor work with you and learn from you. Then I want to thank everyone I met in Bruxelles: Andrea G., Andrea S., Luca V., Anne, Inge, Gianmarco P., Silvia, Inês, Licia, Livio, Stefano, Alessandro, Giuseppe, Ulderico, Luca P., Mattia, Marco, Leone, Giusy, Xavi, Keo and Fabiana: my stay was fantastic also because of special person like you, for the amazing moments inside and outside the company.

A great thank goes to my family: my grandmother, my parents, my brother, my uncles and cousins that, even from far away, always encouraged me to achieve my personal and professional goals. I always felt your love, as I felt my grandfather guidance from very long distance. Without you all this would have been impossible.

I also want to thank all my old friends Claudio, Mario, Roberto, Davide, Luigi, Gabriele, Simone, Gianluca and Stefano that distant or not, always gave me endorsement every time I needed.

A huge gratitude goes of course to my girlfriend, best friend, cohabitant and women of my life Andrea. This program allowed me to meet you and I will never regret one of the choices we made

together. You always supported and tolerated me during all the time. Looking forward to a life with you. I love you!

Thanks everyone for the advices and support!

Gianmarco Colace

UNIVERSITAT ROVIRA I VIRGILI
MODIFICATION OF POLY(VINYL ALCOHOL) FILM TO MAXIMIZE BARRIER PROPERTIES
Gianmarco Colace

Anyone who has never made a mistake

has never tried anything new.

Albert Einstein

UNIVERSITAT ROVIRA I VIRGILI
MODIFICATION OF POLY(VINYL ALCOHOL) FILM TO MAXIMIZE BARRIER PROPERTIES
Gianmarco Colace

LIST OF ABBREVIATIONS

%SW	Percentage of gravimetric swelling
BVOH	Butenediol-vinyl alcohol copolymer
DC %	Crystallinity degree
DH	Difference in Partition
DP	Degree of Polymerization
DPG	Dipropylene glycol
DSC	Differential scanning calorimetry
EBM	Equivalent Box Model
ESEM	Environmental scanning electron microscopy
EVOH	Ethylene vinyl alcohol
FWA49	Fluorescent whitener agent 49
MCCa	Micro Crystalline Cellulose 20 μm size
MCCb	Micro Crystalline Cellulose 50 μm size
MFC	Micro-fibrillated cellulose
$MgCl_2$	Magnesium chloride
Mw	Molecular weight
NMR	Nuclear Magnetic Resonance
OTR	Oxygen transmission rate
Pdiol	Propylene glycol
PET	Polyethylene terephthalate
PEG	Polyethylene glycol
PMVE	Poly (methyl vinyl ether)

PP	Polypropylene
PVA, PVOH, PVAL	Poly (vinyl alcohol)
PVAc	Poly(vinyl acetate)
RH%	Relative humidity
Tc	Crystallization temperature
Tg	Glass transition temperature
WVP	Water vapor permeability
WVTR	Water vapor transmission rate
XRD	X-ray diffraction

TABLE of CONTENTS

UNIVERSITAT ROVIRA I VIRGILI
MODIFICATION OF POLY(VINYL ALCOHOL) FILM TO MAXIMIZE BARRIER PROPERTIES
Gianmarco Colace

1. General Introduction and Objectives

1.1 Poly(vinyl alcohol)

Poly(vinyl alcohol) (PVA), also known as PVA, or PVAL, is a polyhydroxy polymer: is the largest volume, synthetic water-soluble polymer produced in the world. It is effective in film forming, as an emulsifying, and it has an adhesive quality. It has no odor and is not toxic, and is resistant to grease, oils, and solvents. It is ductile but strong, flexible, and functions as a high oxygen and aroma barrier. While other vinyl polymers are prepared by polymerization of its corresponding monomer, PVA is commercially manufactured by the partial or full hydrolysis of poly(vinyl acetate), because monomeric vinyl alcohol is the tautomer of acetaldehyde, and only acetaldehyde exists in a high extent at equilibrium (**Figure 1.1**): [1-3]

Figure 1.1 Scheme of the tautomer of acetaldehyde

Therefore, vinyl alcohol cannot be obtained in quantities that makes polymerization to PVA feasible.

PVA was discovered by Haehnel and Herrmann who, through the addition of alkali to a clear alcoholic solution of poly(vinyl acetate), were able to obtain the ivory-colored PVA. [4]

PVA has a quite simple chemical structure with pendant hydroxyl groups. It is obtained by radical polymerization of vinyl acetate to poly(vinyl acetate) (PVAc) followed by hydrolysis of PVAc to PVA, or from others polyvinyl esters (**Figure 1.2**).[5]

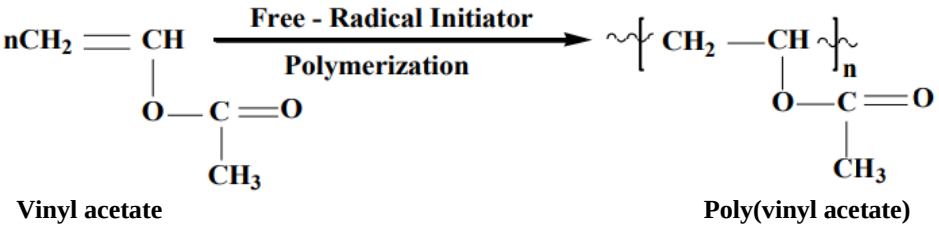

Figure 1.2 Chemical reaction for Poly (vinyl acetate) production

Polymerization of vinyl acetate monomer can occur by bulk, solution, or emulsion techniques. The poly(vinyl acetate) formed is then dissolved in a solvent and hydrolyzed or alcoholyzed with acidic or basic catalysts (**Figure 1.3**). [6]

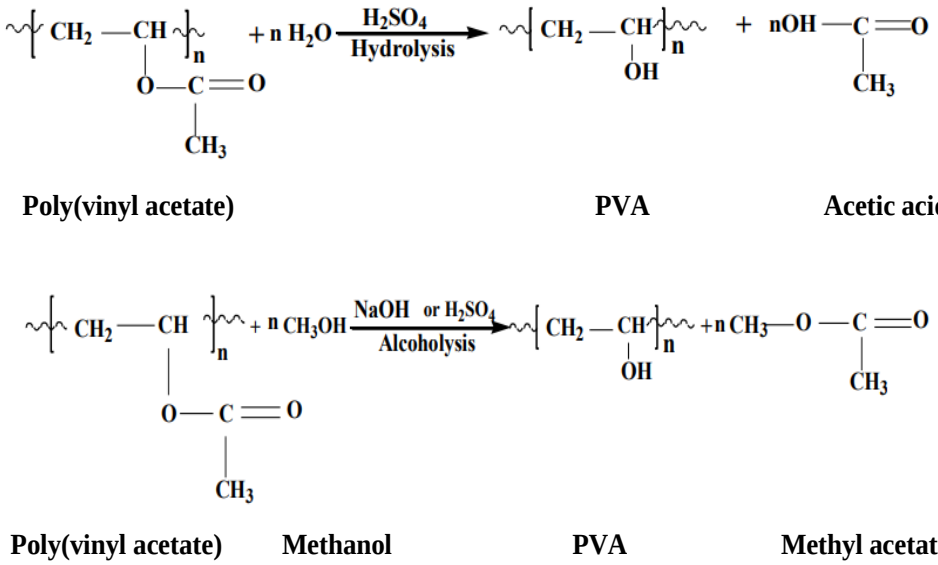

Figure 1.3 Scheme of PVA preparation

The excellent chemical and physical properties of PVA resins have resulted in broad industrial use. Poly(vinyl alcohol) films exhibit high tensile strength, abrasion resistance, and oxygen barrier properties which under dry conditions are superior to those of most polymers.

The main uses of PVA are in textile sizing, adhesives, protective colloids for emulsion polymerization, fibers and paper sizing. Significant volumes are also used in the production of concrete additives and joint cements for building construction and manufacturing bags for detergents, agrochemicals and laundry.

1.1.1 Physical Properties

The physical properties of PVA are highly correlated with the method of preparation. The final properties are affected by the polymerization conditions of the vinyl acetate, the hydrolysis conditions and drying. Further, the term PVA refers to an array of products that are copolymers of vinyl acetate and vinyl alcohol.

The degree of hydrolysis determines the physical characteristics, chemical properties, and mechanical properties of the PVA. [7] The effect of hydrolysis degree and molecular weight is illustrated in **Figure 1.4**.

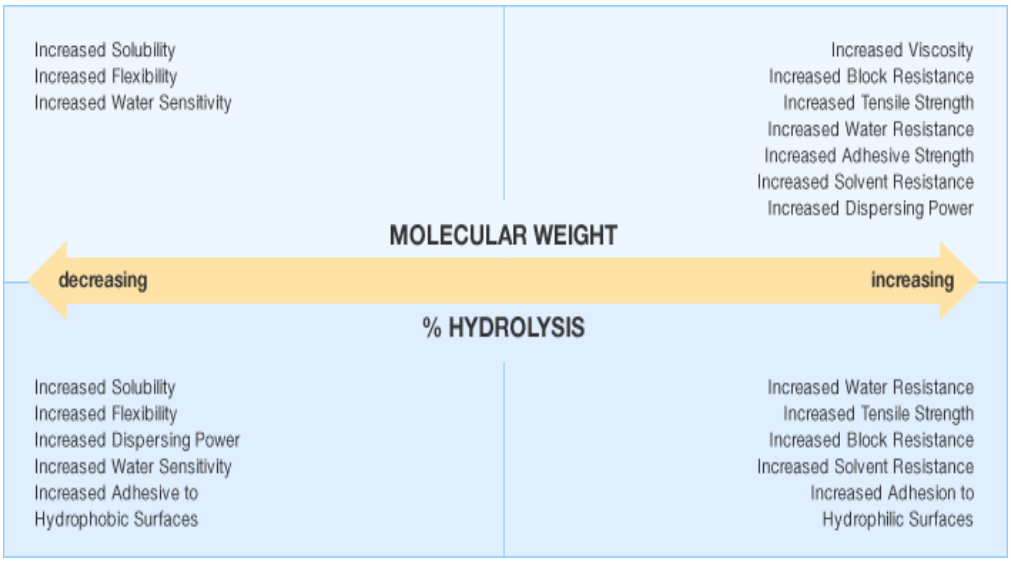

Figure 1.4 Effect of molecular weight and hydrolysis degree on PVA properties

1.1.2 Crystallization and Melting Point

The ability of PVA to crystallize is the single most important physical property of PVA as it controls water solubility, water sensitivity, tensile strength, oxygen and gas barrier properties, and thermoplastic properties. These features have been and continue to be studied in deep for academic and industrial research. [8-10]

The size of the crystals determines the melting point. Reported values for the melting point of PVA range between 220 ºC and 267 ºC for fully hydrolyzed PVA. Exact determination of the melting point using conventional techniques is difficult as incipient decomposition of PVA starts above 140ºC.

1.1.3 Solubility

Poly(vinyl alcohol) is soluble in highly polar solvents, such as water, dimethyl sulfoxide, dimethylacetamide, glycols, and dimethylformamide. The solubility in water is a function of the degree of polymerization (DP) and hydrolysis. Degree of hydrolysis, which is related with the presence of acetate groups in the polymer, strongly affects polymer properties. It has been reported that PVA with high degree of hydrolysis (above 95%) has lower solubility in water. [11]

Fully hydrolyzed PVA is only completely soluble in hot to boiling water. Partially hydrolyzed grades are soluble at room

temperature, although grades with a hydrolysis of 70–80% are only soluble at water temperatures of 10–40ºC. Above 40ºC the solution first becomes cloudy (cloudy point), followed by precipitation of PVA. The hydroxyl groups in PVA contribute to strong hydrogen bonding both intra- and intermolecularly, which reduces solubility in water. The presence of residual acetate groups in partially hydrolyzed PVA weakens these hydrogen bonds and allows solubility at lower temperatures.

Heat treatment or drying of a few minutes increases crystallinity and greatly reduces the solubility and water sensitivity, as shown in **Figure 1.5**. [12]

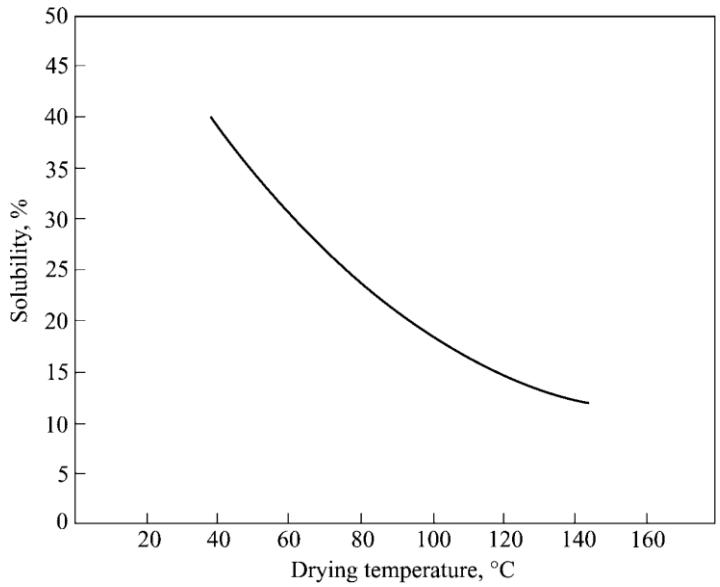

Figure 1.5 Influence of heat treatment on solubility (DP = 1700, 98–99 hydrolyzed)

Prolonged heat treatment doesn`t further increase crystallinity. The heat treatment melts the smaller crystals, allowing for diffusion and reformation of crystals with a melting point higher than that of the treatment temperature. The presence of acetate groups reduces the extent of crystallinity; thus, heat treatment has little or no influence on low hydrolysis grades.

1.1.4 Mechanical Properties

The tensile strength of no-plasticized PVA depends on degree of hydrolysis, molecular weight, and relative humidity (RH%). Heat treatment and molecular alignment resulting from drawing increase the tensile strength; plasticizers reduce tensile strength disproportionately because of increased water sensitivity. Tensile elongation of PVA is extremely sensitive to humidity and ranges from <10% when completely dry to 300–400% at 80 % RH. Addition of plasticizer can double these values. Elongation is independent of degree of hydrolysis but proportional to the molecular weight. Tear strength increases with increasing relative humidity or with the addition of small amounts of plasticizer.

1.1.5 Thermal Decomposition

The thermal decomposition of PVA in the absence of oxygen occurs in two stages. The first stage begins at about 200ºC and is mainly dehydration, accompanied by the formation of volatile

products, like water and acetic acid) Further heating to 400–500ºC yields carbon and hydrocarbons. [13, 14]

1.2 Uses of Poly(vinyl alcohol)

Poly(vinyl alcohol) is widely used to strengthen textile yarn and papers, particularly to make the latter more resilient to oils and grease. PVA may also be used as a coating agent for food supplements and does not pose any health risks as it is not poisonous. One of the leading industrial uses of PVA is for food packaging, accounting for 31.4 % of the global share in 2016. [15] To combat moisture formation from foodstuff, PVA film is created to be thin and water-resistant.

1.2.1 PVA in multi-compartment pouch

Water-soluble polymeric films, as PVA ones, are commonly used as packaging materials to simplify dispersing, pouring, dissolving and dosing of a material to be delivered. Pouches made from water-soluble film is commonly used to package household care compositions such as laundry or dish detergent. A consumer can directly add the pouched composition to a mixing vessel, such as a bucket, sink or washing machine. Advantageously, this provides for accurate dosing while eliminating the need for the consumer to measure the composition, avoiding wasteful overdosing or

underdosing. The pouched composition may also reduce mess that would be associated with dispensing a similar composition from a vessel, such as pouring a liquid laundry detergent from a bottle. In sum, soluble pre-measured polymeric film pouches provide for convenience of consumer use in a variety of applications. [16-20]

Typically, the detergent pouch comprises multi compartments: a pouch for use in a laundry application has typically at least two compartments, wherein one comprises a liquid detergent and in the other usually a whitening agent is contained, [19] but can comprise three, four or five compartments. [21]

A water-soluble film is shaped, such that the compartment is completely surrounded by the film: it may be formed from two films which are sealed together (e.g. heat sealed, solvent sealed or a combination thereof). The film is sealed such the composition doesn't leak out during the storage. The final package may provide at least a partial moisture barrier.

The pouches are suitable for cleaning applications including cleaning laundry, dishes and the body. The film can have any suitable thickness (typical value is 76 μm) able to confer such characteristics, especially in terms of dissolution time and tensile strength, the most important properties, together with moisture barrier.

Upon addition of the pouch to water, the film dissolves and releases the internal contents into the wash liquor. The following

scheme represents the dissolution process of a pouch in contact with water (**Figure 1.6**):

- When the pouch is in contact with the water environment, a hydration of the film surface starts;
- After few seconds, film swelling takes place;
- Pouch rupture allows the release of the different detergent components;
- The process continues until no film residue is in the machine.

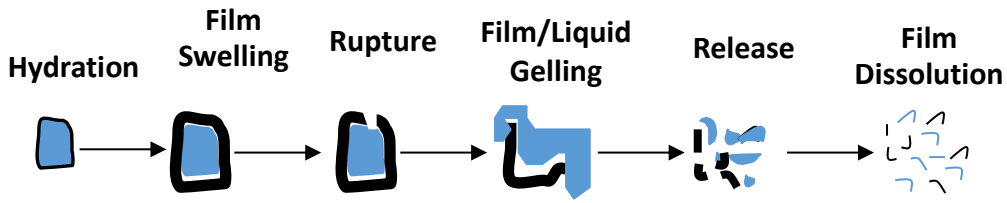

Figure 1.6 Pouch dissolution scheme in a laundry machine

1.2.2 Drawbacks of PVA in pouch

The PVA film is susceptible to water ingress from external environment that can affect the product stability in high humidity ambient, accelerating surfactant diffusion through the material, causing a not wanted greasy product feeling and dye migration through the compartments, which leads to a color alteration as shown in **Picture 1.1**.

Picture 1.1 Fresh pouch (left) vs aged one (right)

In the previous picture, a color modification (yellowing) is easily visible on the white composition, but the migration concerns all the three compartments.

The migration of chemicals from inside to the external environment, causes a weight loss that it is strictly related to lost in hardness (**Picture 1.2**)

Picture 1.2 Softness due to film permeability

The transfer of water from the external environment inside the pouch through the external layer, also affects the compositions effectiveness over time.

The aim of this work is to reduce the permeation of water and detergent components through PVA film, during storage and in the supply chain, while keeping the film functionality in terms of dissolution and mechanical properties, until the moment of use by the customer.

1.2.3 Possible approaches

Poly(vinyl alcohol) is suitable for several modifications to improve or, most in general, change its physical and chemical properties. The state of art comprises different technologies which can be applied to the aim of this work.

A first technique investigated was the chemical modification of the PVA film surface: one example is constituted by improving oxygen and vapor barrier due to an outer layer surface esterification. [22] Chemical grafting using fatty acid chlorides, allows surfaces to be esterified. [23, 24] This increases the water repellence and humidity resistance and reduces the water permeability of poly(vinyl alcohol) coatings since, as Shaikh *et al*. showed, grafting of PVA with fatty acid chloride renders the material hydrophobic (**Figure 1.7**). [25]

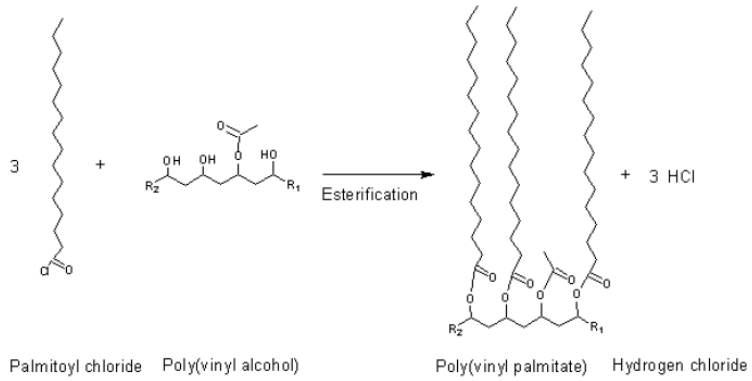

Figure 1.7 Example of PVA reaction with fatty acid chlorides

The proof of concept was studied in deep by Stinga *et al* and called the transfer method : [26, 27]

- A support is immersed in a solution of fatty acid chloride (2%) and petroleum ether (98%);
- After drying, the support is put on the PVA layer;
- The system is placed in the oven for 7 minutes where the grafted took act.

The final structure obtained is shown in **Figure 1.8**.

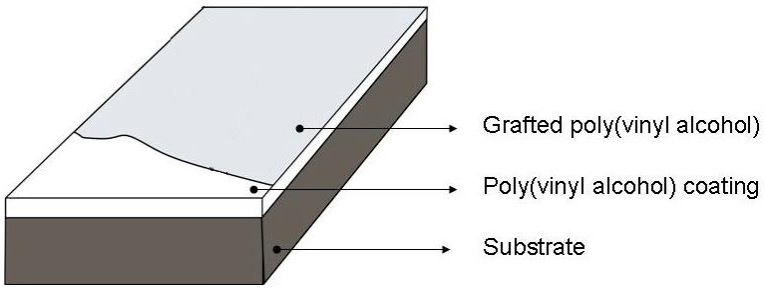

Figure 1.8 Schematic representation of PVA substrate grafted with fatty

After the process, the Water Vapor Transmission Rate (WVTR) was determined according to the standard DIN 53122-1 [28] and the results showed decreased value of WVTR of grafted PVA, up to 19 times in comparison to the virgin layer.

This technique could be applied to the purpose of the work, but some considerations have to be done:

- The transfer method seems work for increasing water vapor barrier, but the studies also claim a drastic change in the hydrophilicity of the surface, with an increase in hydrophobicity upon treatment with fatty acid chlorides, that can sure negatively affect the dissolution of the film, one of the most important property for the material studied in this work; [22, 29, 30]
- This technique has also drawbacks in apply it to the plant scale, in terms of cost of the material and arrangement of equipment.

  So the aim of this work moved on to look for other technological solutions.

Another answer to the purpose could be the mixture of PVA with a second material; in this option we can actually have two approaches: immiscible materials will create composites, meanwhile miscible polymers will generate blends.

A simple model has been developed to describe the permeability in filled polymers. [31, 32]

The model aims to predict the observed permeability based strictly on tortuosity arguments. The filler presence (spherical, lamellar, cylindrical, etc. shaped) introduces an indirect path for a penetrant. The reduction of permeability is due to the longer and more difficult route that the diffusing moieties must travel in the presence of the loading filler. The tortuosity factor (τ) is defined as the ratio between the actual distance (d') that a penetrant has to travel and the shortest distance (d) that it would have traveled in absence of the filler, and is expressed in terms of face's length of a filler particle (L), thickness of the filler (W) and volume fraction of the filler (ϕ_F) as in the *equation 1.1* : [31, 33]

$$\tau = \frac{d'}{d} = 1 + \frac{L}{2W}\phi_F \qquad (1.1)$$

In addition to the tortuosity factor, permeability is cut down because not all of a given cross section of material is pure polymer. As approximation, the following *equation 1.2* is used: [34]

$$\frac{P_F}{P_u} = \frac{\phi_u}{\tau} \qquad (1.2)$$

Where P_F and P_u are the permeabilities of the filled and unfilled polymer respectively and ϕ_u is the volume fraction of the polymer.

According to this equation, the fractional area occupied by polymer in any cross section is equal to the volume fraction of the polymer. [35]

Combining *equation 1.1* and *1.2*, the permeability equation becomes:

$$\frac{P_F}{P_u} = \frac{\phi_u}{1+\frac{L}{2W}\phi_F} \qquad (1.3)$$

This generic model, illustrated in **Figure 1.9**, is adapted for gases, taking into account the hypothesis of filler particles with cubic or rectangular shape with an uniform and completed dispersion in the matrix and parallel orientation to the film surface. [31]

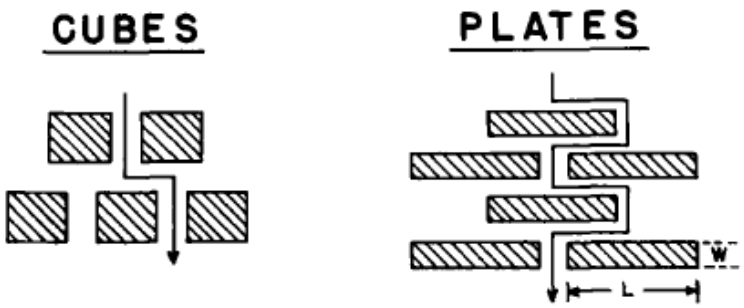

Figure 1.9 Simple model for the path of a diffusing moiety through a filled polymer

In general, incomplete filler dispersion and only partial orientation of the particles should result in higher permeation property than this simple theory predicts.

On the other hand, liquid permeability through filled polymers is more complex than gas one: it is defined as the amount of liquid passing through a membrane of unit area and thickness in unit time when one side of the membrane is in contact with the liquid and the other side is swept by an air flow. [31] In general, the liquids have some solubility in the polymer, so that the polymer becomes swollen and the liquid can interfere with the polymer-filler interface, giving different solubility of the polymer at the interface from the bulk polymer.

A diffusing molecule can get through the filled system by going only through the polymer, or it can diffuse along a path of both polymer and the interface: so, the permeability can be divided into two parts:

$$P_{FL} = P_1 \left(\frac{\phi_{Li}}{\tau^i}\right) + P_2 \left(\frac{\phi_u + \phi_{LP}}{\tau}\right) \qquad (1.4)$$

Where P_{FL}, P_1 and P_2 are the permeabilities of the filled polymer, the interfacial and the bulk part respectively; τ^i is the tortuosity factor for the interfacial part; ϕ_{Li} is the volume fraction of liquid collected in the interfacial region; ϕ_{LP} it is the one of liquid dissolved in the polymer; ϕ_F and ϕ_u are volume fraction of the filler and polymer respectively.

The whole system volume fraction will be equal to 1, as

$$\phi_u + \phi_{LP} + \phi_{Li} + \phi_F = 1 \qquad (1.5)$$

The permeability P_1 through the interfacial region will be calculated first. In this region reciprocal permeabilities are additive, accordingly to the following equation

$$\frac{1}{P_1} = \frac{\theta_i}{P_i} + \frac{\theta_P}{P_{PL}} \qquad (1.6)$$

Where θ_i and θ_P are the fractional length of diffusion for the interface and polymer; P_i and P_{PL} are the permeabilities of the liquid in the interface and the polymer itself respectively.

Combining the formulas (1.4) and (1.6), the equation for P_{FL} becomes:

$$P_{FL} = \frac{P_i P_{PL}}{P_{PL}\theta_i + P_i\theta_P}\left(\frac{\phi_{Li}}{\tau^i}\right) + P_{PL}\left(\frac{\phi_u + \phi_{LP}}{\tau}\right) \qquad (1.7)$$

All the quantities in the previous equation are obtainable empirically, except P_i, θ_i, τ_i that have to be checked experimentally. In general, θ_i is function of the volume fraction of filler and tortuosity factor. [31, 36]

Accordingly to the permeation theory for filled polymers, several examples of PVA film composites are present in literature: interesting for our purpose, cellulose and wax composites were considered. [37-45] Most of these works underline improved mechanical and barrier properties. [37, 40, 43-45]

Cellulose is one of the most abundant biomaterials on earth, and it has been successfully used for the preparation of nano- and micro-composites, [46, 47] showing numerous applications that make it a promising candidate for industrial scale use: filtering, modifying rheology, enforcing the strength, formation of complex networks that provide good mechanical and barrier properties. [48] For instance, pure micro-fibrillated cellulose (MFC) films have shown a potential for food packaging due to their oxygen and water vapor barrier features, related to the high crystallinity. [49, 50] Using natural fibers to reinforce composite structures is also a potential solution for reducing the dependency on petroleum-based and non-biodegradable materials. Other properties that can favorably change with nano – microcellulose PVA composite, are the E-modulus and the tensile strength (both increase), [44, 45] probably due to the intermolecular forces between cellulose and the base PVA matrix: they keep the inherent tensile strength of the fibrils intact and result in enhancement of the mechanical strength of the tensile properties of the films. [51]

These studies and results had addressed this work to the preparation of a PVA composite film by adding micro-sized cellulose fibers. In general, the use of nano-sized particles will increase the cost of the final film, as cost increases as size particles decreases. [37]

Another aspect of adding to PVA a second material, is the blends production, when a miscible polymer is mixed with it.

The permeation phenomena on blended polymers, are widely studied, [52] and the most important aspect related to transport processes involves the phase behavior. [53] The key equation for predicting the permeability of miscible blends is

$$\ln P_b = \phi_1 \ln P_1 + \phi_2 \ln P_2 \qquad (1.8)$$

Where P_b, P_1 and P_2 are the permeability coefficients of the blend and the two unblended components respectively and ϕ_1 and ϕ_2 are the respective volume fractions of components 1 and 2. [54] The theoretical derivation of this equation is attributed to Paul. [55]

The relationships for phase separate blends are more complex as the blend composition changes from component 1 as the continuous phase to component 2 as the continuous phase. At the extremes of composition, the series and parallel models used for upper and lower limits of the expected transport behavior.

These models are expressed by the following equations:

$$P_b = \phi_1 P_1 + \phi_2 P_2 \qquad \text{[parallel]} \qquad (1.9)$$

$$P_b = P_1 P_2 (\phi_1 P_2 + \phi_2 P_1) \qquad \text{[series]} \qquad (1.10)$$

A third more complex model is commonly employed: it involves spheres of one component dispersed in a matrix of the second component. In this case, the permeability can be expressed according to the following Maxwell`s equation: [53]

$$P_b = P_m \left[\frac{P_d + 2P_m - 2\phi_d(P_m - P_d)}{P_d + 2P_m + \phi_d(P_m - P_d)}\right] \qquad (1.11)$$

Where b, m and d represent the blend, the matrix and the dispersed phase respectively. The parallel and series models and Maxwell`s model offer reasonable predictions where one phase is entirely the continuous phase at both ends of the composition range. In the intermediate compositions, these relationships do not apply. The best approach in the intermediate range is referred to as the Equivalent Box Model (EBM) proposed by Kolarik. [52]

This more complete model employs a combination of parallel and series model contributions: so, the equations for EBM are

$$P_b = \frac{P_1\phi_{1p} + P_2\phi_{2p} + \phi_s^2}{\left[\frac{\phi_{1s}}{P_1} + \frac{\phi_{2s}}{P_2}\right]} \qquad (1.12)$$

where

$$\phi_s = \phi_{1s} + \phi_{2s} \qquad (1.13)$$

and ϕ_{1p}, ϕ_{2p}, ϕ_s,ϕ_{1s}, ϕ_{2s} are defined by the expressions

$$\phi_{1p} = [(\phi_1 - \phi_{1cr})/(1 - \phi_{1cr})]^{T1} \quad ; \quad \phi_{1s} = \phi_1 - \phi_{1p} \qquad (1.14)$$

$$\phi_{2p} = [(\phi_2 - \phi_{2cr})/(1 - \phi_{2cr})]^{T2} \quad ; \quad \phi_{2s} = \phi_2 - \phi_{2p} \qquad (1.15)$$

where P_b, P_1, and P_2 are the respective permeabilities of the blend and components 1 and 2; ϕ_{1cr} and ϕ_{2cr} are the critical threshold percolation values of components 1 and 2 and T1 and T2 are the critical universal exponents for the components. A 3-dimensional array theory, developed by De Gennes *et al*, predicts the value for ϕ_{1cr} and ϕ_{2cr} . [56]

As already mentioned, the EBM model is a combination of a series and parallel contribution and it is shown in the following scheme (**Figure 1.10**).

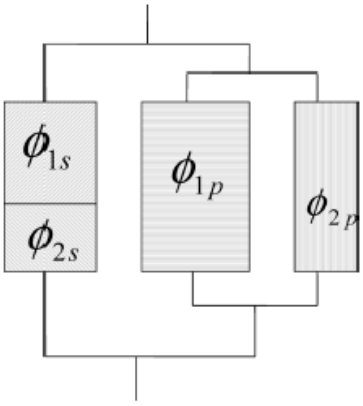

Figure 1.10 Scheme of the combination of parallel and series models for the EBM

A graphical illustration of these models can help to understand the physical approach to the blend permeability (**Figure 1.11**).

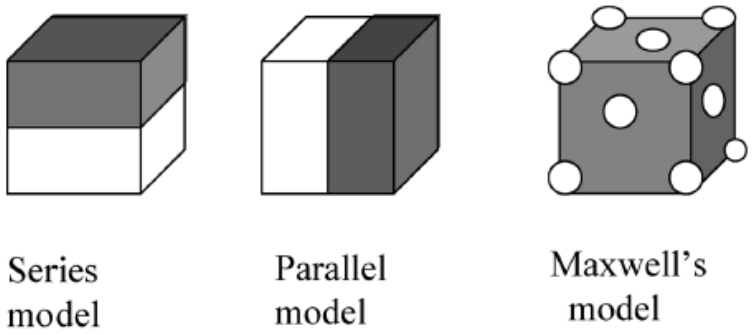

Figure 1.11 Representation of morphology for various permeability models

Several studies demonstrated that the permeability of heterogeneous polymer blends to fluids can be approximately predicted with the aid of these models: in therefore, the blended material final property will be a function of the permeability of the two or more starting polymers. [36, 53, 56]

Considering the permeation theory, different PVA blended polymeric film could be studied in this work. A lot of water-soluble polymer blends with PVA have been studied, like Poly (vinyl acetate), Poly(methyl vinyl ether) (PMVE), Polyethylene glycol (PEG), Polypropylene (PP) and so on. [13, 42, 57-62]

Following these studies, several PVA properties can be improved or more in general modified, blending it with other water-soluble polymers, but this work is focused on a blend with a specific material, relatively new: a butenediol-vinyl alcohol copolymer

(BVOH), in particular manufactured by Nippon Gohsei of Japan, known as Nichigo G-Polymer®.

A lot of patents report the benefit of this material that is a high amorphous vinyl alcohol copolymer. In addition to the biodegradable, compostable and high water solubility properties, it is claimed a high gas barrier property. [63-68] Some data for transport properties can support the choice of this material (**Table 1.1 – Table 1.2**). [69]

Table 1.1 Oxygen Transmission Rate (OTR) comparison at 20 °C dry condition

Polymer type	**Oxygen Transmission Rate [cc 20µm/m^2 * day atm]**
Nichigo G-Polymer	0.0023
Fully hydrolyzed PVA	0.0050
29 mol % Ethylene vinyl alcohol (EVOH)	0.07
44 mol % Ethylene vinyl alcohol (EVOH)	1.3
Nylon 6	76
Polypropylene	3900

Table 1.2 Hydrogen gas barrier performance comparison at dry condition for different polymers

Polymer type	**Hydrogen Transmission rate [cc 20µm/m^2 * day atm]**
Nichigo G-Polymer	<3
29 mol % EVOH	26
44 mol % EVOH	440
Nylon 66	900
Nylon 11	5600

Water-soluble films formed from BVOH copolymers may exhibit improved barrier properties due to the relatively large size of butenediol monomer units, which apparently reduce crystallization in the copolymer while still allowing the polymer backbone to be both tightly packed and highly hydrolyzed. [63]

Another important aspect for the work purpose is the high-water solubility and the Nippon Gohsei reports some interesting data of an improvement of dissolution time in water (also in cold water), as shown in **Figure 1.12**. [70]

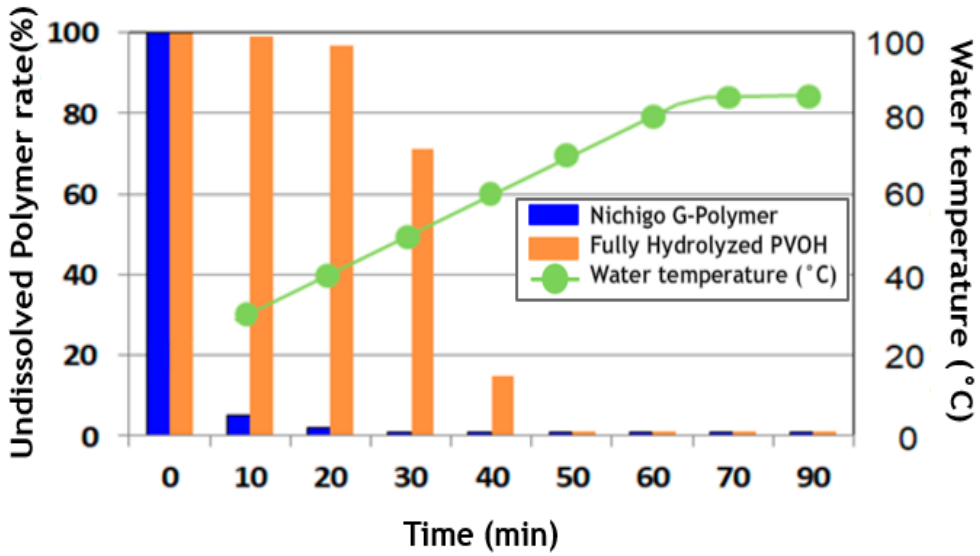

Figure 1.12 Chart of water solubility of Nichigo G-Polymer compared to fully hydrolyzed PVOH

General G-Polymer properties claimed from Nippon Goshei are: [69]

- Biodegradability
- Compostability
- Low crystallinity
- High gas barrier
- Non-foaming
- Oil and solvent resistance
- High transparency
- Good processability

1.3 General Objectives

This PhD thesis aims to modify the PVA film that builds up the laundry pouches (unit dose) currently commercialized by Procter and Gamble Company, in order to decrease the permeability of the film being in contact with the detergent juice.

To do so, this work is focused on two kinds of modification:

- Loading the PVA with micro sized cellulose particles;
- Blending the PVA with high amorphous Nichigo G-Polymer® from Nippon Gohsei.

The tendency to water ingress from ambient humidity, decreases the product stability: it can accelerate surfactant diffusion through the film, promote dye migration from one compartment to another, and negatively affect cleaning effectiveness. Another aspect to take into account, is the oxygen permeation, which oxidizes the enzymes in the detergent, affecting the washing performance and reducing the shelf life of the product.

So, the goal of this work is to decrease the permeability through the film of water, oxygen and detergent, maintaining dissolution and mechanical properties.

The objectives of this thesis can be summarized as follows:

- ✓ Production by casting solution of new films, modifying currently applied PVA characteristics used in unit dose application;
- ✓ Characterization of the films: tensile properties, solubility and permeability;
- ✓ Determination of the physical/chemical structure of the new materials.

2. Materials and Methods

2.1 Materials

2.1.1 Poly(vinyl alcohol)

Three kinds of PVA were used in this work. The PVA Mowiol® 18-88 resin (pellets form) without carboxylic acid groups was supplied by Sigma Aldrich and used as received. It has a M_w of about 130000 and residual acetate content 10.0-11.6%. The second PVA used was the M8630 film supplied by MonoSol approximately 87-89% hydrolyzed and with a thickness of 76 µm (±10%) : it's a mixture of PVA/monocarboxylate copolymer, chitosan and other components. [71] The last PVA film utilized was a patented film from MonoSol, a hydrolyzed copolymer consisting of vinyl acetate and itaconic acid , with a degree of hydrolysis, expressed as a percentage of vinyl acetate units converted to vinyl alcohol units, of about 98%. [20] For the last type of PVA we will refer to it as *Olympus film* and also in this case it has a 76 µm (±10%) thickness.

2.1.2 Cellulose

Micro-sized cellulose particles were supplied by Sigma-Aldrich in 20 µm and 50 µm average size. The **Figure 2.1** shows the chemical structure of the material. It was used as received.

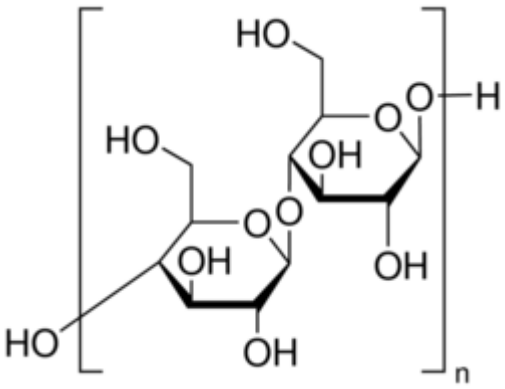

Figure 2.1 Chemical structure of Cellulose

2.1.3 Nippon Goshei® Nichigo G-Polymer

Nichigo G-Polymer or just G-Polymer was supplied by Nippon Goshei (grade BVE8049Q) (**Figure 2.2**). It was used as received.

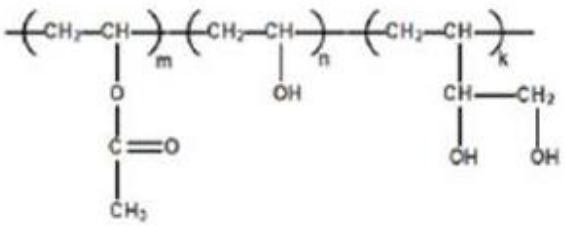

Figure 2.2 Chemical structure of Nichigo G-Polymer

2.2 Methods

2.2.1 Film preparation

Film formation from polymeric solutions is a straight forward process since the polymer is in the dissolved state. The solution is spread onto the substrate and, as the solvent evaporates, the polymer chains interpenetrate, going through a gel state then forming the film with further drying.

Solvent evaporation depends on temperature, atmospheric pressure and in the case of water, relative humidity (RH %): these variables can be adjusted by manipulating the process conditions.

Many coating processes today use aqueous-based systems to avoid issues associated with the use of organic solvents. Improvements in drying efficiency of the processing equipment was necessary to shift from organic based film coating toward aqueous-based systems, since the latent heat of water evaporation is significantly higher than that of organic solvents. [72] In this work, water is used as solvent, since the polymeric matrix is made of PVA, a high water-soluble material.

Solvent evaporation from solution is commonly used for lab-scale film preparation, but also is adaptable in plant scale.

Three are the most important tools used for film formation after solvent evaporation in lab-scale:

- Petri dish
- K-hand coater
- Casting knife

In the first case, the polymeric solution is gently swirled to coat the bottom of the dish; then the system is preferably placed on a level surface.[73] An oven drying or room temperature evaporation, is chosen in according to the solvent. In water/PVA system, 1 hour to the room temperature and 3 hours at 80°C dry oven is recommended. [37]

The **Figure 2.3** shows the schematic representation of the film formation using petri dish.

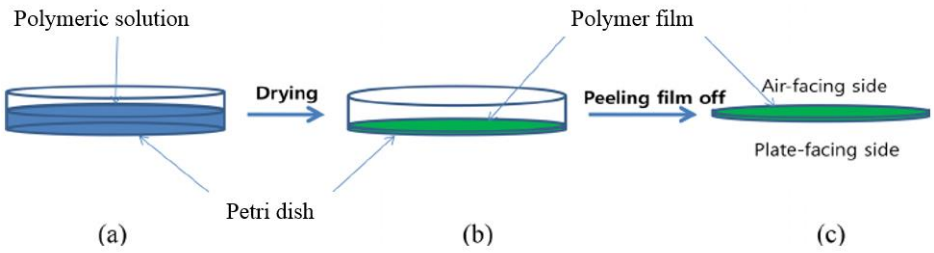

Figure 2.3 Scheme of petri dish film formation

On the other hand, the second tool called K-hand coater or K-bar, shown in next **Picture 2.1** and supplied by RK Print Coat Instrument Ltd., provides a simple but effective means of applying the solution on the substrate. It is composed by a stainless-steel wire wound onto a stainless-steel rod.

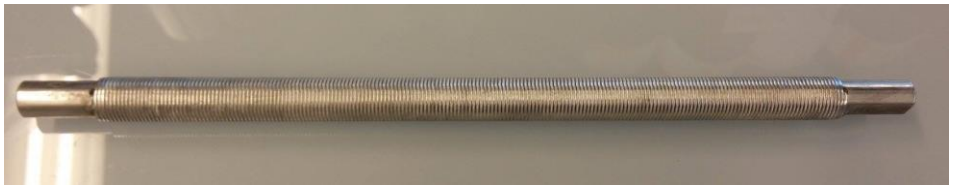

Picture 2.1 K-hand coater

The film thickness depends on the diameter of the wire and the distance between each section of the wire (**Figure 2.4**).

Figure 2.4 Section of K-hand coater

In this case, the polymer solution is poured on the chosen support (glass, Teflon or others) and the material is spread over, forming a wet film. The **Picture 2.2** shows how to use K-bar. The drying conditions are the same explained for petri dish casting.

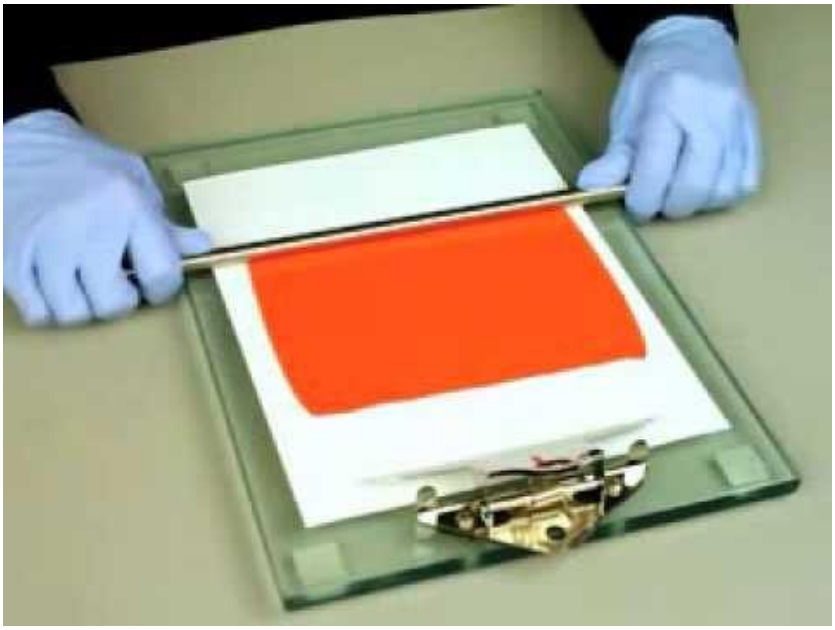

Picture 2.2 Example of K-hand bar coating

The last simple but effective instrument used for the film formation is the casting knife or Film applicator (**Picture 2.3**) supplied by Elcometer. This tool was the one used mostly during the work. It has two screws on the sides which modify the level of the knife (wet thickness of the film).

Picture 2.3 Casting knife

The film preparation process applied in this work, using the casting knife is described as follow (**Figure 2.5**):

- Polymer resin powder/film scratch are dosed in distilled water to prepare a 20 % in weight solution. The mixture is heated at 80 °C with stirring (350 rpm) for 3 hours in a 50 ml glass bottle with plastic lid; to ensure the homogeneous temperature over the all bottle, a Dipropylene Glycol bath is used;
- The well-mixed solution is poured onto a glass support;
- A knife is used to spread the solution into a thin layer (for our application the wet thickness goes from 350 μm to 450 μm);

- The resulted membrane is left at ambient condition (22 °C-35 % RH) for 1 hour and then is placed in a dry oven at 80 °C for 3 hours;
- The supported membrane is taken out from the oven and kept at room temperature for 1 hour more; then it can be peel off from the support. [37]

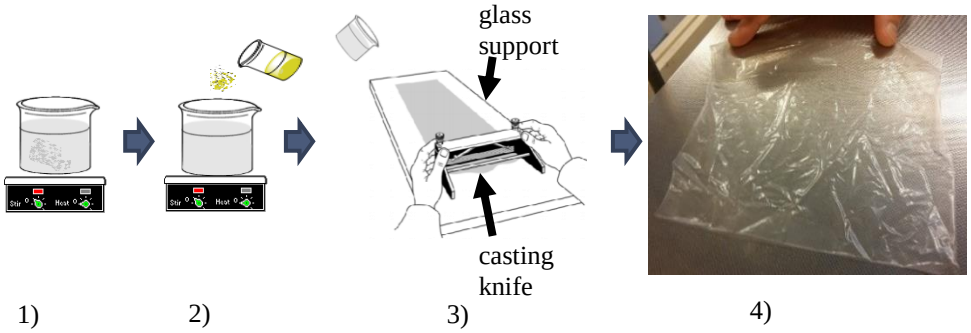

Figure 2.5 Casting knife process: 1) polymer dissolution 2) particles loading/polymer adding 3) pouring the mixture on the support and spread it with the knife 4) film after solvent evaporation

For K-hand coater and casting knife, the spread wet layer it will have a thickness different from the actual one desired: for PVA/water system, around a fifth part of the wet layer will be the dry thickness, but depending on the chosen solvent for each application, the ratio will change. [62]

2.2.2 Differential scanning calorimetry (DSC)

Differential Scanning Calorimetry, or DSC, is a thermal analysis technique that looks at how a material's heat capacity (Cp) is changed by temperature. The DSC is the most applied technique for study the thermal events on polymers like melting temperature, heat of fusion, latent heat of melting, reaction energy and temperature, glass transition temperature, crystalline phase transition temperature and energy, precipitation energy and temperature and specific heat or heat capacity. It's based on the heat flow difference between a substance and a reference, during a controlled temperature program. DSC analysis measures the amount of energy absorbed or released by a sample when it is heated or cooled, providing quantitative and qualitative data on endothermic (heat absorption) and exothermic (heat evolution) processes. The **Figure 2.6** shows a schematic illustration of the apparatus.

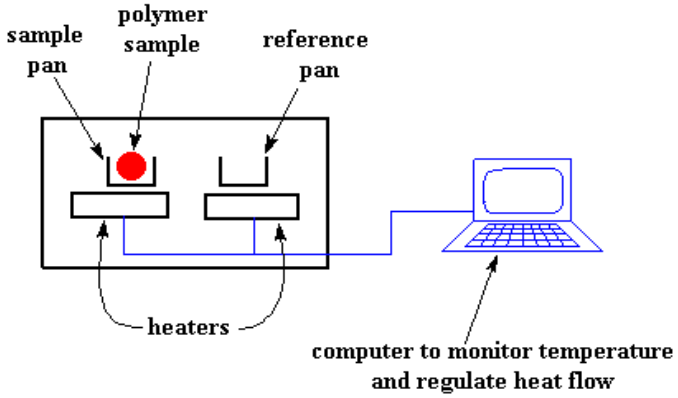

Figure 2.6 Scheme of DSC equipment

It consists of two pans, the sample one where the operator puts the polymer and the reference pan that will be left empty. Each pan is on top of a heater and using a software, the heat/cool cycle can be set. When a sample undergoes a physical transformation such as a phase transition, more or less heat will need to flow to it than to the reference to maintain both at the same temp. Whether more of less heat must flow to the sample depends on whether the process is exothermic or endothermic. [74]

Generally, the temperature program for a DSC analysis is designed such that the sample holder temperature increases linearly as a function of time. Only a few mg of material are required to run the analysis. DSC is the most often used thermal analysis method, primarily because of its speed, simplicity, and availability. It is mostly used for quantitative analysis.

There are different DSC instruments; in this work we focused mostly on two types:

- Heat flux DSC
- Modulated DSC (MDSC)

In *heat flux DSC*, the difference in heat flow into the sample and reference is measured while the sample temperature is changed at the constant rate. The main assembly of the DSC cell is enclosed in a cylindrical, silver heating black, which dissipates heat to the specimens via a constantan disc which is attached to the silver block. The disc has two raised platforms on which the sample and reference pans are placed. A chromel disk and connecting wire are attached to the underside of each platform, and the resulting chromel-constantan thermocouples are used to determine the differential temperatures of interest. Alumel wires attached to the chrome discs provide the chromel-alumel junctions for independently measuring the sample and reference temperature. A separate thermocouple embedded in the silver block serves a temperature controller for the programmed heating cycle. An inert gas is passed through the cell at a constant flow rate (**Figure 2.7**).

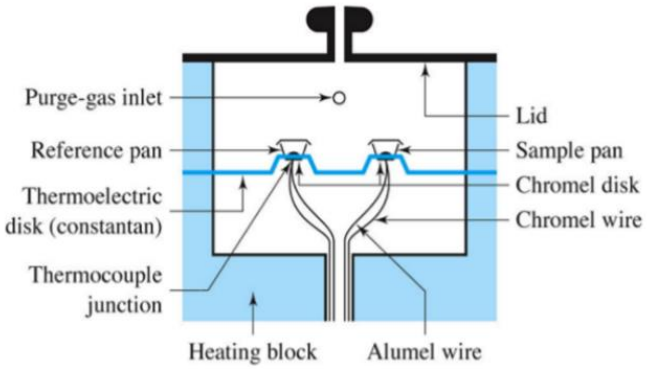

Figure 2.7 Heat Flux DSC scheme

In this system, it is possible to write the equation:

$$\frac{dH}{dt} = \frac{C_p}{dT} + f(T, t) \qquad (2.1)$$

Where H is the enthalpy in J mol^{-1}, C_0 is the specific heat capacity expressed in JK^1mol^{-1} and f (T, t) is the kinetic response of the sample in $Jmol^{-1}$. The result of a DSC experiment is a curve of heat flux versus temperature or time (**Figure 2.8**). This curve can be used to calculate enthalpies of transitions, by integrating the peak corresponding to a given transition.

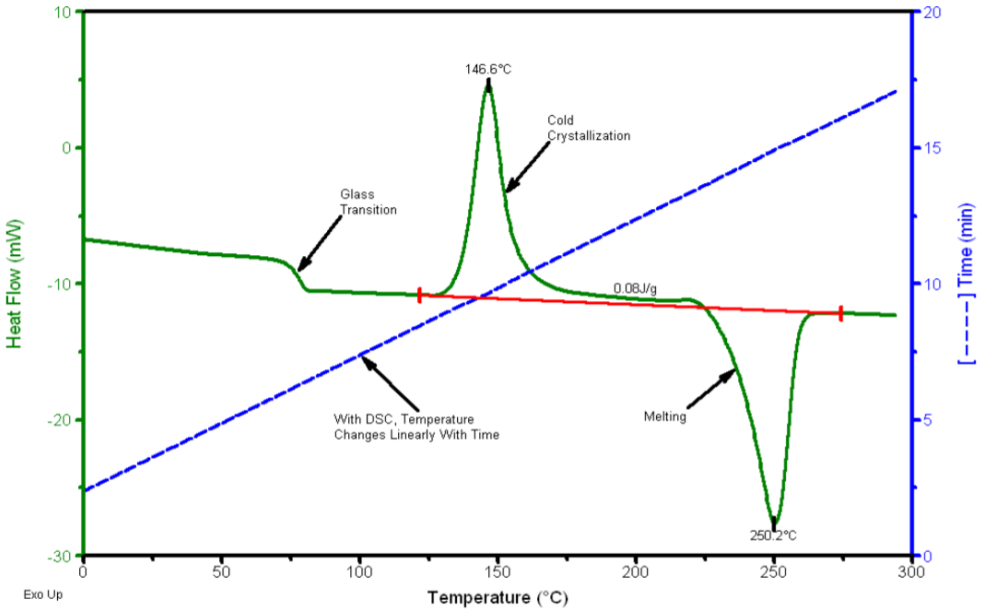

Figure 2.8 Typical DSC curve (example of PET)

Area under the peak is directly proportional to heat absorbed or evolved by the reaction. Height of the peak is directly proportional to rate of the reaction. [75]

About of the first peak on the **Figure 2.8**, it is mean there is more heat flow and so an increase in the heat capacity of the polymer. This happens because the polymer has just gone through the glass transition (Tg). After glass transition, the polymers have a lot of mobility. They wiggle and squirm, and never stay in one position for

very long time. But when they reach the right temperature, they will give off enough energy to move into very ordered arrangements, which are called crystals. When polymers fall into these crystalline arrangements, they give off heat. So, it doesn't have to put out much heat to keep the temperature of the sample

pan rising. This drop in the heat flow as a big peak in the plot of heat flow vs. temperature. The temperature at the highest point in the peak is usually considered to be the polymer's crystallization temperature, or Tc. Also, the area of the peak can be measured, which tells us the latent energy of crystallization of the polymer. But most importantly, this peak tells us that the polymer can in fact crystallize. If 100% amorphous polymer is analyzed, this peak cannot be obtained. If polymer is heated past its Tc, eventually reach another thermal transition, called melting. When polymer's melting temperature is reached, Tm, the polymer crystals begin to fall apart, that is they melt. It comes out of their ordered arrangements and begin to move around freely that can be spotted on a DSC plot. The heat which polymer give off when crystallized is absorbed when reached at Tm. That is a latent heat of melting like latent heat of crystallization. When the polymer crystals melt, they must absorb heat in order to do so.

On the other hand, the operating principle of MDSC differs from standard DSC in the use of two simultaneous heating rates - a linear heating rate that provides information like standard DSC, and a sinusoidal or modulated heating rate that permits the simultaneous measurement of the sample's heat capacity. **Figure 2.9** shows the temperature profile from a MDSC experiment.

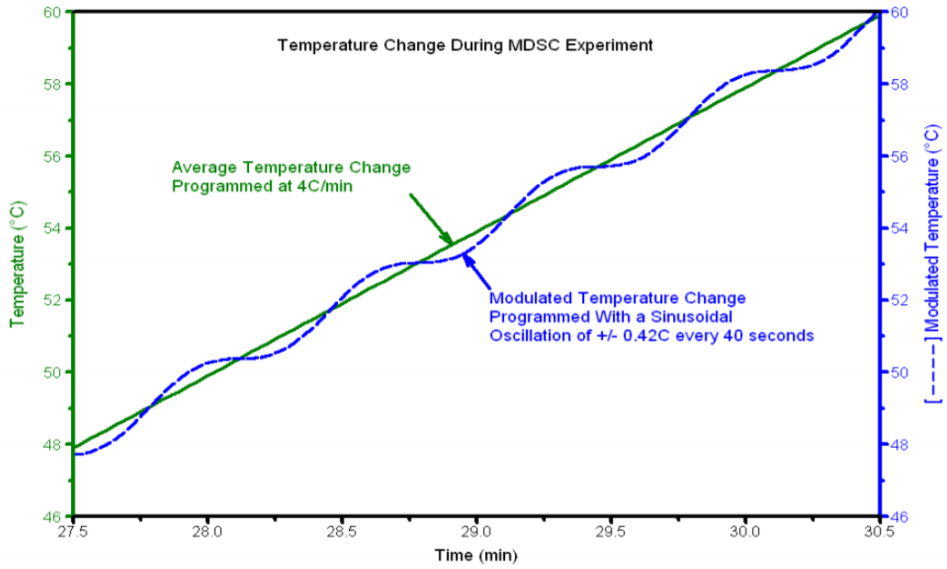

Figure 2.9 Sinusoidal and linear temperature profiles for a MDSC

Figure 2.10 shows the three most often used MDSC signals and the benefits of the dual heating rates. The Total signal (green) is equivalent to standard DSC; the Reversing signal (blue) provides information on heat capacity and melting, while the Non-reversing signal (brown) shows just the kinetic processes of enthalpic recovery at Tg, cold crystallization and crystal perfection. [58, 76]

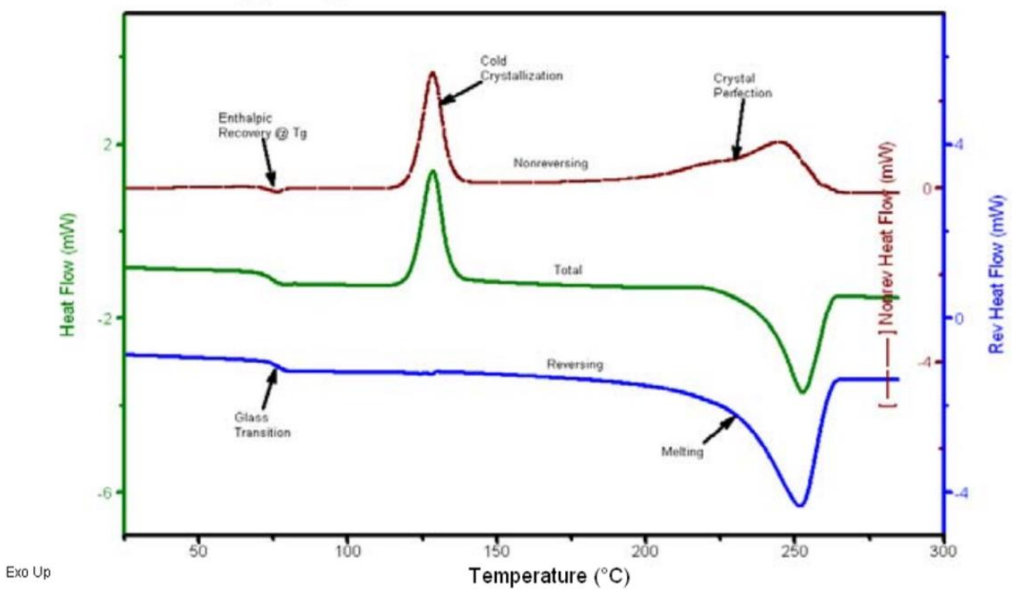

Figure 2.10 Common signals involved in a MDSC experiment

The heat flux calorimetric studies of this work were performed in aluminum standard 40 µl crucibles with a TA instruments Q2000 DSC (Z01023) thermal analyzer at the heating rate of 10˚C/min using between 3 and 10 mg of sample, nitrogen as a purge gas (50 ml/min) and liquid nitrogen for the cooling system. Same equipment and pan were used for MDSC; the differences were on the heating rate (3˚C/min) and the addition of a modulate heat (± 1˚C every 60 seconds).

2.2.3 Slide Dissolution Test

This method purpose is the determination of the time required for a water-soluble film to break apart.

The test is a standard method utilized by the supplier Monosol (MSTM 205) and described in several patents. [63, 64, 77]

First step to do is measure the thickness of the film using the digital micrometer Thwing- Albert Model 89-100" SOP FHCM1021. Once be sure of the thickness, in this work 76 ± 4µm, place the film in a plastic frame (**Picture 2.4**) avoiding wrinkles and repeat the operation until have 5 samples to test.

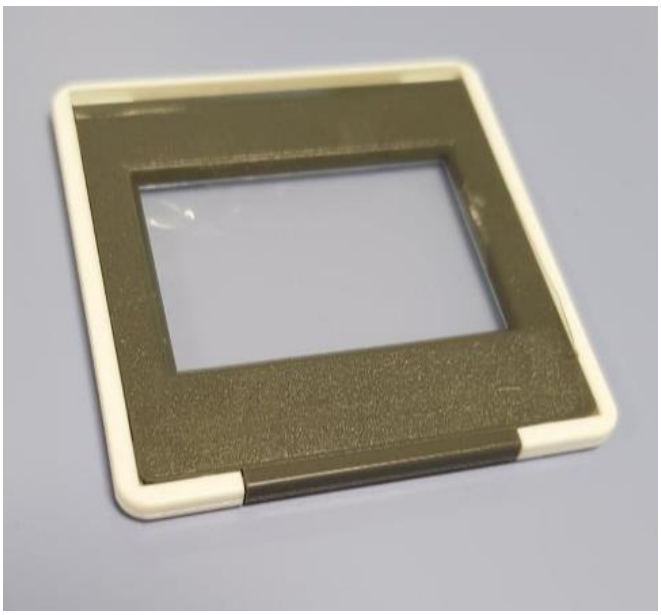

Picture 2.4 PVA film framed for Dissolution test

After the sample preparation, the procedure is the following:

1. Fill a 600 ml beaker with 500 ml of distilled water and adjust the stirring speed to control the vortex height so the final water level is 4/5th of the original water height (400 ml level)
2. Record the water temperature; it has to be maintained at 10˚C (± 1 ˚C)
3. Insert the slide into the water using a system of clamps and immediately start the stopwatch for the measure
4. Record the time when the film breaks. This value is called *disintegration time*, meanwhile *complete dissolution* is the time when no film is more framed
5. Stop the stirring, clean the equipment and repeat for all the specimens.

The final set up is shown in **Picture 2.5.**

Picture 2.5 Slide test setup

2.2.4 Environmental Scanning Electron Microscopy

ESEM analysis was performed using a low-vacuum ESEM FEI Quanta 600 apparatus, without sputter coating. The film samples were fractured by impact after cooling them with liquid nitrogen. In the resulting specimens a brittle fracture was obtained. Before the analysis, samples were coated with a gold-palladium layer (about 15 nm thick) by means of an Emitech K575X sputter coater.

2.2.5 Tensile Properties

The stress of a film at 100% elongation is measured utilizing the ASTM D 882, "Standard Test Method for Tensile Properties of Thin Plastic Sheeting".[78] The test is conducted on a Model 5567 Instron® Tensile Tester. The Instron® grips utilized in the test may impact the test results. Consequently, the present test is conducted utilizing Instron® grips having model number 2702-032 faces, which are rubber coated and 25 mm wide.

Since the final application of the new PVA film is a soluble unit dose, Procter & Gamble developed an additional method to measure the shift in film properties for film when brought into contact with a cleaning liquid. This experiment is called internally *Immersion Test*. The detergent contains mainly water, Glycerol, Dipropylene glycol [DPG] and Propylene glycol [Pdiol]: the

glycerol for example is also the plasticizer content in the films and the experiment is focused on understand if the film plasticizes, changing not only tensile features, but also dissolution, permeation and tightness ones.

A 12 cm by 17 cm film is placed in a flat clean inert glass tray, where a total of 150 ml of detergent is poured. To avoid bubbles and wrinkles, firstly a part of the liquid is poured in the recipient to cover the bottom (**Figure 2.11 a)**) and, once the film is situated in it (**Figure 2.11 c)**), gently the remaining liquid is poured. Then the tray is sealed, and the system is stored in controlled temperature and relative humidity room (20°C–35%RH) for 5 days.

After this time, the vessel is removed from the storage and left for 24 hours at room conditions. The excess of detergent is removed with paper and then 5 stripes of 25 mm width are cut as specimen and tested in according to the ASTM D 882.[78] This experiment leads to the effect of solvents content in the cleaning liquid, like plasticizers and water, on the PVA film and simulate the storage condition of a finished pouch.

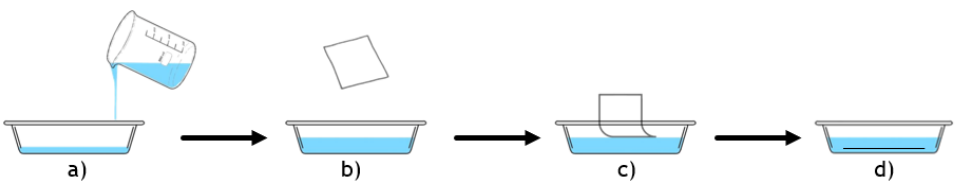

Figure 2.11 Immersion test procedure

2.2.6 Water vapor permeability (WVP)

The ASTM E96-95 standard method was used to examine the WVP of the composite and blend films. [79] The test is run using a SPSx-1μ High Load Vapor sorption analyzer supplied by ProUmid (**Picture 2.6 a)**).

a) b)

Picture 2.6 a) SPS equipment b) Carousel

The basic operation principle of a sorption analyzer is to measure the change in mass of a sample that is kept in an environment of controlled constant temperature and relative humidity. Change in mass takes place either by water sorption from the surrounding air to the sample or water desorption from the sample.

There are two methods to test the water vapor permeability: dry cup or wet cup. These two tests are similar in setup, but the service

conditions are different. Water or desiccant is placed in the cup leaving an air gap between it and the material (**Figure 2.12**).

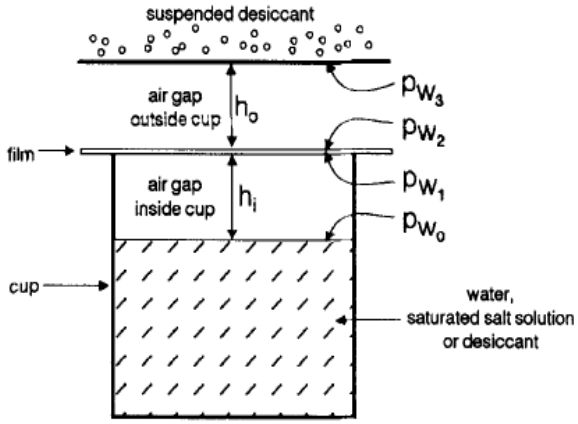

Figure 2.12 Dry/wet cup method scheme

The water method measures weight loss due to water vapor from the cup transmitting through the material to the test atmosphere as well as the humidity of the test chamber; meanwhile, the desiccant method measures weight gains due to water vapor from the environment transmitting through the material due to the desiccant absorbing feature.

In this work, the dry cup method was applied for the purpose.

The equipment is basically a relative humidity and temperature controlled chamber, wherein a carousel (**Picture 2.6 b)**) with up to 5 film samples is placed plus a reference cup. The specimen is a cup (**Picture 2.7**) where inside a desiccant is placed (e.g.

molecular sieve), closed by the film of interest and sealed thanks to six screws.

Picture 2.7 Specimen for WVP experiment; film covers the desiccant

The weight system is automatic due to a software (usually every 10 minutes the equipment weights the sample), which also controls the environment conditions. After several hours of test, a chart like **Figure 2.13** is obtained: the X-axis reports the experiment time (hours), meanwhile the Y-axis are the milligrams on the primary (left) and temperature (°C)/ relative humidity (%) on the right. T and RH share the secondary vertical axis. During the first 6 hours the system is still conditioning, and the humidity is on 35% RH, meanwhile after the increasing to 50 % RH, the cups start to gain weight. The firsts 2 hours with 50% RH show a not-linear slope, not interesting for the purpose, while from 8 hours to 19 hours, the slope is linear and it`s used for the WVP calculation.

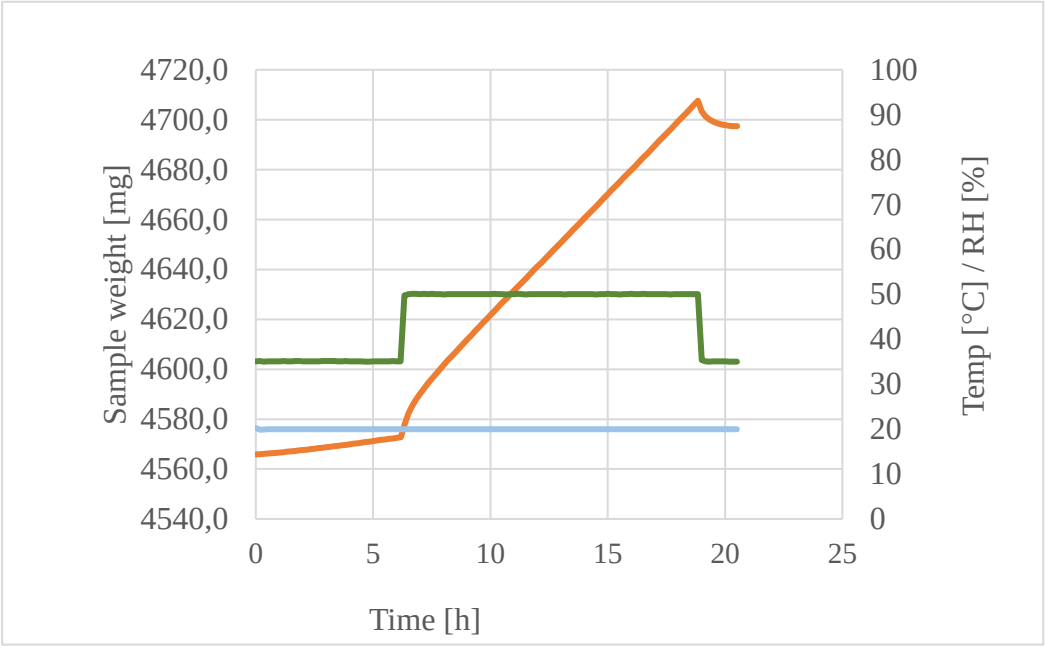

Figure 2.13 Typical chart for WVP experiment: Temperature in light blue (°C), Relative Humidity in green (%) and a sample kinetics in orange

The slope of the linear portion of this plot represented the steady state amount of water vapor diffusing through the film per unit time [g/h]. These values are insert in the following formula (2.2) to calculate the water vapor permeability.

$$WVP = \frac{Mass \ * Thickness * 24}{Time * Area \ * \Delta Vapor \ Pressure} =$$

$$WVP = \frac{m*T*24}{t*A* S(R1-R2)} = \ [\mathrm{g}\ Pa^{-1}day^{-1}m^{-1}] \qquad (2.2)$$

Where the Thickness of the film is expressed in [m], the Area of interface contact between the film and the atmosphere is in [m^2] and the ΔVapor Pressure it is equivalent to the saturation vapor pressure at test temperature S (e.g. S at 20º C = 2338,8 Pa) multiplied by the difference of the relative humidity at the source expressed as a fraction R1 (e.g. R1 = 0.5) and R2, the relative humidity inside the cup expressed as a fraction (R2 = 0 for dry cup method).

2.2.7 Detergent-film system compatibility

Due to the final application of the new films, a compatibility study of the film with the detergent used in pouches and the most used solvents in the compositions, is fundamental to understand the behavior of the system.

The **Figure 2.14** represents the system utilized for this purpose:

- the film of interest is weighed;
- 20 ml of detergent (also called juice) or solvent content in it (e.g. Glycerol, Dipropylene glycol [DPG], Propylene glycol [Pdiol]), is poured in a polystyrene transparent cup;
- the film is placed in the half full cup, paying attention to avoid air bubbles that can create interface air/film;
- other 20 ml of liquid are poured in the cup;
- after seal the cup with a lid, the system is placed in a controlled temperature room (50°C) for 3 days;

- when this time is passed, the film is removed from the cup and gently and accurately cleaned with paper;
- now the sample can be weighed again.

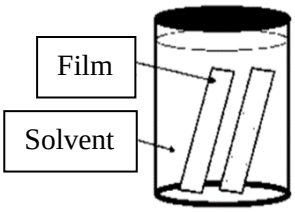

Figure 2.14 Representation of the system used for compatibility studies

This method is a gravimetric technique and, having the initial weight (W_i) and the final one (W_f), the gravimetric percentage of swelling (%SW) can be calculated thanks to the following formula:

$$\%SW = \frac{(W_f - W_i)}{W_i} \cdot 100 \qquad (2.3)$$

The technique is applied to understand how the material interacts with solvents in terms of swelling or dissolving.

2.2.8 Migration of a brightener through the film

The purpose of this test is monitoring the migration, meant as liquid to liquid diffusion of a molecule or active through a film.

The molecule that diffuses is a brightener (Fluorescent Whitener Agent FWA49) that is in low percentage inside the detergent of pouches: it converts UV light into "blue" light and increase consumer whiteness perception. The chemical name is Sodium 2,2'-([1,1'-biphenyl]-4,4'-diylbis(ethene-2,1-diyl))dibenzenesulfonate and following image is the structure and some properties.

Molecular Formula	$C_{28}H_{20}Na_2O_6S_2$
Molecular Weight	562.6 g/mol
CAS NUMBER	56776-28-4

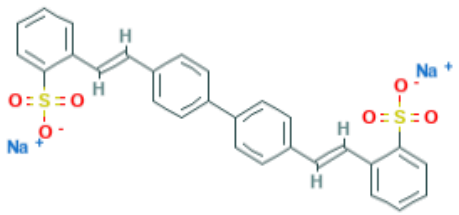

Structure 2.1 FWA49 molecule structure and compound summary

The diffusive flux across per unit area of film is described by [80]

$$j = \frac{DH}{l}(\Delta Concentration) \quad (2.4)$$

Where H is the partition coefficient which reflects the migration from liquid interface, $\frac{DH}{l}$ the permeability and *l* is the thickness of the film sample. Partition coefficient (H) is defined as the relative concentration of a molecule in film versus the concentration in the detergent.

The method uses metallic cells (**Picture 2.8**) separated by the film, where inside of each one there is detergent: the differences between the 2 compositions, is the presence of a brightener molecule (FWA49), used as a migration tracer; a blue dye is added to the composition that includes this molecule (**Picture 2.8** left cell), while the yellow (**Picture 2.8** right cell) detergent is not containing it.

Picture 2.8 Metallic migration cells

Each step has to be followed accurately:

- After measure the thickness of the film, which will be used for the DH calculation, the sample is located between the two metallic cells, using a rubber O-ring to avoid leak and permit a perfect an adhesion between the two sides;
- Using screws and torque screwdriver that ensure 2.5 N force, avoiding wrinkles on the film, the cells are assembled;
- Around 67 g of detergent for each side are placed (one side with FWA49 and the other one without) and transparent lids close the system: the cover with the silicone cork will be placed on the top of the juice without brightener molecule (**Figure 2.15**);
- When all the systems are ready (3 reps each sample), the cells are carefully placed on stirrer hotplate (40°C – 350 rpm) (**Picture 2.9**).

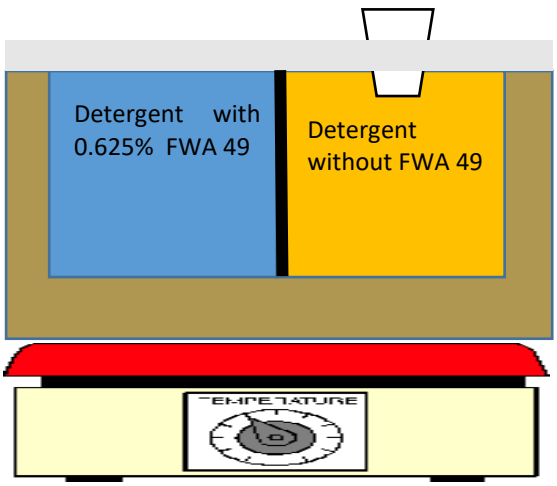

Figure 2.15 Design of migration experiment setup

Picture 2.9 Migration experiment cells on hot-stirring plate

After 3-4 days, the sampling can start; every 2-3 days a sample from yellow compartments has to be taken, until have 5-8 samples for cell during time. The sample consists in 1 drop of juice (around 0.020 g) that must be dilute with distilled water about 100 times (total weight around 2 g), always recording the drop and total dilution weight.

Once all 5-8 samplings are ready, the actual measurement can take place:

- the diluted samples are dilute further with distilled water (e.g. from 0.3 g to 15 g) and gently mixed;
- now these final solutions can be studied thanks to fluorimeter supplied by Perkin Elmer Luminescence Spectrometer, Model LS55 with FL WinLab software.

The equipment will respond with intensity values between 0 and 1000 (if higher, another dilution is mandatory). Taking in account the dilution and the intensity of the fluorimetry, the concentration of brightener in the cells over time is calculated.

An example is following:

- The drop from the cell weights 0.0226 g and with the first water dilution give a weight of 2.0242 g (sample concentration $S1 = \frac{0.0226}{2.0242} * 1000$ =11.1649 g/l). A sample of 0.2584 g of the first dilution is further diluted up to 35.7536 g ($S2 = \frac{11.1669}{35.7536} * 0.2584$ = 0.0807 g/l). The specimen can be evaluated with fluorometry and give an intensity of 202.899 and, taking into account the calibration of the equipment on the brightener molecule, the final concentration of FWA 49 in the detergent is C_p = 22.20.

- The permeability DH of a film can be calculated using the following equation: [81]

$$DH = slope\ of\ Ln\left(\frac{Cr,0}{Cr,0-2Cp}\right) versus\ time/CC \quad (2.5)$$

where $C_r,0$ is the initial concentration of FWA49 in the detergent (0.625% = 6250 ppm), C_p is the detergent concentration of brightener that as migrated and CC is a cell constant expressed by the equation $CC = \frac{A}{l}(\frac{1}{V1} + \frac{1}{V2})$ with A as film surface (m^2), l as film thickness (m) and V1,V2 the volumes of the juice in cell 1 and 2 (m^3).

Charting the $Ln\left(\frac{Cr,0}{Cr,0-2Cp}\right)$ versus time (**Figure 2.16**), fitting the values, the slope is obtained.

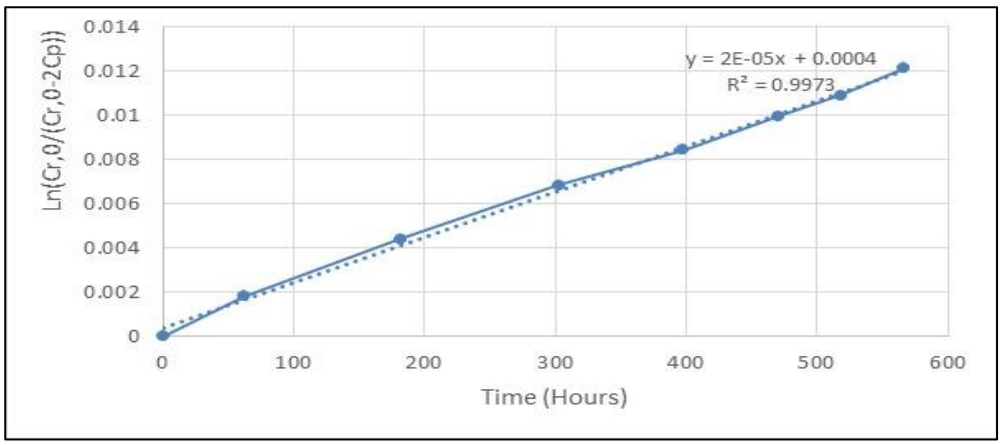

Figure 2.16 Example chart of migration experiment

2.2.9 X-Ray Diffraction (XRD)

The degree of crystallinity of polymer is very important. It defines the physical and mechanical properties of the polymer system. The chemical resistance, moisture absorption and mechanical properties like tensile properties and stiffness are directly proportional to the crystallinity. The X-ray diffraction technique is the most reliable technique for determining the crystallinity of the semi crystalline polymer system. [82, 83] The X-Ray diffraction studies of this work were carried out with Bruker AXS diffractometer, using a source provided by copper (Cu) tube with 1.5418Å wavelength.

2.2.10 How produce a pouch

A typical pouch for laundry has 3 compartments with different compositions, 2 on the Top side and 1 at the Bottom. The top part is formed by 2 films and 1 film forms the bottom side (**Picture 2.10**).

Picture 2.10 Lateral view of a typical multi-compartment pod

The **Figure 2.17** shows a schematic representation of a converter producing multi-compartments pouches for laundry.

The process consists in:

- The *bottom* film is pulled by rollers to the belt, where the molds with rectangular shape are situated;
- Heating up the film, helps the formation of the bottom shape due to vacuum system;
- Once the bottom pocket is formed, the belt continues and dispenser, dose the exact amount of detergent;
- at this time, the top part is created with the same principles (usually with 2 compartments within 2 different compositions) but closed between *middle* and *top* film;
- Now the bottom side and the top are sealed together applying water;
- The pods are ready to be cut and divide.

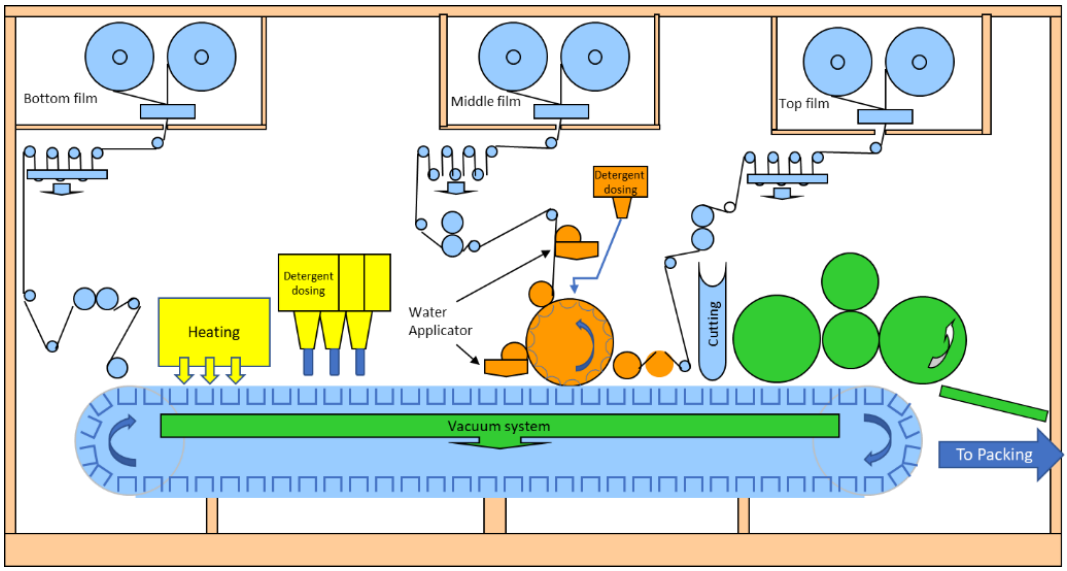

Figure 2.17 Converter scheme for pouch making

This process can be repeated with a 1-up machine that mimics a plant converter but in lab-scale.

The equipment used for the purpose is a thermo/vacuum forming machine (**Picture 2.11**).

Picture 2.11 Thermo/vacuum machine used for producing a single pouch

First step for prepare a classic multi-compartment pouch, is start with the top compartment. A piece of film is placed on a plastic mold with the desire shape and fixed to avoid wrinkles. A heat gun is used to heat up the film for the deformation (**Picture 2.12**).

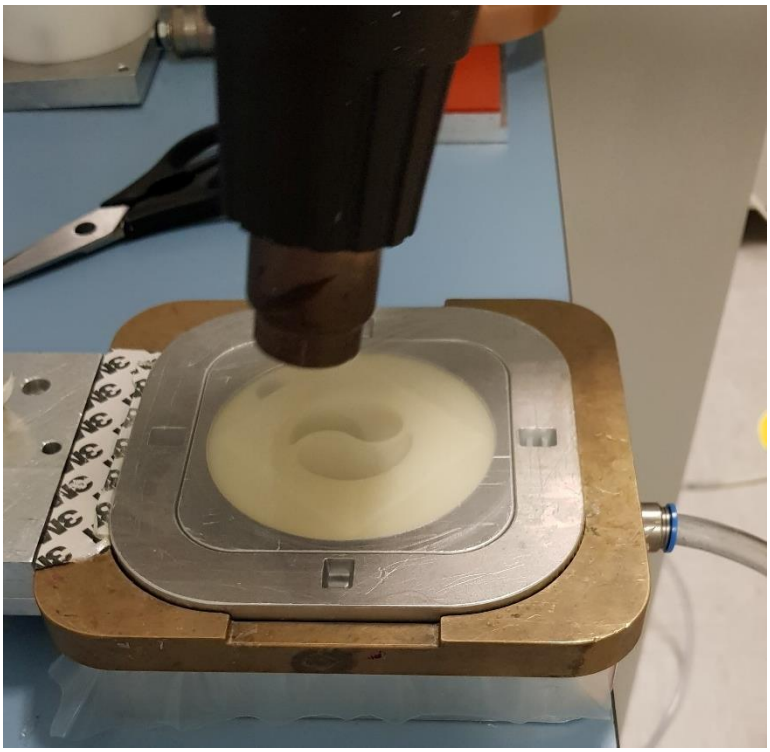

Picture 2.12 Heating the film with a gun

After about 10-15 seconds (time depends on the material) the film is ready, and the vacuum in started to shape the compartment. The detergent is now inserted in the pouch with a syringe or dispensator (**Picture 2.13**).

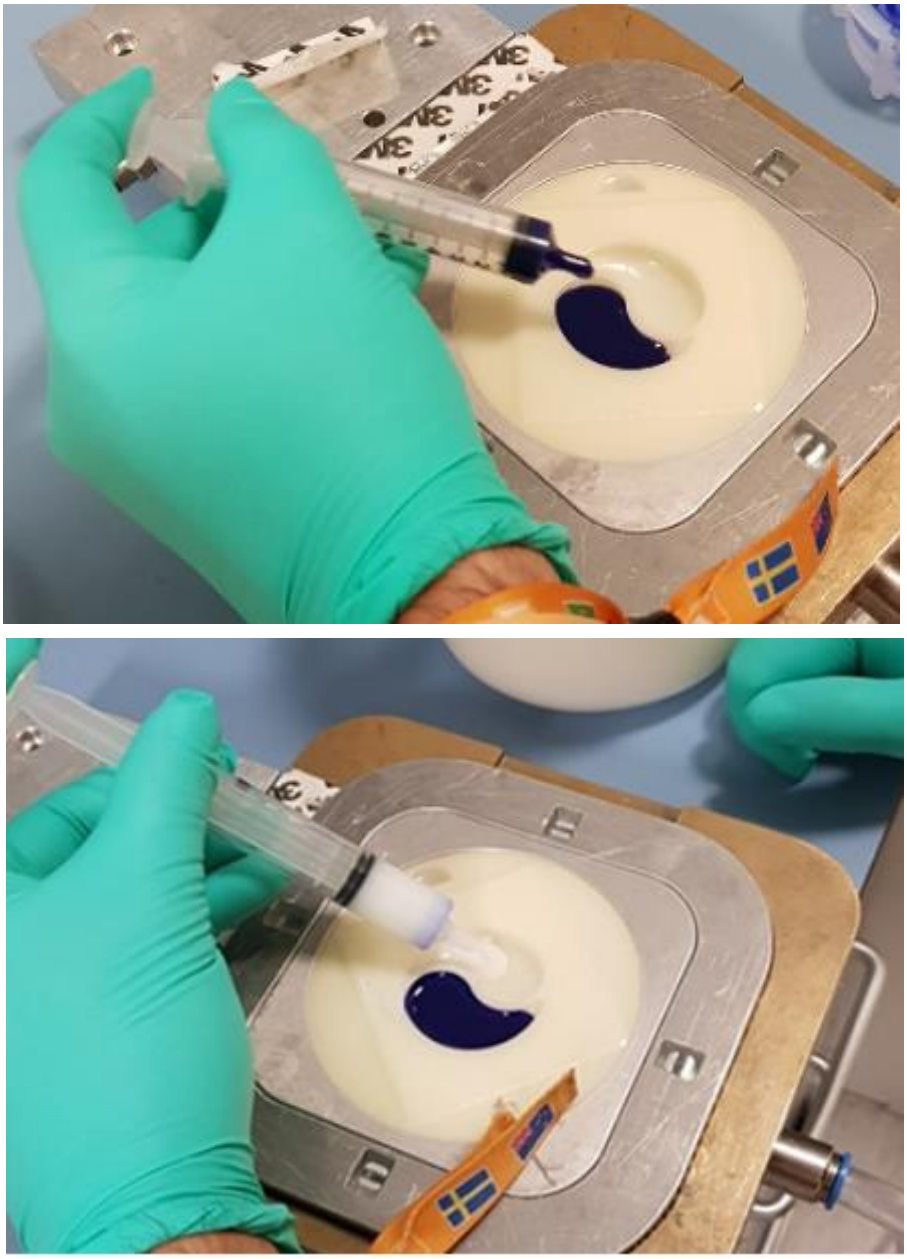

Picture 2.13 Filling the two compartments with two different detergents

Now the top compartment is ready to be completed: a piece of film (about 25 x 40 cm) is placed on a rubber support (**Picture 2.14**) and, avoiding wrinkles, a frame encloses it. With a pipette, few ml of sealing solution (usually water or PVA water solution) are poured on the top of the middle film and using a metallic bar, the liquid is spread over the whole area.

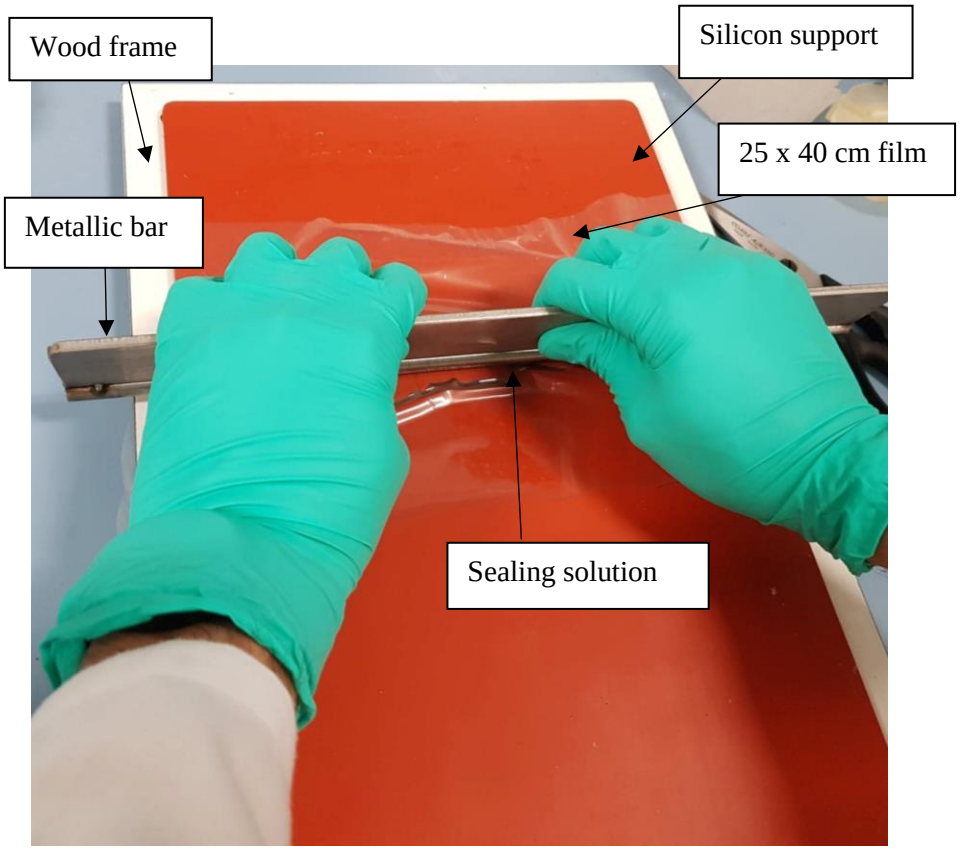

Picture 2.14 Silicone support used for framing the middle film and spreading the sealing solution

The wet film is now placed on the top compartment, paying attention to avoid wrinkles and a metallic plate of the machine, heated up at around 115°C, seals the first side of the pouch pressuring the film with the filled cavities. The result is showed in following **Picture 2.15**.

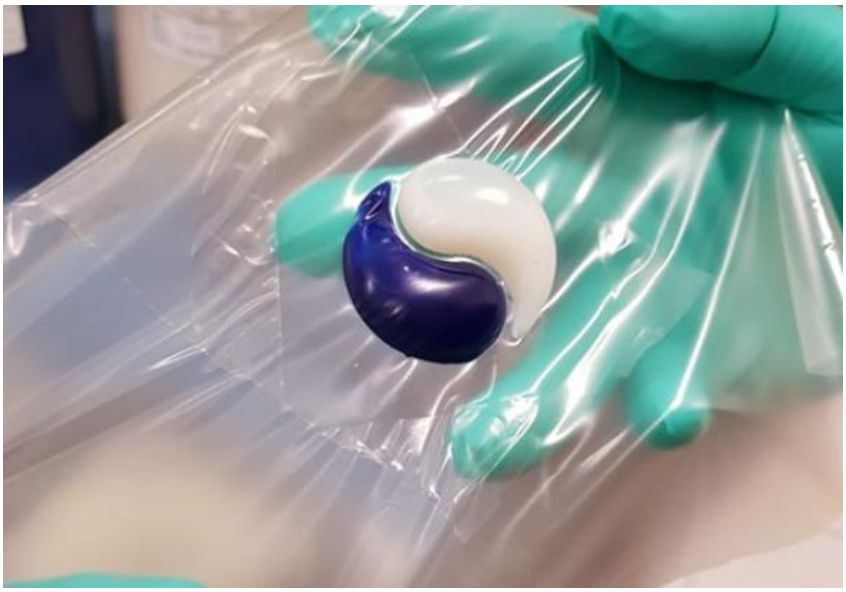

Picture 2.15 Completed top compartment

To complete the process, a bottom compartment is produces following the same steps as before (with different mold) (**Picture 2.13**) and, instead of sealing it with a film wet by water/PVA solution, is it covered by the top part, previously produced (**Picture 2.16**).

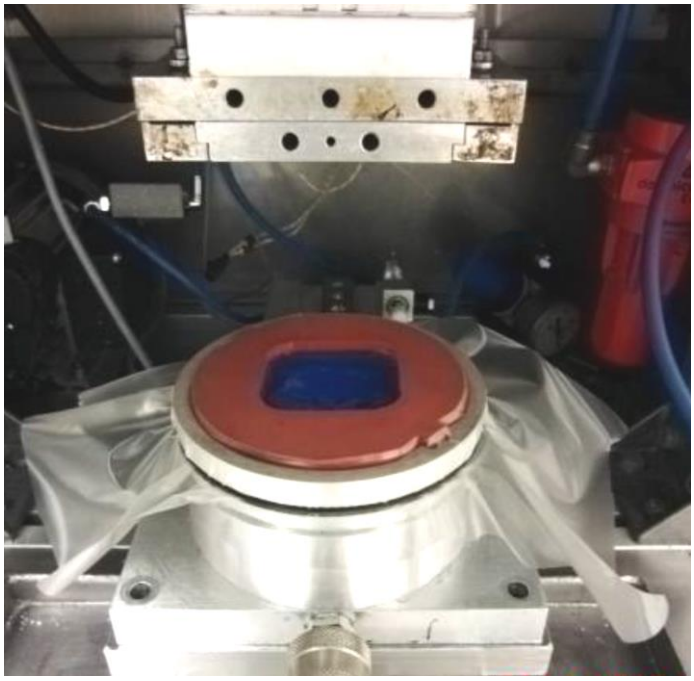

Picture 2.16 Bottom compartment filled with detergent, ready to be sealed with top part

The following images illustrate the sequence of the final sealing:

- **Picture 2.17 a)** shows how to apply the sealing solution on the finished top compartment using a brush;
- In **Picture 2.17 b)** the operator is placing the top section, paying attention to the perfect alignment between the 2 parts;
- **Picture 2.17 c)** presents the final pouch after the hot plate sealed the top and bottom compartments.

a)

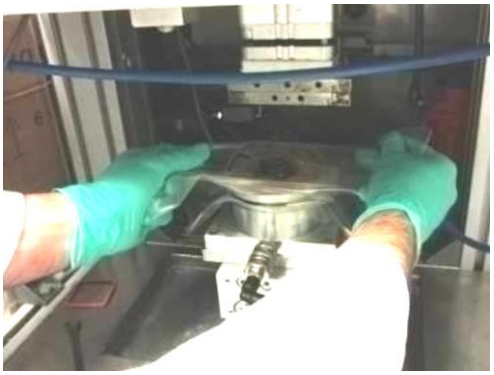

b)

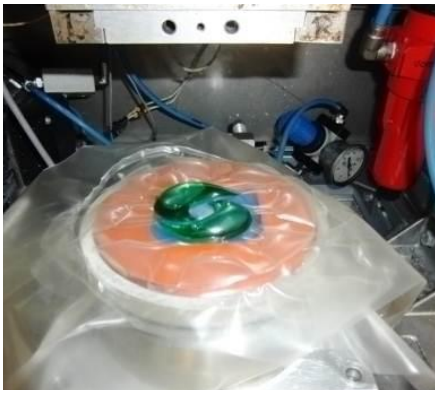

c)

Picture 2.17 Bottom compartment filled with detergent, ready to be sealed with top part

Once the seal is complete, the pouch is completed: then is cut and ready to be tested.

2.2.11 Beaker test: dissolution of a pouch

To determine the dissolution time in water of pouches, Procter & Gamble, developed a procedure called *Beaker test*. This method use a conductivity meter (Seven Excellence supplied by Mettler Toledo) to measure what is called completion, defined as:

$$\%\ Completion\ (t) = \frac{Cond.(t) - \min Cond.}{MAX\ Cond. - min\ Cond.} \qquad (2.6)$$

Where Cond(t) is the conductivity in time function and min and MAX Conductivities are the lower and higher value of the conductivity for a specific sample.

At least 3 specimens per sample have to be analyzed. First step to follow is the pouches conditioning: they are placed in 23 °C and 50% RH chamber for at least 24 hours, helping the equilibration of system film/detergent. Usually at least 2 weeks aged pouches are tested.

For the test itself, 5 l beakers are filled with 3 l of demineralized water at 20 °C wherein impellers for the stirring and homogeneous dispersion of the detergent and conductivity probes are inserted (**Picture 2.18)**.

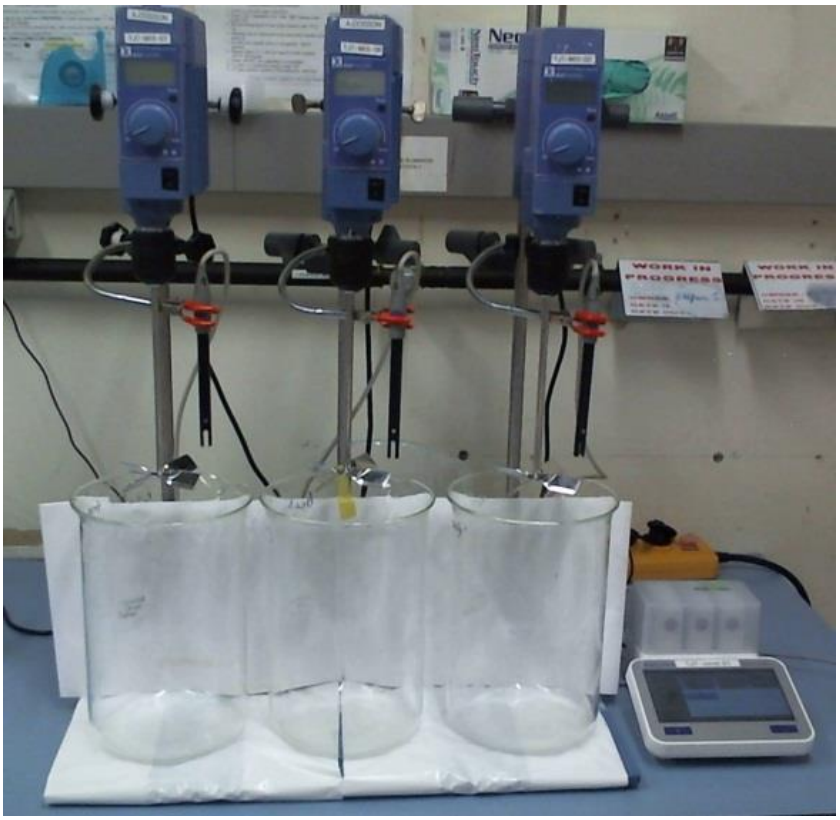

Picture 2.18 5 liters beakers with mechanical stirrers and conductivity probes

In **Figure 2.18** is shown the actual setup for the test: first, the water conductivity is measured and must be < 5μS/cm. When the experiment starts, the pouches, placed in metallic cages standing on the seal area (as shown in following picture), are inserted in the beakers (water stirring at 70 rpm): a software linked to the probes, record the values over 15 minutes and gives as results an excel file, where the conductivity over time is charted.

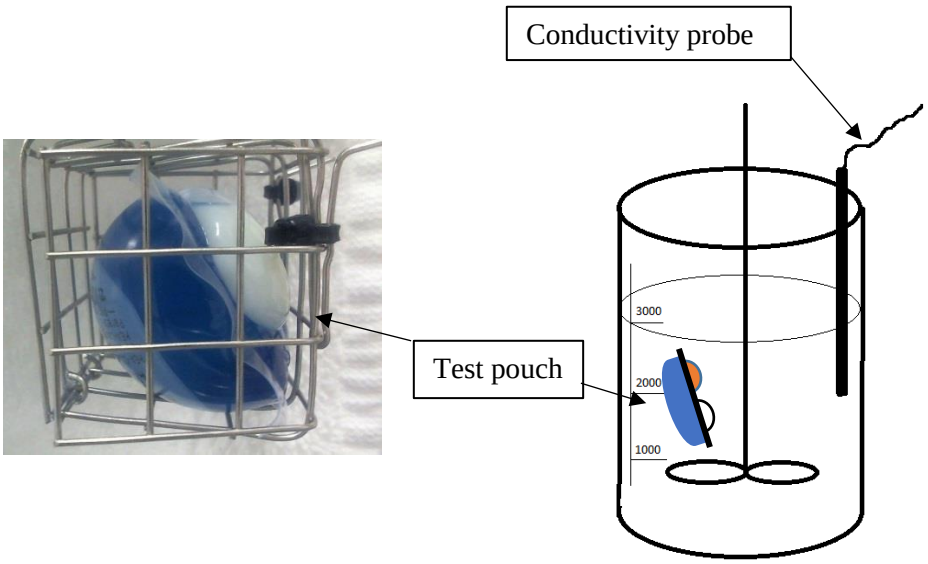

Figure 2.18 Scheme of setup for beaker test

After 15 minutes, the pouches are completely dissolved and chart like **Figure 2.19** Conductivity [µS/cm] versus Time [s] is generated.

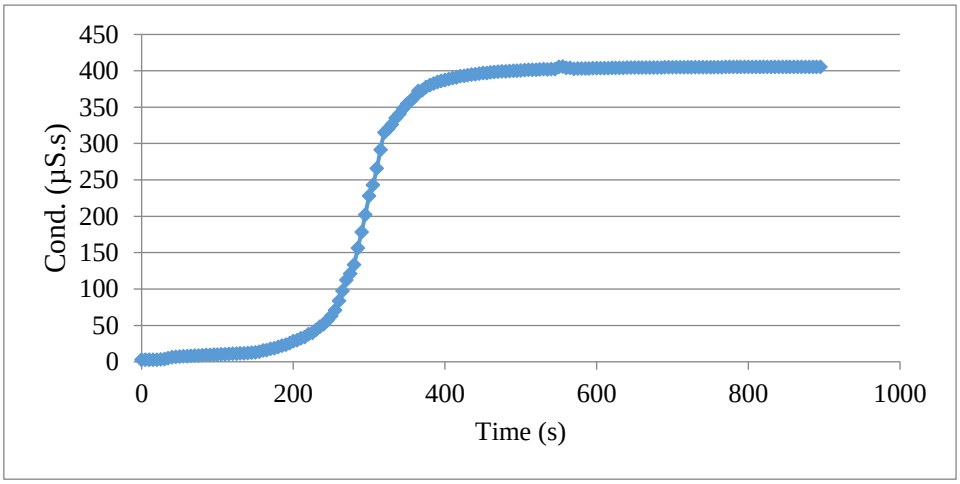

Figure 2.19 Typical chart after beaker test: Conductivity[µS/cm] vs time[s]

It is clear that the plateau reached corresponds to the maximum Conductivity of the liquid, so the pouch is completely dissolved and all the detergent contents in, now is in the water.

This test is used to understand, not only the dissolution time of the pouch in water, but coupled to a camera which records the process, it can help to understand the mechanism of it.

The general charts are reported in completion percentage (**Formula 2.6**) versus time because this kind of *normalization* allows to compare different samples.

3. Preparation and Characterization of M8630 microcomposite films

3.1 Introduction

Following the purpose of the work, the first modification for PVA film studied was the filled system with microfibrillar cellulose.

The study was performed on modifying M8630 film: this film is branded and commercialized by MonoSol®. According to the patent literature, [84, 85] MonoSol's M8630 water-soluble film is a commonly used grade for detergent capsules. The film is a mixture of PVA, chitosan, plasticizers, like glycerin, and other components: usually around 72% in weight is PVA, while around 7% in weight is water.

In this work, we decided to start with the modification of this film, since it was already broadly studied in all the chemical and physical aspects. The common thickness is 76 ± 4 μm and this value was the goal for the films casted by solvent evaporation.

The state of art is plenty of applications for PVA film loaded with several particles, like wax and cellulose. [40, 43-45, 48] The choice of micro sized cellulose particles was based on some results of the filled PVA film, like those reported by Ali *et al* [86] who claim a decreasing permeability for PVA/Microcrystalline Cellulose Composites in packaging application and other results on PVA film loaded with nano particles of cellulose, like those reported by Sun-Young *et al* [45] who claim an improved tensile strength linked to the nanocellulose loading.

This work is focused on the study of a PVA composite loaded with micro-sized cellulose particles, since the goal properties we want to improve are the permeation ones, and also because we want to avoid the final cost of film to increase, as cost rises with particles size decreasing.

First experiments on this new material were directed to the study and choice of the film casting process, meanwhile the other investigated properties, as tensile strength, water permeation and dissolution ones, are the most important for the material screening taking into account the final application as soluble unit dose for laundry.

All the experimental results of the new loaded polymer were compared with virgin M8630 film supplied by MonoSol, to understand the actual differences between these materials.

3.2 Results and Discussion

3.2.1 Film preparation and characterization

In the previous chapter (**Section 2.2.1**), the film preparation was deeply reported, but before having the optimized procedure, some trials were run to understand how and whether the casting support and the solvent evaporation procedure, could affect the final film morphology.

In **Picture 3.1,** the two different surfaces tried for the film casting are shown: Teflon and glass.

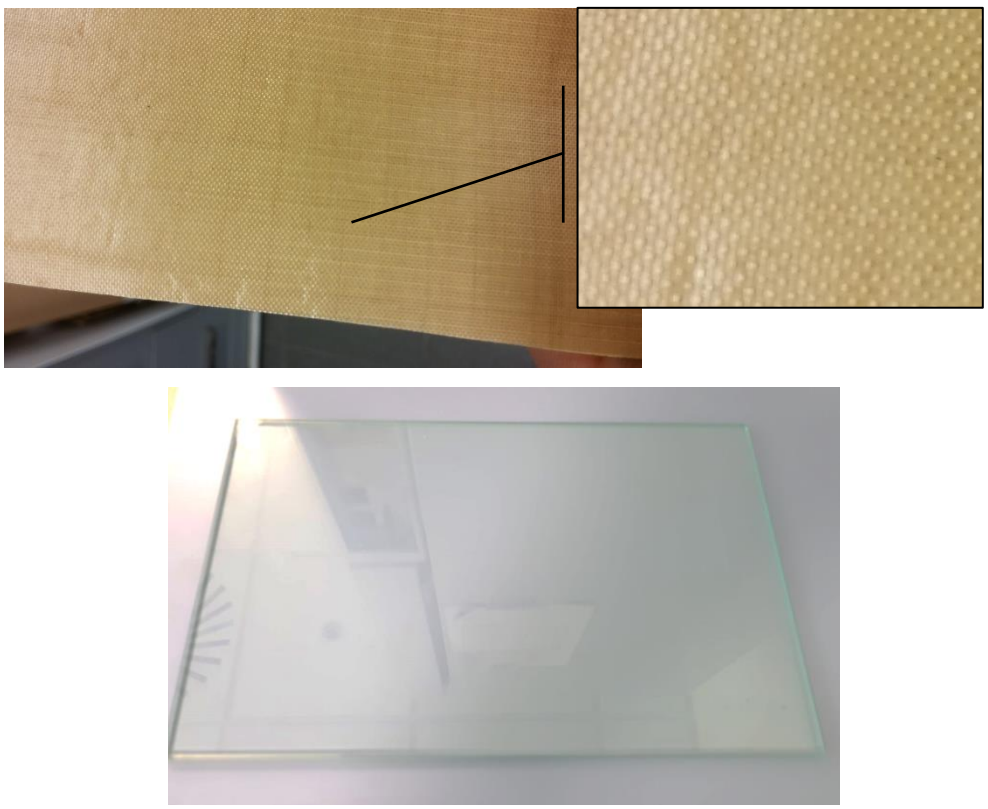

Picture 3.1 On top the Teflon surface with a zoom on the right; at the bottom, glass support

Teflon supports are widely used due to their non-stick property, as different studies confirm, [39, 87] meanwhile the glass is very common for dense polymer casting. [45, 48]

The choice of the support was focused on two aspects:

- Ease of the peeling of the film, avoiding wrinkles or cracks;
- Possible prints that can affect the film properties.

The simplicity of detaching the film after the drying process, was observed in both cases, meanwhile the Teflon support was leaving some marks on the film side in contact with the substrate; the zoom in **Picture 3.1** underlines the path. To validate the formation of pattern and understand the morphology, Environmental Scanning Electron Microscopy (ESEM) observation were performed (**Figure 3.1**).

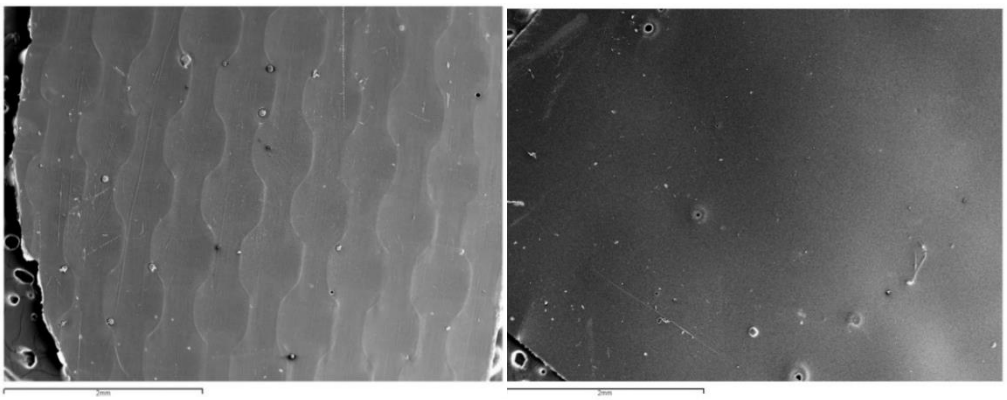

a) ***Film casted on Teflon support*** ***b) Film casted on glass support***

Figure 3.1 ESEM observation of casted film on different supports

These ESEM pictures show the film faces which were in contact with the casting support: the left film has a rough pattern resulted from Teflon support, meanwhile the film casted on glass has a perfectly smoother surface. The marks on the surface could mean a non-homogeneous thickness and can promote variation in the permeation.

An irregular pattern on the surface can negatively affect or, at least, significantly change the properties of this kind of material, even more so if the focus point of the work is the modification of the barrier properties of the PVA membrane.

For these reasons, the glass was chosen as support for the casting process.

Another aspect studied was the evaporation process after spreading the polymeric solution on the glass with the casting knife. Virtanen *et al*, [37] for nanofibrillated cellulose PVA film, dried the solution for 7 days at room conditions, until the weight of the system is constant. On the other hand, Lee *et al*, [45] for nanocellulose PVA film, choose as drying procedure a dry oven at 80 °C for 4 hours. In this work, both drying conditions were tested; then ESEM morphological analysis was performed.

Figure 3.2 shows the cross section of two different films, casted from the same solution. The solution was prepared adding 40 % in weight of 50 µm average size cellulose to a M8630 dissolved film solution. With % in weight of loading, from now on, will be referred to a percentage in weight of the dry polymer (e.g. 30% in weight for 1 g of M8630 film, it means 0.3 g of cellulose particles).

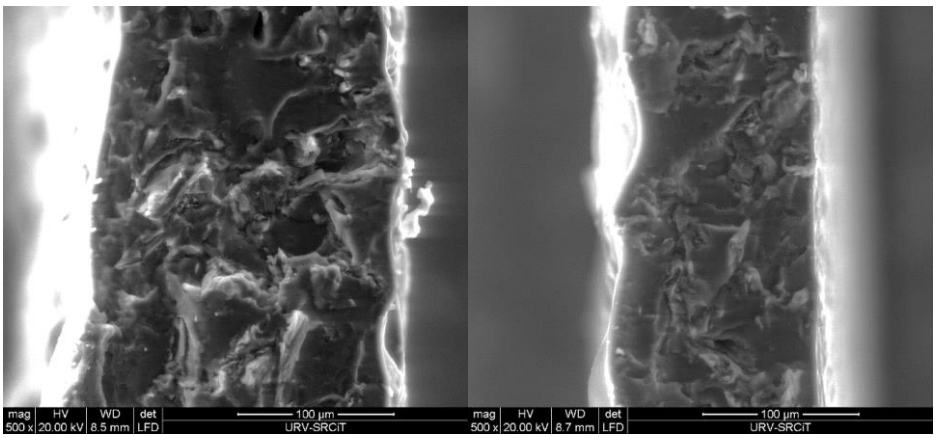

Figure 3.2 ESEM observations: on the left a cross section of a loaded film after 7 days drying at room temperature; on the right a cross section of a film dried in an oven for 4 hours at 80 °C

The cross section of the film was obtained by cooling in liquid nitrogen and cutting the sample in fragile break to prevent deformation of the original microstructure.

The hypothesis assumed for the 7 days drying process, was a sedimentation of the particles to the bottom side of the film; this assumption was disproved by the homogeneity of the cellulose distribution over the whole thickness, displayed in the **Figure 3.2** as the white prominences.

Since no significant differences were observed for the two processes, the evaporation procedure in dry-oven at 80 °C was adopted. As detailed in the *Materials and Methods* chapter, before the oven time, the films are left at room temperature for 1 hour, to start the water evaporation and give the possibility to handle the support avoiding leakage from it that affects the thickness homogeneity.

For the films nomenclature it was chosen a name indicating the two size of micro crystalline cellulose used: MCCa indicates particles with 20 µm average size, meanwhile MCCb was used for 50 µm average sized. A filled film is indicated with the name of particles and the amount in weight percentage of M8630 loading: e.g. MCCa-20% stays for a M8630 film loaded with 20 % in weight of particles with 20 µm average size.

3.2.2 Solubility properties

One of the pillar properties, due to the final application of the new films, is the solubility. This is evaluated with the procedure recommended by the film supplier MonoSol (MSTM 205), [88] described in the previous chapter. Complete dissolution times, reported in seconds, are collected in **Table 3.1** for different films.

Table 3.1 Dissolution times (expressed in second) for different films

Film Name	Thickness [µm]	% in weight of particles loaded	Particles average size [µm]	Complete Dissolution [s]
M8630	76.0 ± 2.1	0	/	60.2 ± 0.2
MCCa-10%	76.1 ± 3.2	10	20	70.5 ± 1.9
MCCa-20%	75.1 ± 3.1	20	20	71.3 ± 2.6
MCCa-30%	76.2 ± 3.0	30	20	76.3 ± 1.4
MCCa-40%	75.5 ± 2.5	40	20	78.1 ± 3.1
MCCb-10%	75.7 ± 2.4	10	50	74.2 ± 1.2
MCCb-20%	76.0 ± 1.9	20	50	75.5 ± 2.4
MCCb-30%	77.1 ± 3.4	30	50	77.3 ± 1.1
MCCb-40%	76.9 ± 3.9	40	50	81.2 ± 2.2

The film thicknesses were chosen to be comparable, since the dissolution time is strongly affected by them. [89] Solubility properties of the new loaded materials are compared to the ones of the pure film coded M8630, supplied from MonoSol and used as received.

The values of **Table 3.1** show an increase in dissolution time for the new films, passing from 60 seconds to 81 seconds for the film loaded with 40 % in weight with 50 µm size particles. These values, even if seem worse than before, are still reasonable for the final function. The longer dissolution times are probably related

to the more obstructed pattern that the water has to cross through the thickness, created by the cellulose particles. [90]

3.2.3 Tensile properties

The mechanical properties of unloaded M8630 and several films loaded with micro-sized cellulose were studied by the tensile test.

Prior to performing the test, all the films were conditioned for 24 hours in a desiccator containing $MgCl_2$ saturated aqueous solution that gives a constant 33% RH at 25°C [91] since the relative humidity of the environment wherein the films are stored, affects several properties of water-soluble films as permeability or tensile properties. [92]

First step was to understand whether the casting process could affect the tensile properties. **Figure 3.3** shows the comparison between a M8630 film from plant and a M8630 film cut in pieces, dissolved and recasted following the same procedure used for the composite film.

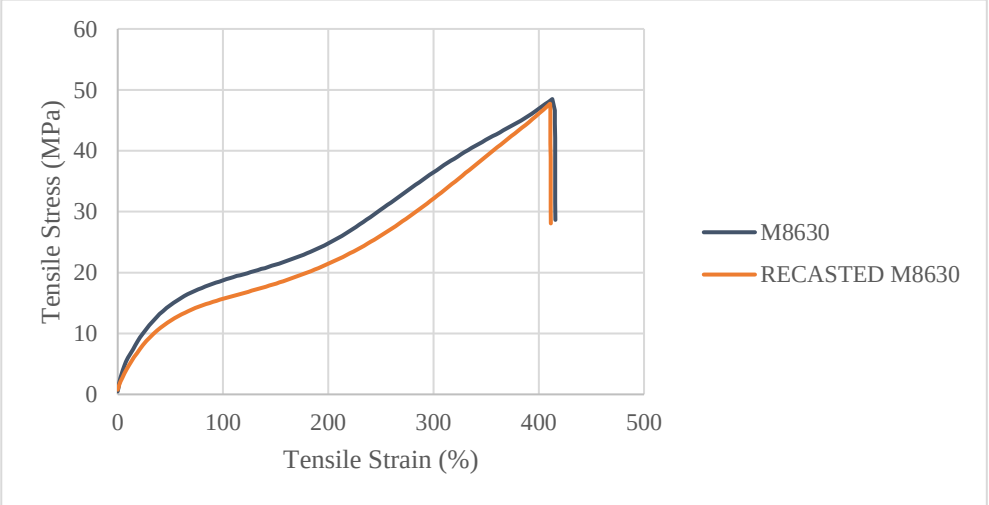

Figure 3.3 Stress-Strain representative curves of M8630 and recasted M8630

The behaviors are comparable, also taking into account that the chart is an average of 5 specimens tested. From this study, non-influence of the casting process on the tensile features of the film has been evidenced.

Once this understood, tests on the various composite films were performed. **Figure 3.4** shows the representative Tensile Stress - Tensile Strain curves of M8630 and filled films.

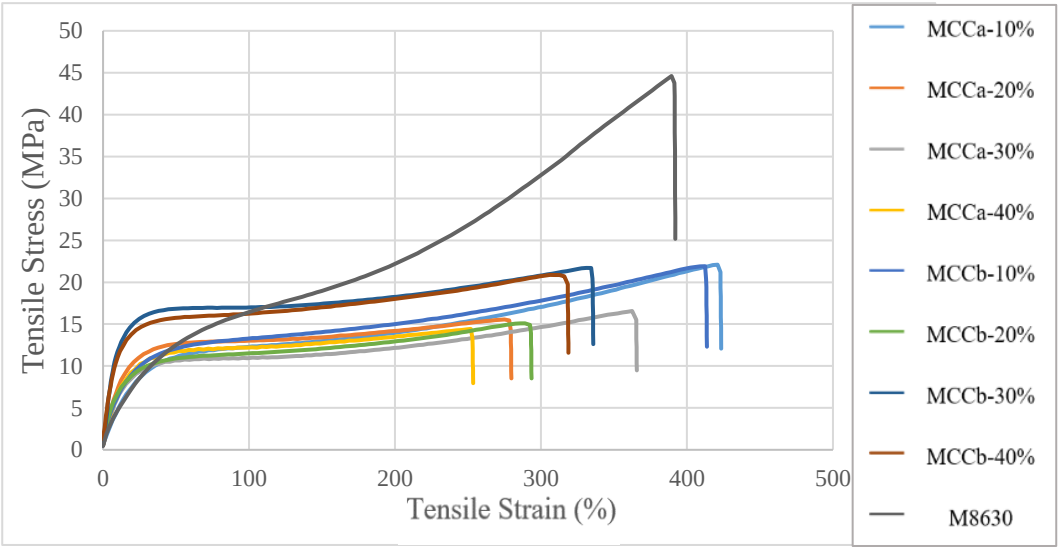

Figure 3.4 Stress-Strain representative curves of M8630 and its composites

It's clear that the addition of micro cellulose particles didn't improve the mechanical properties of M8630, but the loading affected on the mechanical performance. In order to understand more in deep the behavior, **Table 3.2** and **Table 3.3** report the data of the key tensile values. The values of variance from the values, expressed after the sign ±, represent the standard deviation.

Table 3.2 General results of tensile experiments

Film Name	Stress at 5% Strain (MPa)	Stress at 100 % Strain (MPa)	Load at Break (N)
M8630	3.2 ± 0.7	16.6 ± 1.8	90.1 ± 2.4
MCCa-10%	3.0 ± 0.2	12.0 ± 0.4	36.4 ± 0.1
MCCa-20%	4.4 ± 0.3	12.6 ± 0.6	24.6 ± 1.2
MCCa-30%	3.8 ± 0.2	11.1 ± 0.2	32.9 ± 0.3
MCCa-40%	7.3 ± 0.6	11.9 ± 1.1	23.6 ± 1.5
MCCb-10%	4.7 ± 0.6	13.7 ± 0.6	31.9 ± 1.6
MCCb-20%	4.7 ± 1.1	11.5 ± 0.8	29.8 ± 1.1
MCCb-30%	7.5 ± 0.2	16.8 ± 0.3	47.2 ±0.7
MCCb-40%	7.0 ± 0.7	15.8 ± 0.7	37.6 ± 2.5

Table 3.3 Results of tensile test at break

Film Name	Tensile Strain at Break (%)	Tensile Stress at Maximum Load (MPa)	Tensile Extension at Maximum Load (mm)
M8630	416 ± 3	47.4 ± 1.2	101.6 ± 2.4
MCCa-10%	417 ± 4	22.1 ± 0.1	105.5 ± 0.2
MCCa-20%	265 ± 9	15.0 ± 0.8	66.3 ± 4.6
MCCa-30%	353 ± 13	16.5 ± 0.2	89.5 ± 1.5
MCCa-40%	252 ± 4	12.8 ± 0.9	63.0 ± 0.3
MCCb-10%	397 ± 22	22.1 ± 0.3	98.3 ± 6.8
MCCb-20%	292 ± 6	15.1 ± 0.9	71.4 ± 2.2
MCCb-30%	327 ± 9	21.5 ± 0.3	82.3 ± 0.9
MCCb-40%	312 ± 6	20.1 ± 1.1	76.5 ± 0.1

Table 3.2 underlines noticeable differences in terms of *Load at Break* reached during the experiment. On the other hand, **Table 3.3** shows and confirms what is it possible to see from the comparison chart (**Figure 3.4**): microcomposite films seem less ductile compared to pure M8630. Another result clear from the chart and confirmed in values at **Table 3.3**, is the marked reduction of *Tensile Stress at Maximum Load* from around 47 MPa to around 15- 20 MPa. No linear correspondence between loading percentage and decline of the tensile properties is observed but, in general, load polymers show lower tensile values.

3.2.4 Water vapor permeability studies

Barrier performance of M8630 and its composites was studied by the water vapor permeability (WVP). WVP measures the rate at which water vapor permeates through a film of a specific thickness at a specified temperature and relative humidity (%RH).

In **Section 2.2.6** the WVP experiment was discussed in deep. As done for tensile properties, excluding the casting process influence on the films behavior was the first step.

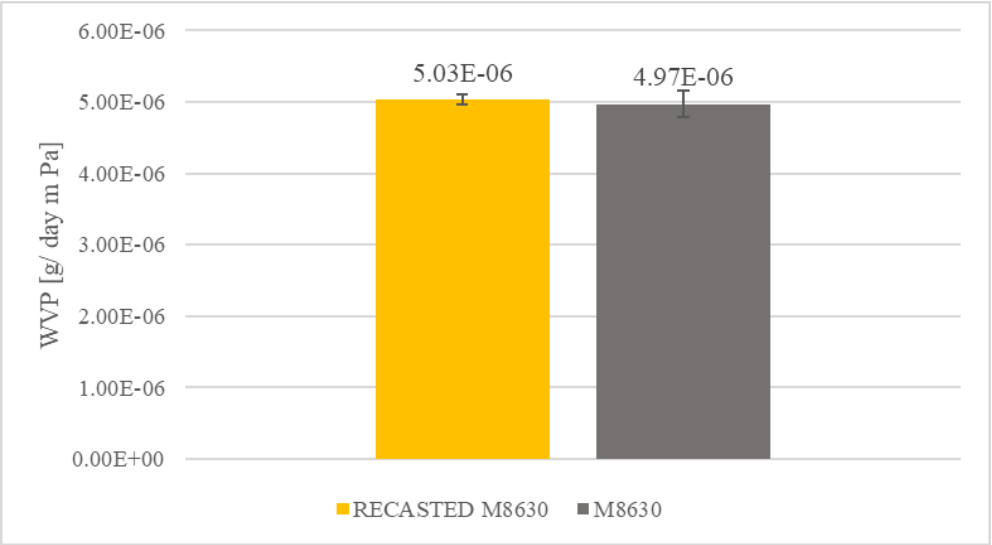

Figure 3.5 WVP chart for virgin M8630 film supplied by plant and same film recasted

The values reported in **Figure 3.5** demonstrate zero impact of the recasting procedure on the M8630 film for WVP: the values are average of three experiments ran with different films and, considering the standard deviation expressed by the bar, the data are strongly comparable. Therefore, as for tensile properties, dissolving the M8630 film and casting it again, doesn't affect the feature.

As shown in **Figure 3.6**, increasing particles average size and filler percentage, both reduce the permeability to water passing from a mean value of $4.97 \cdot 10^{-6}$ g/Pa m day for M8630 film to a $3.08 \cdot 10^{-6}$ g/Pa m day for a composite loaded with 40 % weight and with average size of the particles of 50 µm.

Overall, the barrier for water vapor for the composite films, increases up to about 1.6 times, compared to the virgin film obtained from the plant.

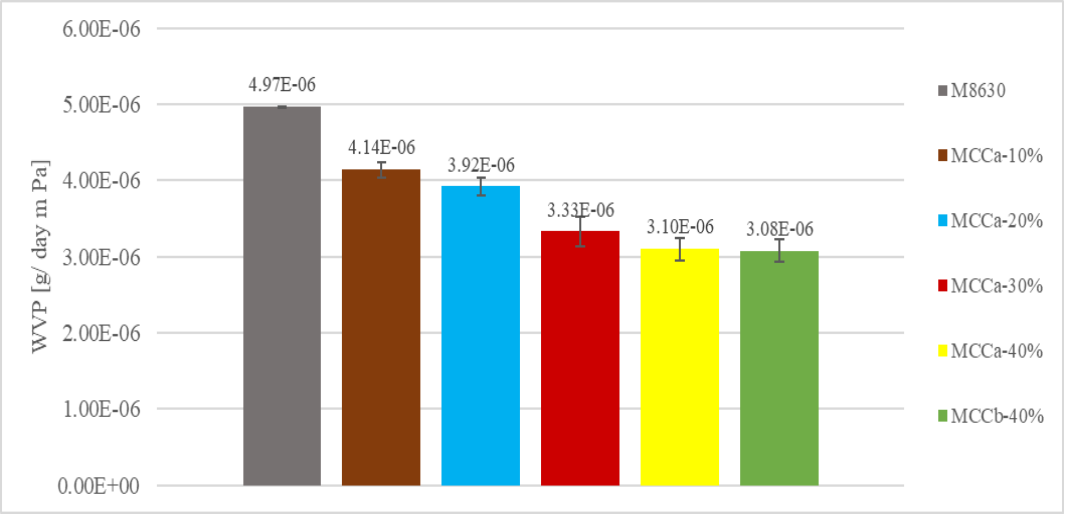

Figure 3.6 WVP chart for M8630 film and its micro composites loaded with cellulose particles

In the **Section 1.2.3** (Introduction Chapter) a simple model for permeability in filled polymers was discussed. Its final *equation 1.3* which describes permeability for a simplified system loaded with rectangular shape fillers is reported here again:

$$\frac{P_F}{P_u} = \frac{\phi_U}{1+\frac{L}{2W}\phi_F} \qquad (3.1)$$

Where P_F and P_u are the permeabilities of the respectively filled and unfilled polymer respectively and ϕ_u is the volume fraction of the unfilled polymer.

This equation includes the tortuosity factor τ as dependent on length (L), width (W) and volume fraction of the filler particles (ϕ_F):

$$\tau = 1 + \frac{L}{2W}\phi_F \qquad (3.2)$$

This model makes the key assumption that the fillers are placed such that the sheet normal is coincident with the direction of

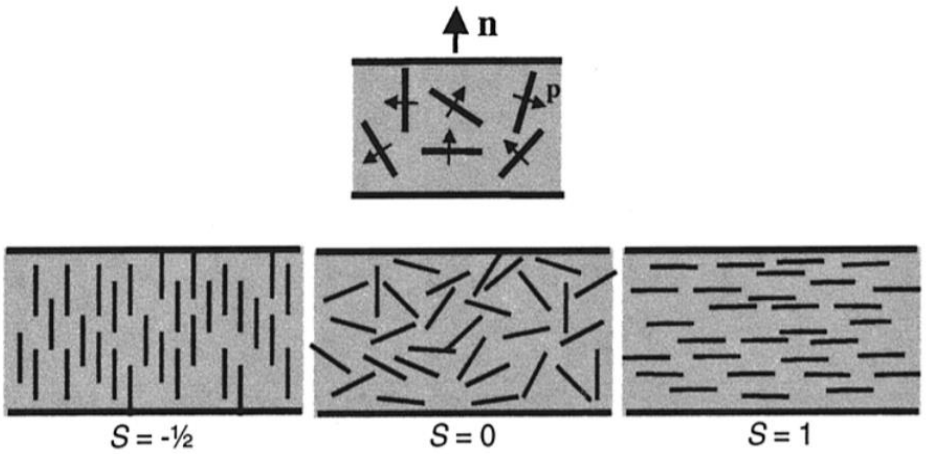

*Figure 3.7 Examples of several orientations of the sheets (**p**) with respect to each other and the preferred orientation (**n**),normal to the film plane*

The two extremes, planar and orthogonal alignment of the sheets, may be treated by simply interchanging L and W in *equation 3.2*. However, considering that a range of orientations is possible, it would be more instructive to modify *equation 3.2* to consider the dependence of the tortuosity factor on the orientational order of the fillers in a continuous manner. An order parameter *S* was

introduced by Bharadwaj [32] which includes the orientation effect for rectangular shaped fillers, and defined as

$$S = \frac{1}{2} < 3cos^2\theta - 1 > \quad (3.3)$$

where θ represents the angle between the direction of preferred orientation (**n**) and the filler normal (**p**), vectors shown in **Figure 3.7**. This parameter can range from 1 (θ=0), indicating parallel orientation of the fillers with the film plane, to $-\frac{1}{2}$ ($\theta = \frac{\pi}{2}$), meaning a perpendicular orientation, passing by the value of S=0 for random orientation of the particles. In this way, the tortuosity factor τ is modified to include the new orientational parameter and the *equation 3.1* of permeability, becomes:

$$\frac{P_F}{P_u} = \frac{\phi_U}{1+\frac{L}{2W}\phi_F\left(\frac{2}{3}\right)\left(S+\frac{1}{2}\right)} \quad (3.4)$$

The above formula reduces to a planar arrangement with S=1, meanwhile with $S = -\frac{1}{2}$ the equation converges to a pure polymer value.

Before starting the modeling, the assumption of comparable density between the polymer and the filler has to be done, hence the volume fractions ϕ correspond to the weight portion percentage in the composite material.

To evaluate which parameter S fits and so estimate the actual particles orientation, least squares approach to find the optimal S value in the model was used.

The **Figure 3.8** shows the experimental data of WVP and the model values for MCCa composites, charted versus the percentage of loading : the parallel (S=1) and normal (S=0) orientations and the random particles distribution are represented.

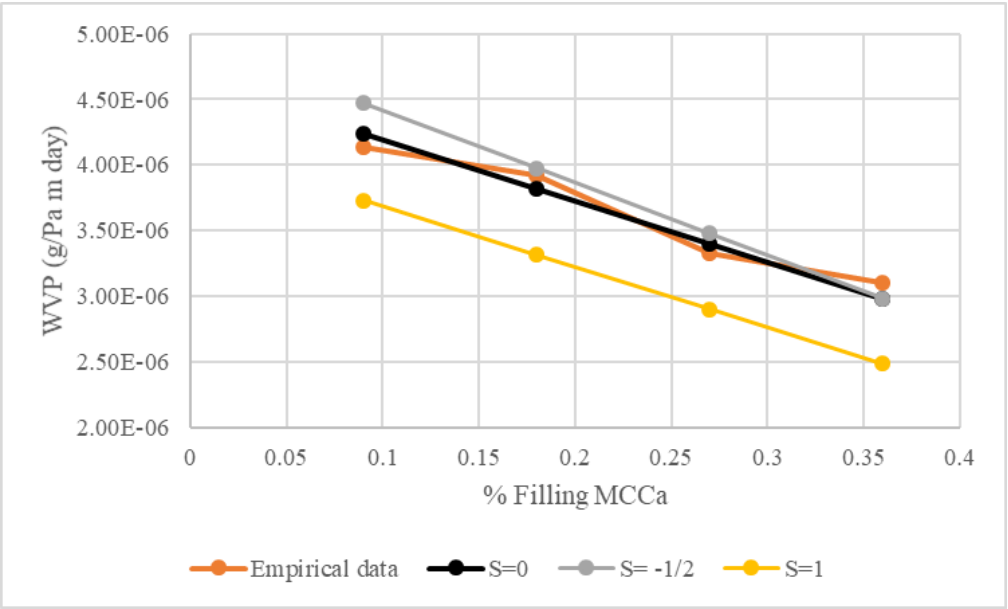

Figure 3.8 Fitting of experimental data versus different S values for composite loaded with MCCa particles

In agreement with least squares analysis, the value which better fits the measured data is S=0, which is a confirmation of random particles disposition of the theory in Bharadwaj adjusted model.

[32] Once established this, we can claim a total random distribution of the micro-sized particles.

With these assumptions the *equation 3.4* can be written in an alternate form:

$$P_F = \frac{6\phi_U P_u W}{\phi_F L + 6W} \qquad (3.5)$$

An example of calculation for a 10% in weight loaded with 20 µm average size composite is reported.

Taking the following values $P_u = 4.97 \cdot 10^{-06}$ g/(Pa m day); $\phi u = 0.91$; $\phi_F = 0.09$; $W = 5\ \mu m$; $L = 20\ \mu m$. the *equation 3.5* becomes:

$$P_F[\,20\ \mu m\ 10\%] = \frac{6\phi_U P_u W}{\phi_F L + 6W} = \frac{6*0.91*4.97*10^{-06}*5}{0.09*20+6*5} =$$

$$=4.24\cdot10^{-06}\frac{g}{Pa\ m\ day}$$

In this way, all the predicted values according the model were obtained and compared to the experimental ones (**Table 3.4** – where Δ(%) indicates the percentage variation between the empirical values and the predicted ones).

Table 3.4 Comparison between measured and predicted WVP data

Film Name	ϕu	ϕ_F	L (µm)	W (µm)	Empirical WVP · 10^{06} [g/(Pa m day)]	Model (S=0) WVP · 10^{06} [g/(Pa m day)]	Δ (%)
MCCa-10%	0.91	0.09	20	5	4.14	4.24	2 %
MCCa-20%	0.82	0.18	20	5	3.92	3.82	2 %
MCCa-30%	0.73	0.27	20	5	3.33	3.40	2 %
MCCa-40%	0.64	0.36	20	5	3.10	2.98	3 %
MCCb-40%	0.64	0.36	50	10	3.08	2.93	5 %

As can be seen, the model introduced by Nielsen and then updated for random fillers orientation by Bharadwaj has a good agreement with the permeation values obtained. The maximum difference detected is about 5 % for the MCCb-40%, composite loaded with 50 µm cellulose particles.

Overall the model works and the deviation from the empirical values measured is not huge, also taking into account the approximation done on the cellulose size: the particles were considered as regular shape with 20 x 5 µm size or 50 x 10 µm, meanwhile these can be just averaging of the actual dimension.

3.3 Conclusions

In this chapter composites of micro sized cellulose particles and M8630, a film supplied by MonoSol widely used in laundry pods application, were prepared and studied. The choice to start to modify this film is associated to the deep knowledge on the film in terms of dissolution, tensile and barrier properties. In fact, the three pillar features for the soluble unit dose application were studied: dissolution time, tensile properties and water vapor permeability (WVP).

The dissolution times measured were slightly affected by the loading passing from about 60 seconds to a range of 70-80 seconds, meanwhile the mechanical performance, of the loaded films, dropped significantly in comparison with virgin M8630 film, taking into account the final application for laundry pouches.

The most important feature studied was the water vapor permeability. The theoretical model proposed by Nielsen and generalized by Bhardwaj, predicts values with low deviation from the empirical data, up to 5 % for MCCb-40%, composite. The least squares analysis applied to the model, confirms a random orientation for micro sized crystalline cellulose particles.

The data from the WVP experiments, reveal a decreasing of the film permeability up to 1.6 times for the 40 % in weight loading: the modification, even if it seems to work, it didn’t give decreases desired.

Overall, filling the M8630 film with micro-sized cellulose, doesn't change the features as scheduled, and for the reasons discussed previously, the microcomposite study was set aside for new types of modification.

4. Preparation and Characterization of M8630 or Olympus based blended films

4.1 Introduction

The second modification choice for this work was the blending of current PVA used in laundry application from Procter & Gamble with a different kind of PVA branded by Nippon Gohsei with the name of Nichigo G-Polymer®. In the general introduction, an overview on the benefits of this new material was done.

The supplier itself and several patents of inventions that use this material, [63-65] claim a biodegradability, high water solubility and above all a very high barrier to gas features: Nippon Gohsei declares even a 30 times better oxygen barrier compared to ethylene and vinyl alcohol copolymer (EVOH).

The Nichigo G-Polymer or G-Polymer, as called from now on in this work, is a copolymer of butenediol and vinyl alcohol (BVOH). A copolymer is a polymer formed by two or more types of monomeric repeating units.

On the other hand, the PVAs used were M8630, described in the previous chapter, and the film coded PXP20655 and named internally from Procter & Gamble `*Olympus*`. The latest film is a blend itself of a homopolymer and an anionically polymerized copolymer of PVA: it is not still branded by MonoSol and has higher water solubility than its predecessor M8630. As indicated in the previous chapter, M8630 is a mixture of PVA, chitosan and other components (i.e. glycerol).

The choice of modifying two kind of films used by Procter & Gamble was based on the differences in the two materials: understanding whether blending with G-Polymer is affecting one film more than the other, could help to understand on the chemical differences among the three types of materials.

For the both blends (M8630 blended with G-Polymer and *Olympus* blended with G-Polymer) the target thickness was 76 ± 4 μm, since this value is the one of M8630 and Olympus film supplied.

In this chapter the three key properties of the films for soluble unit dose were studied: solubility, tensile stress and barrier properties. Moreover, solvent compatibility, thermal features and studies on complete pouch were performed.

All the experimental data obtained were compared with those obtained from no blended films from manufacturing scale to figure out how the blending affects the most important properties of the films.

4.2 Results and Discussion

4.2.1 Film preparation and characterization

Once optimized the film casting procedure for the M8630 composites, the same process was applied for the blended materials. Therefore the polymer is dissolved in water and forms a solution with a certain concentration and viscosity; the second water-soluble polymer is loaded in the heated (80 °C) and stirred system; after 3 hours, the viscous mixture is poured on a glass support and spread across it manually with a casting knife set at different gaps. So, the wet film is left to stand to evaporate the solvent and leave a dry film. Clearly the main difference was the type of material added to the PVA water solution (in this case M8630 or *Olympus*). No experiments on the drying procedure effect on the film were ran, but ESEM morphological analysis on the blended film cross section were run, to observe the compatibility of the polymers. **Figure 4.1** shows the cross section of two different film: on the left side a cross section of pure M8630 film is shown, meanwhile on the right a cross section of a blended film with 70 % in weight of M8630 and 30 % in weight of G-Polymer is displayed.

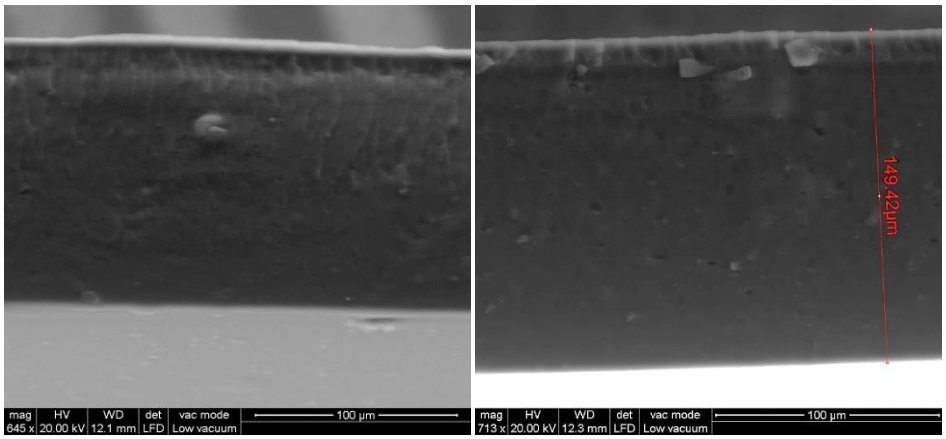

Figure 4.1 On the left a cross section of a M8630 film; on the right a cross section of a M8630 blended with G-Polymer, with a composition 70 % in wt. of M8630 and 30 % in wt. of G-Polymer

From this figure it is clear that no phase separation between the two polymeric components is evidenced. This result will be also confirmed by thermal analysis. As described in previous chapter, the cross sections of the films were obtained by fast cooling in liquid nitrogen and cutting the samples to have a fragile break to avoid structure deformations.

From now on the nomenclature of these films will follow the one just described: the first percentage will be the amount of M8630 or Olympus, meanwhile the second value will be the quantity of G-Polymer.

4.2.2 Thermal properties

For the film processing purpose of the final films application, a thermal analysis was performed on the pure films and blends. Even if the G-Polymer is part of the PVA family, differential scanning calorimetry (DSC) analysis was run to understand also the miscibility of the components and if and how the blending could affect the thermal performance: for this scope the thermal features have to be compared with those of virgin films. The 2nd heating curves of the materials are shown in the following Figures.

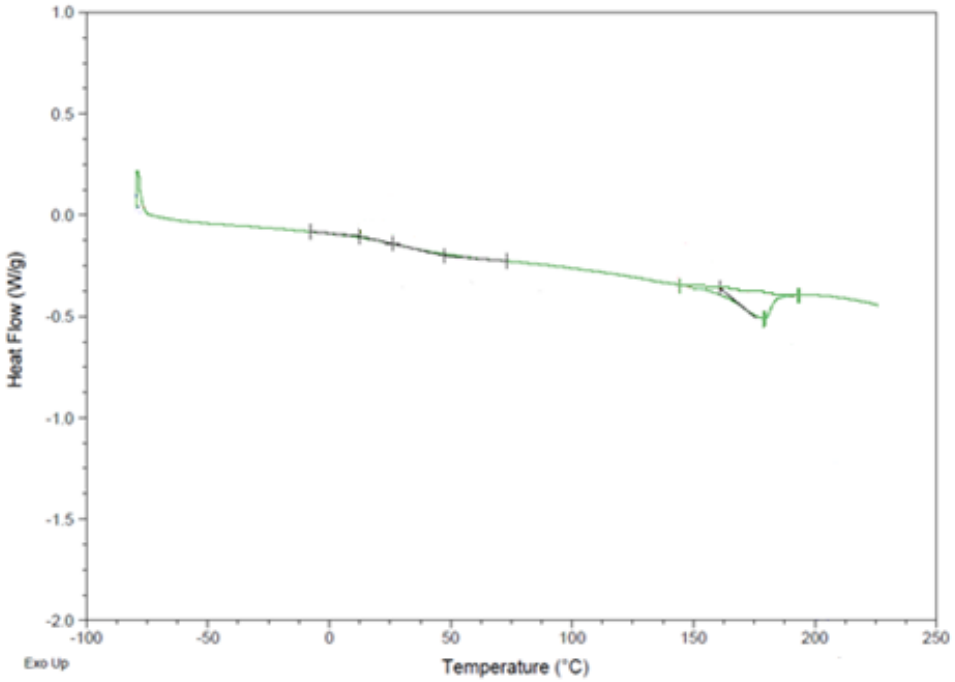

Figure 4.2 2nd heating DSC curve for virgin M8630 (exo up)

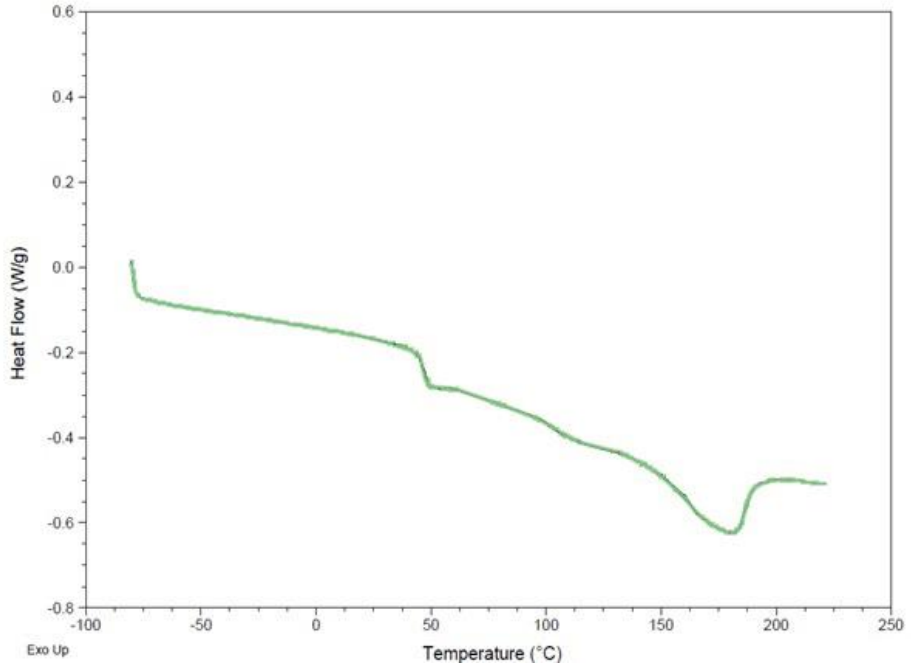

Figure 4.3 2nd heating DSC curve for virgin G-Polymer (exo up)

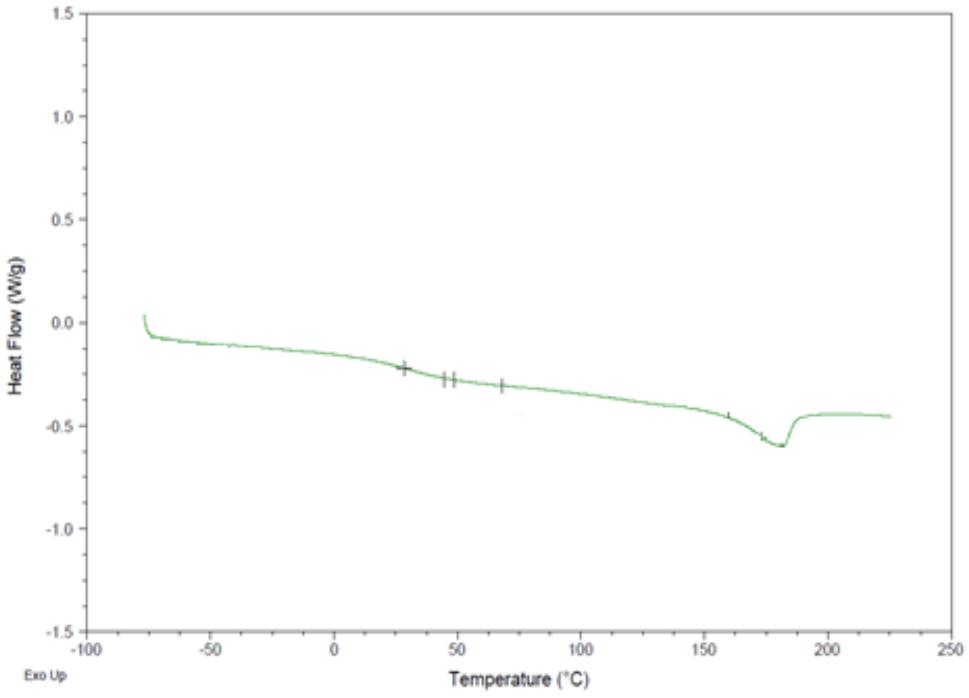

Figure 4.4 2nd heating DSC curve for a sample 75 % in wt. of M8630 and 25 % in wt. of G-Polymer (exo up)

The thermal characteristics of the components and the blended films reported in **Table 4.1** were determined from the second heating scans, since the first ones were excluded because they contained latent heat of water absorbed in the samples.

Table 4.1 Thermal properties obtained by DSC for virgin G-Polymer and M8630 and their blended films

Sample Name	Tg (°C)	Tm (°C)	ΔH^0 Melting enthalpy (J/g)
G-Polymer	46/102	169	24
M8630/ G-Polymer (60:40)	40	188	18
M8630/G-Polymer (65:35)	34	185	18
M8630/G-Polymer (70:30)	29	182	20
M8630/G-Polymer (75:25)	28	184	17
M8630	26	179	13

The G-Polymer itself, showed a double Tg (40 °C and 100 °C), due its composition as block copolymer. In despite of this, the blends only showed one Tg, indicating good compatibility of all the components.

The glass transition temperature (Tg) is observed to increase from 26 °C of M8630 up to 40 °C for the blended film containing 40% of G-Polymer. In general terms, melting temperature (Tm) also increase as the G-Polymer percentage grows up from 0% to 40 %. Overall little differences between the blended and no blended samples are observed, but the M8630 is most likely responsible

for most thermal events. The Tg also shift higher in the second heating scan with respect to the first because of evaporation of the plasticizer (mostly water).

Another point to underline with the thermal analysis, is the clue of a perfect miscibility of different kind of PVA used (M8630 and G-Polymer), confirming what it was seen in morphological experiment (**Figure 4.1**): if the two polymers were immiscible, the DSC curves would show more than one glass temperature transition; in this study a single common Tg is obtained for the polymer blend, meaning that the initial polymers are completely miscible. [93]

4.2.3 Solubility properties

The G-Polymer is claimed to have a higher barrier property compared to other PVAs: does this barrier affect in some way the dissolution of the film? In works like the one of Limpan *et al*, [94] the water vapor permeability and solubility of several types of Poly(vinyl alcohol) were studied: the results showed an inversely proportional behavior, so a higher barrier to the water vapor means lower solubility.

Accordingly to this result, the solubility study was fundamental for the blends of M8630 and *Olympus* with G-Polymer, taking into

account of the final application of soluble pouches containing detergent.

As done in the previous chapter, the method called Slide Dissolution test from the film supplier MonoSol (MSTM 205) was used for the measurement. [88]

In **Figure 4.5** are charted the performances of M8630 and *Olympus* virgin films and blended ones versus the percentage of G-Polymer. Two values are graphed for the 0 % of G- Polymer: the symbols ● mean films which were dissolved and casted again (called *recasted*) accordingly to the procedure described in **Section 2.2.1**, while Δ icons represent the values for the no modified film from the plant (*virgin*).

The experiments on the films, that will be called recasted, were ran to verify the eventual role of the casting process on the film, in terms of loss of plasticizer and/or water for example. Moreover the standard deviations of the repetitions ran are reported in a bar for each mean value.

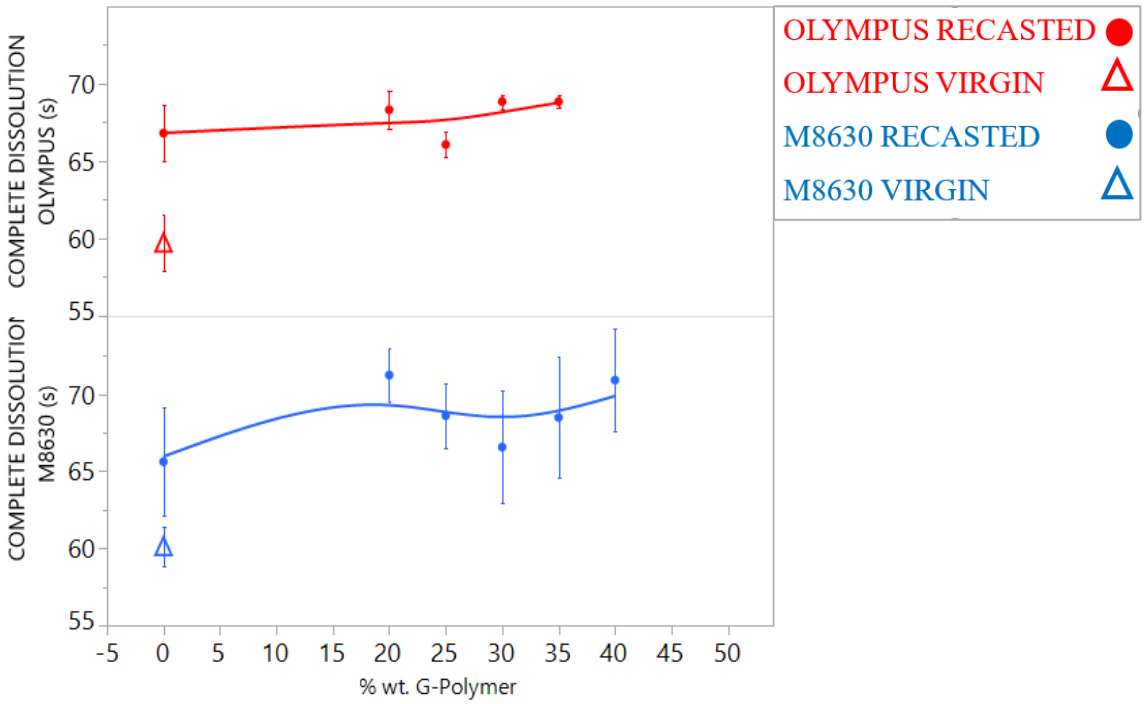

Figure 4.5 Trends of complete dissolution times (s) for Olympus and M8630 blends versus the percentage in weight of G-Polymer of the sample: Δ indicates values for virgin film from the plant, meanwhile the value in seconds at 0 % in weight (●) is the same material but dissolved and recasted according to the casting procedure

The thicknesses of all the samples were comparable in the range of 76 ± 3.0 µm, as the dissolution time depends on it. [87]

There is a visible slight change in the dissolution time from *recasted* films compared to *virgin* films, but in terms of seconds, the deviation is no relevant.

The higher gap observed between a *recasted* film and a blended one, is about 5 seconds for 60 % in weight of M8630 – 40 % in

weight of G-Polymer. On the other hand the discrepancy of the *Olympus recasted* with the blended films touches about 3 seconds.

Taking into account the setup of the test, where the operator has to time the film break manually when by eyes sees it, the results are repetitive, since the error can be higher for this kind of experiment.

Globally the results are even better than the expectations and satisfy the purpose, that is to have similar solubility data for nowadays used film and new blended materials.

4.2.4 Compatibility of film/detergent system

In the **General Introduction Chapter**, the G-Polymer, a butenediol-vinyl alcohol copolymer, was broadly described: even if it is part of the PVA family, looking at the soluble unit dose final application, a study of its compatibility with used detergent and the solvents content in, it`s essential for the blended films. In the **Figure 4.6** are reported the results of gravimetric experiments explained in **Section 2.2.6**. Samples for each material were left 3 days in detergent as its major components Glycerol, Propylene glycol (expressed in the chart as P-diol) and Dipropylene glycol (DPG in the legend). The purpose of the test is to verify the compatibility between the new films and the detergent components. The actual goal is having similar behavior to M8630 and *Olympus* films.

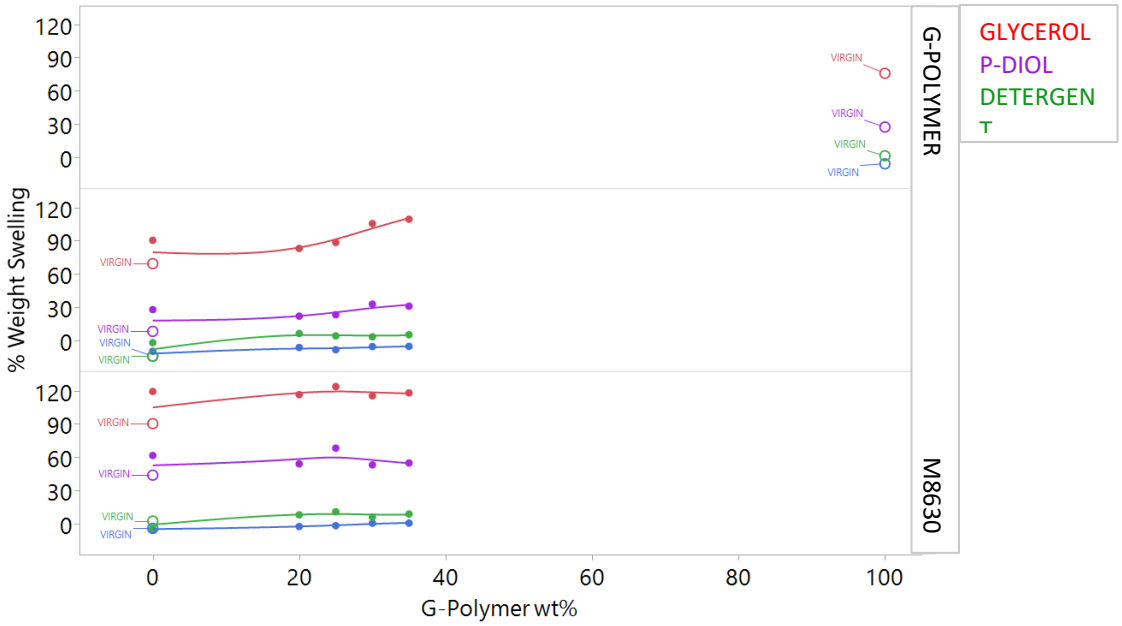

Figure 4.6 Trends of gravimetric swelling for virgin and blended films: the ○ represents virgin film from plant for M8630 and Olympus (0% on X-axis) and a film casted just from G-Polymer solution (100% on X-axis)

In the **Figure 4.6** on the right axis are labeled the 3 primary polymers G-Polymer, M8630 and *Olympus*, while on the X-axis the percentages of G-Polymer in the sample are reported; the actual values of gravimetric swelling also in percentage are on the Y-axis.

It`s easy to observe very similar performances between the *virgin Olympus* and M8630 (indicated by ○) and the blended films: the results underline a bigger swelling in glycerol (higher values on chart) for all the specimens and, above all, a complete compatibility of new materials with detergent. Also discrepancies important discrepancies between the 3 kind of virgin films were

observed, obviously due to the differences on the film compositions.

4.2.5 Tensile properties

In this section, tensile features of M8630, *Olympus* and their blends with G-Polymer are studied. This is so, because the mechanical characteristics have a key role during the pouches thermo-forming.

Same test procedure utilized for the micro-composites films of the previous chapter was applied for these films: 5 specimens for each sample were pre-conditionated for 24 hours in a 33% RH at 25°C environment generated by a magnesium chloride saturated water solution in a desiccant, since the relative humidity strongly affects a lot the performance of water soluble films and the pre-conditioning is crucial. [92]

First step was to study the possible changes of the *Olympus* film properties after the casting process, as well as it was done in previous chapter for M8630 (**Section 3.2.3**).

In **Figure 4.7** the Tensile Stress – Tensile Strain curves of *Olympus* from plant and recasted are reported.

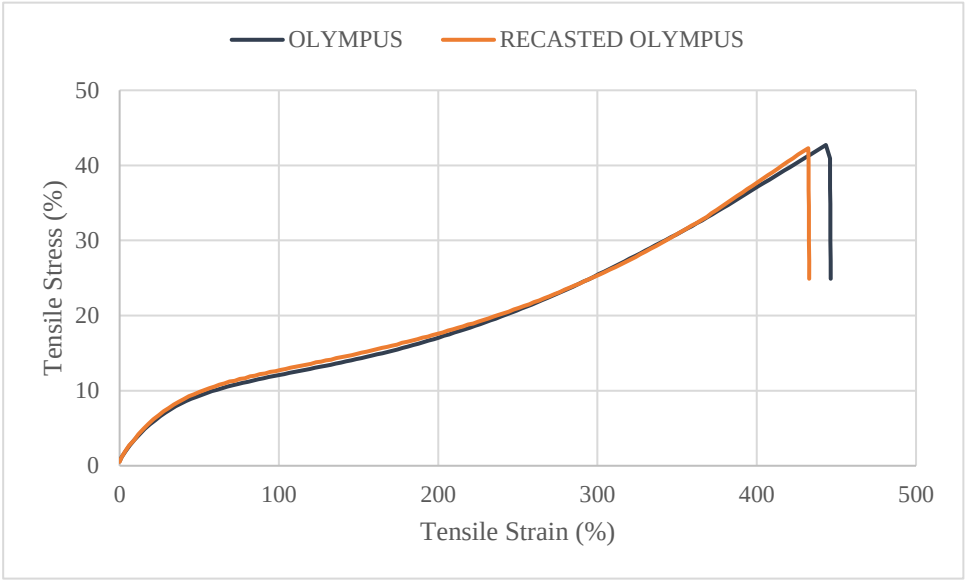

Figure 4.7 Stress-Strain representative curves of virgin Olympus film and recasted Olympus film

The trends are clearly comparable, as observed also for M8630, considering that the curves are averages of 5 specimens per material: these studies confirm that recasting the *Olympus* film doesn't affect the tensile features, as well as verified for M8630 film in previous chapter.

Once established no changes in the mechanical features after the casting process, the following charts will display the trends of the blended films.

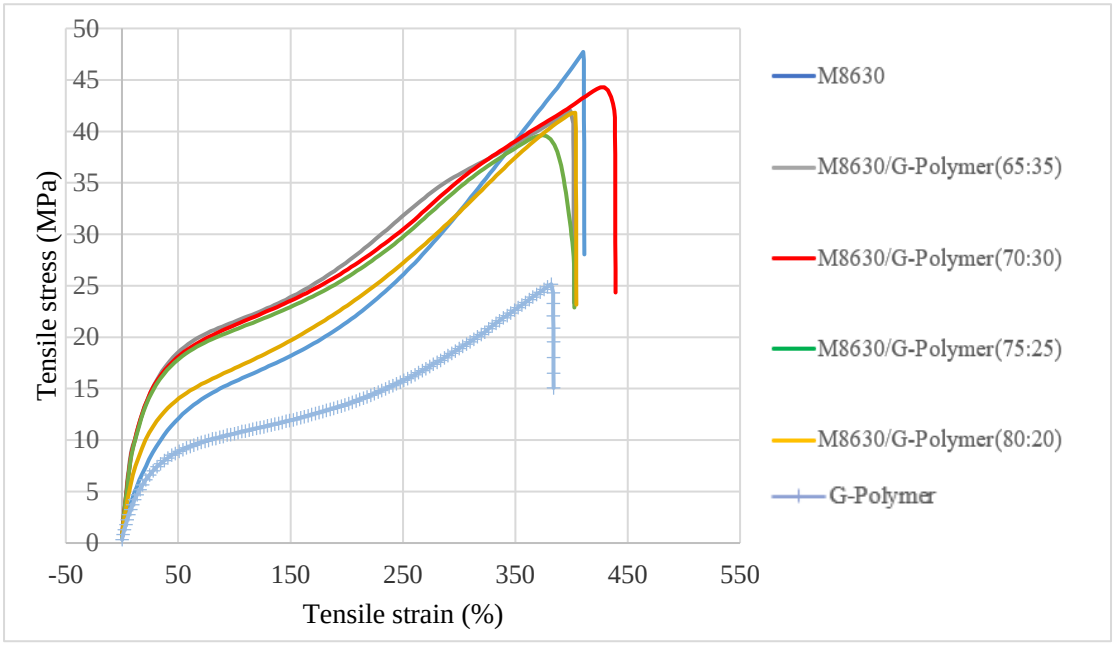

Figure 4.8 Stress-Strain representative curves of virgin M8630, G-Polymer and M8630 blended films with several percentage of G-Polymer

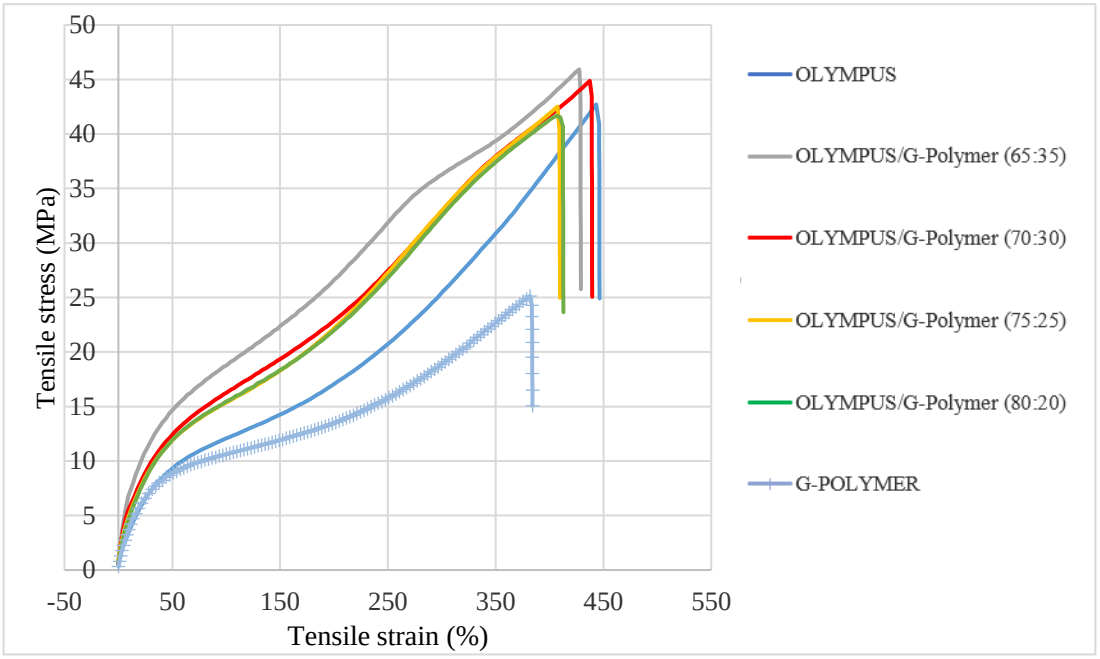

Figure 4.9 Stress-Strain representative curves of virgin Olympus, G-Polymer and Olympus blended films with several percentage of G-Polymer

In **Figure 4.8** and **Figure 4.9** the stress-strain curves of M8630 and *Olympus* themselves and their blends with G-Polymer in several percentage are represented. In terms of global behavior, no important deviations of tensile properties are observed, meanwhile the pure G-Polymer shows lower properties than virgin and blended films. Since the tension features of the blended films are close to *virgin* films, probably some morphological interaction between the polymers took act. [95]

To confirm the similar performances of the *virgin* film with blended ones, key values as *Maximum Load* (expressed in Newton) and Stress at 100 % strain (MPa) are reported in **Figure 4.10**: they are plot versus the G-Polymer percentage in the blend.

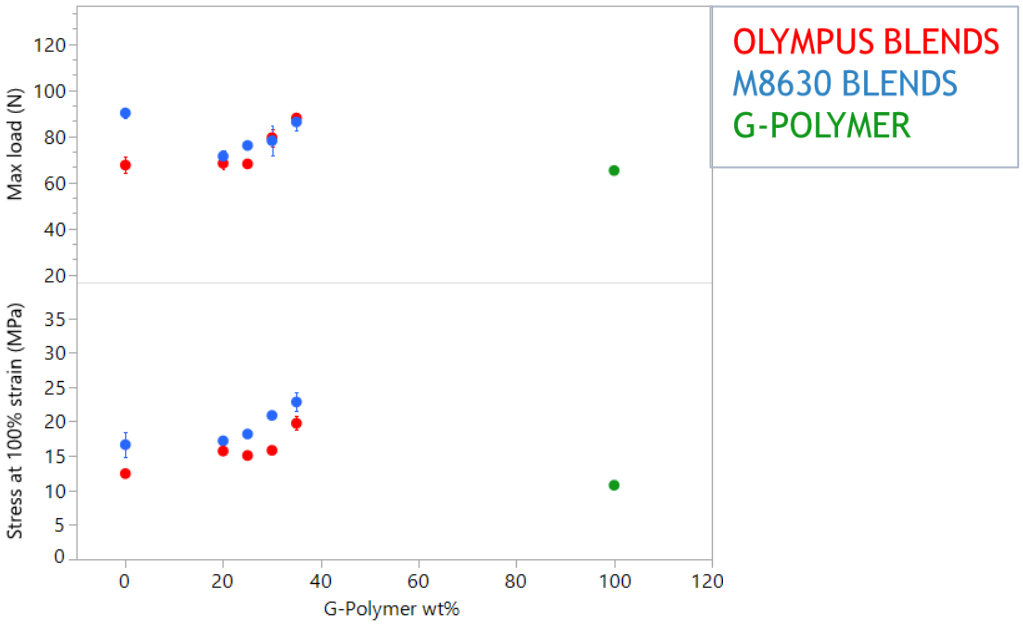

Figure 4.10 Tensile properties overview for Olympus, M8630 and their blends

For 0 % values, we are referring to the *virgin* M8630 and *Olympus* films, while the 100 % indicates a pure G-Polymer casted film.

The aim of the last chart is to underline the limited deviation of mechanical properties of the films, comparing and evaluating key tensile characteristics.

The *Maximum Load* or tensile strength is related with the higher value of energy applied to the material before the break and with blended materials the range of values goes from 70 N to 84 N versus a range of 69-88 N for *virgin* films; the contrast with the range 26-40 Newton for microcomposite with cellulose is evident.

On the other hand, *Stress at 100% strain* is a common parameter considered for film used in water-soluble laundry bags: this datum is the stress needed to apply to the specimen to duplicate the length between the Instron® equipment clamps.

It is important that the values of this parameter for virgin and blended films were comparable, since the first deformation is crucial for the pouch forming: from tensile tests ran on blended films, we have a range 14-20 Mega Pascal, while the virgin films have 12-16 MPa range.

Since the goal was to not weaken the film, tensile experiments gave us satisfactory results.

An additional tensile test ran on films was described in **Section 2.2.5**: we will refer to it as *Immersion Test*. The purpose of this

mechanical test is to study the shift in film properties when brought into contact with a cleaning liquid: it leads to the effect of solvents contained in the detergent like glycerine and water on the film, and it simulates the finished pouches conditions.

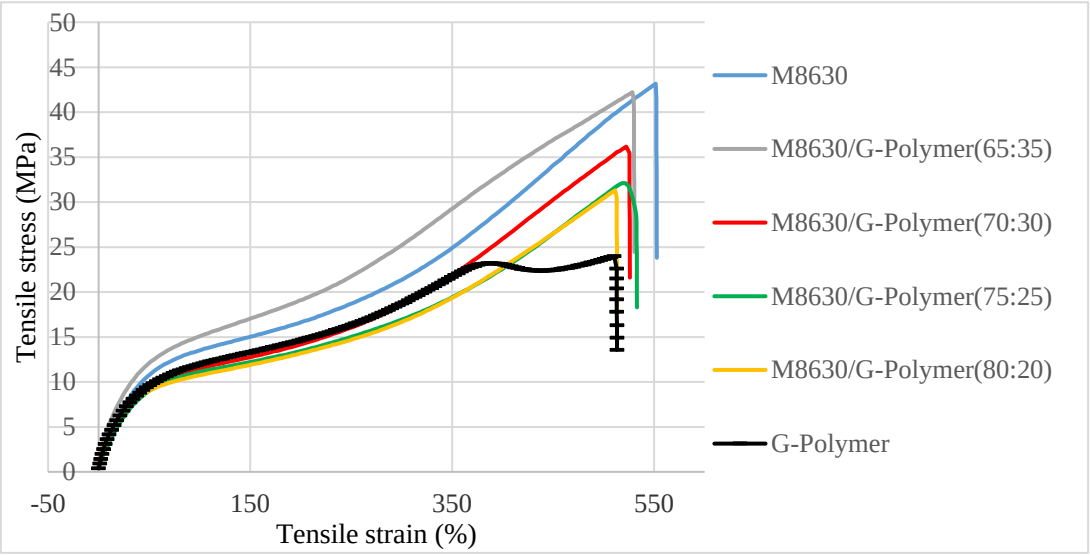

Figure 4.11 Stress-Strain curves of virgin M8630 and its blended films after Immersion procedure

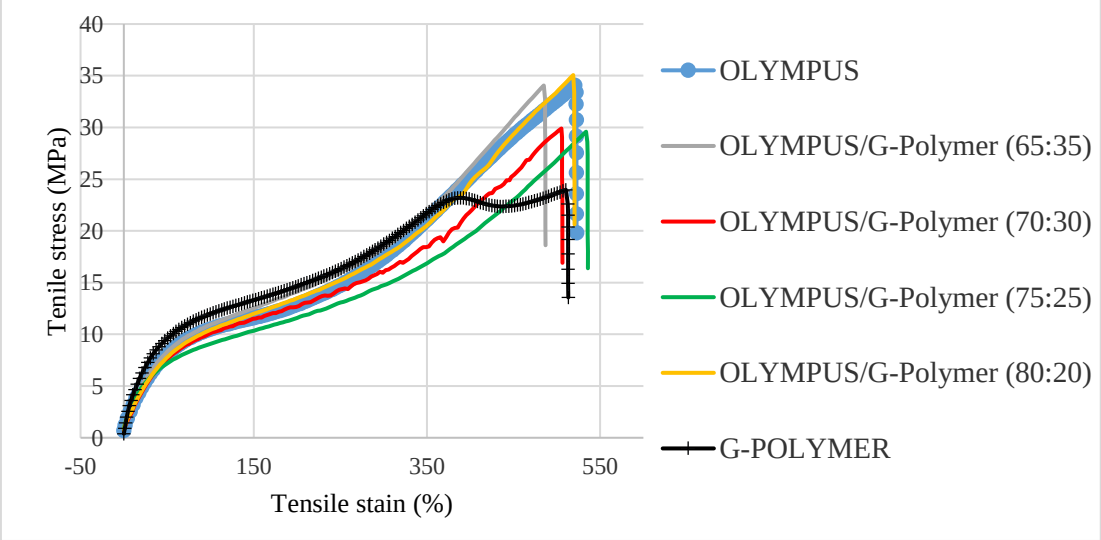

Figure 4.12 Stress-Strain curves of virgin Olympus and its blended films after Immersion

The **Figure 4.11** and **Figure 4.12** chart the tensile trends of the films after the *Immersion* procedure. The most important results we can observe from these charts are the comparable behaviors of *virgin* films and the blended ones: the mixing and casting with G-Polymer is not affecting in important manner the processability of the films, as the loading with particles did (**Chapter 3**).

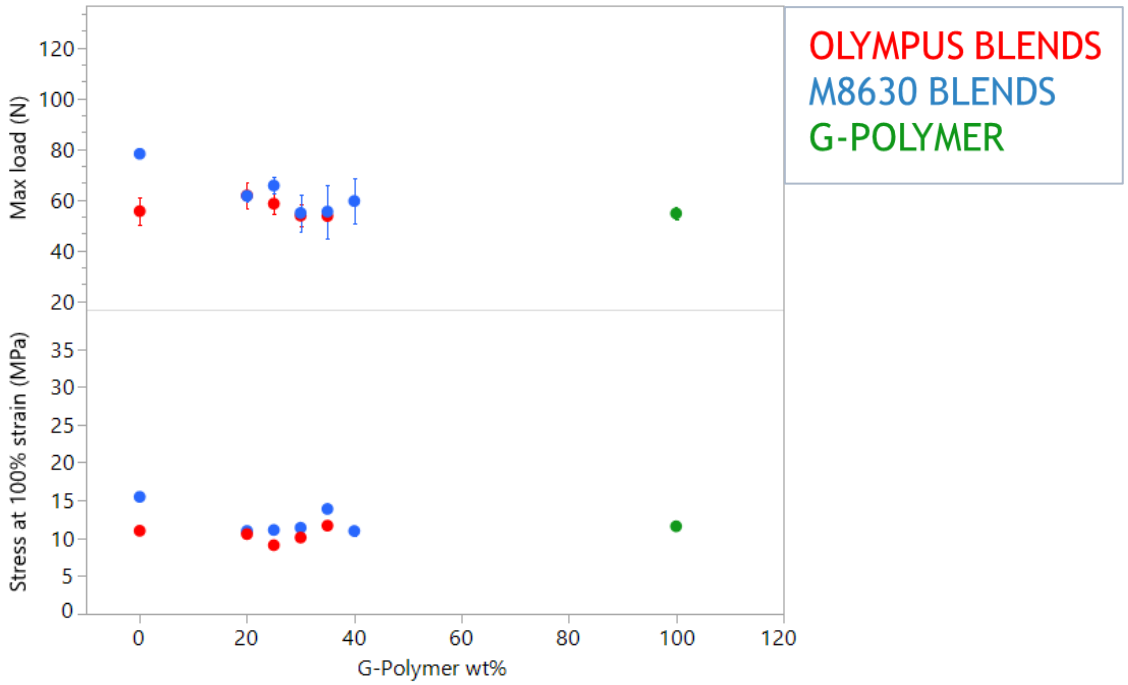

Figure 4.13 Tensile properties overview for Olympus, M8630 and their blends after Immersion procedure: 5 days in detergent and 24 hours at room temperature

As done for the tensile properties of films before the *immersion* procedure, the *Maximum Load* (N) and *Stress at 100 % strain*

(MPa) of the *virgin* films and their blends with G-Polymer are reported in **Figure 4.13**.

The results showed a very small dispersion. The *Maximum Load* for *Olympus* blends varies between 52 N to 61 N meanwhile the *virgin* film has an average of 55 ± 5 N range; for the M8630 blends the values range is 58-66 N and the *virgin* film average is 67 ± 3 N.

The same applied to the *Stress at 100 % strain* : *Olympus* blends range is 9-11 Mega Pascal versus an average of the pure film of 11 ± 1 MPa; for M8630 blends is 10-12 MPa versus 15 ± 1 MPa of *virgin* film.

This study is confirming again no important effects of the mixing with G-Polymer on M8630 and *Olympus* films, even after contact with detergent for 5 days.

Taking into account the lower tensile properties of G-Polymer, we must conclude that M8630 and *Olympus* are giving the most contribution for the blend properties in terms of tensile features.

4.2.6 Water vapor permeability studies

M8630 and *Olympus* blends with G-Polymer water barrier performances were studied following the procedure described in **Section 2.2.6** for water vapor permeability (WVP) measurements, according to ASTM E96-95 standard method.[79]

As already proved in **Chapter 3** for M8630, first step was to preclude the casting process influence on the films features of *Olympus* film: **Figure 4.14** reports the values of WVP for *virgin Olympus* and casted *Olympus* in g/Pa m day, and the values are strongly comparable, so no affection was observed on the film after the casting process also in *Olympus* film case.

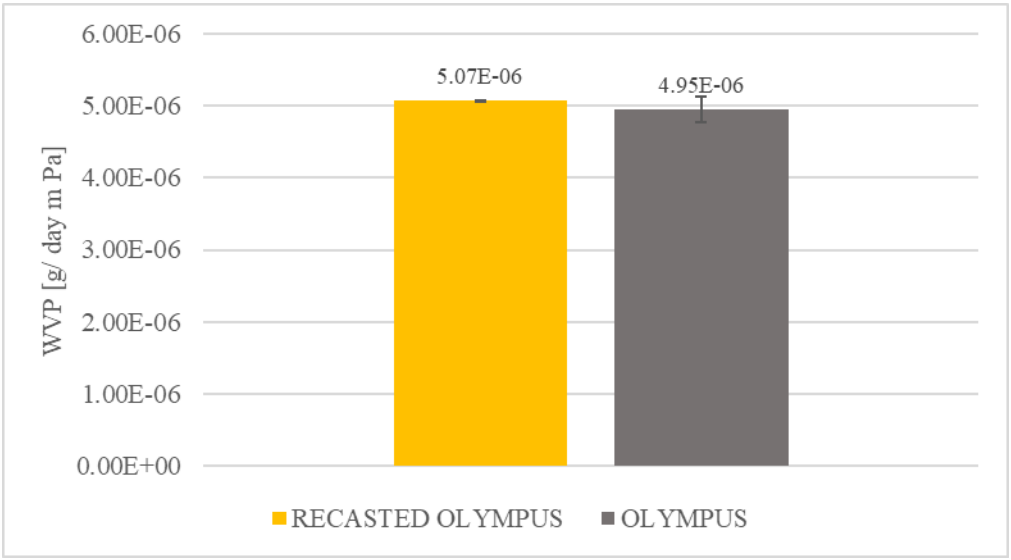

Figure 4.14 WVP chart for Olympus film supplied by plant and same film recasted

The WVP values are means of 3 different experiments and the bars indicate the standard deviation of the three measurements.

Once proved no relevant impact of casting process on the WVP, experiments on blended films were run: **Figure 4.15** graphs a bar chart that compares the values for *Olympus* and M8630 mixed materials.

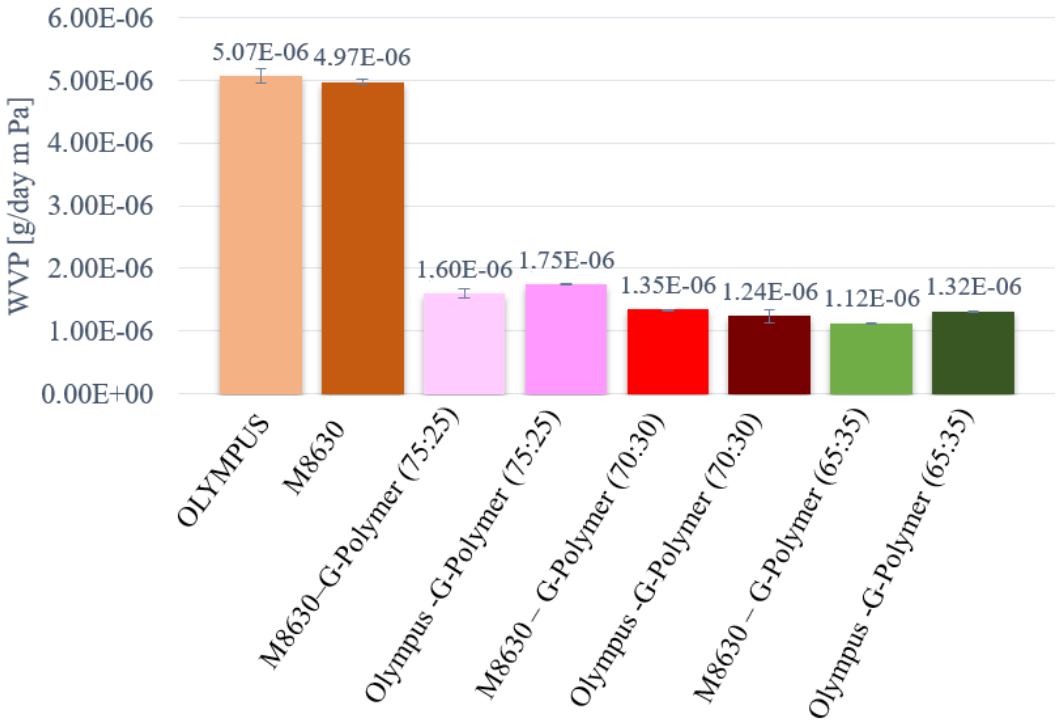

Figure 4.15 WVP chart for blended films with G-Polymer: in brackets are reported the ratio between the M8630/Olympus and G-Polymer

This chart shows a strong decrease in water vapor permeability: it decreases from ca $5.07 \cdot 10^{-6}$ g/Pa m day for not blended films to ca $1.12 \cdot 10^{-6}$ g/Pa m day for film blended with a 35 % in weight of G-Polymer, showing about 5 times more barrier to water vapor.

These results are excellent considering the final purpose established at this work.

In the **Section 1.2.3** (**General Introduction Chapter**) a simple model for permeability for miscible polymers was discussed and was represented by

$$\ln P_b = \phi_1 \ln P_1 + \phi_2 \ln P_2 \qquad (4.1)$$

Where P_b, P_1 and P_2 are the permeability coefficients of the blend and the two unblended components, and ϕ_1 and ϕ_2 are the volume fractions of components 1 and 2, respectively [54, 55]

Another more complex model (also already mentioned) involves one component phase dispersed in a matrix of the second component and follows a Maxwell equation

$$P_b = P_m \left[\frac{P_d + 2P_m - 2\phi_d(P_m - P_d)}{P_d + 2P_m + \phi_d(P_m - P_d)}\right] \qquad (4.2)$$

Where b, m and d represent the blend, the matrix and the dispersed phase respectively. [53]

In accordance with the previous results, the blends of M8630/*Olympus* and G-Polymer can be considered as miscible blends and can be represented by the easier model of *equation 4.1*, but to complete the study, also the Maxwell model was applied (*equation 4.2*).

The *equation 4.1* can be solved for the P_b variable and becomes

$$P_b = e^{\phi_1 \ln P_1 + \phi_2 \ln P_2} \quad (4.3)$$

As done in **Chapter 3**, an assumption of comparable density between the two polymers was done, hence the volume fractions ϕ correspond to the weight percentage in the blended material.

An example of calculation for M8630 blended with 35 % in weight of G-Polymer is reported.

Taking the averages data $P_1 = 4.97 \cdot 10^{-06}$ g/Pa m day; $P_2 = 4.17 \cdot 10^{-06}$ g/Pa m day and the volume fractions $\phi_1 = 0.65$; $\phi_2 = 0.35$, the *equation 4.3* becomes:

$$P_{[M8630/G-Polymer(65:35)]} = e^{0.65 \ln(4.97 \cdot 10^{-6}) + 0.35\, ln(4.17 \cdot 10^{-6})} =$$

$$= 4.67 \cdot 10^{-06} \frac{g}{Pa\ m\ day}$$

Table 4.2 Comparison of experimental data versus miscible polymers and Maxwell predictions models

Film	ϕ_1	ϕ_2	Empirical data WVP · 10^{06} [g/(Pa m day)]	Miscible Model WVP · 10^{06} [g/(Pa m day)]	Maxwell Model WVP· 10^{06} [g/(Pa m day)]
M8630/G-Polymer (65:35)	0.65	0.35	1.12	4.67	4.68
M8630/G-Polymer (70:30)	0.70	0.30	1.35	4.72	4.72
M8630/G-Polymer (75:25)	0.75	0.25	1.60	4.76	4.76
M8630/G-Polymer (80:20)	0.80	0.20	2.10	4.80	4.80
Olympus/G-Polymer (65:35)	0.65	0.35	1.32	4.73	4.74
Olympus/G-Polymer (70:30)	0.70	0.30	1.24	4.78	4.79
Olympus/G-Polymer (75:25)	0.75	0.25	1.75	4.83	4.83
Olympus/G-Polymer (80:20)	0.80	0.20	2.20	4.88	4.88

As shown in **Table 4.2**, both models, for all the samples, have an important deviation from the empirical data measured by the Dry Cup Method: the calculated values are combination of the two data from *virgin* M8630/*Olympus* and pure G-Polymer and to obtain a valued close to the actual, the WVP of G-Polymer should be at least one order of magnitude lower than the actual one. Since the values of WVP for G-Polymer, were measured on films containing 20 % in weight of glycerol as plasticizer, a hypothesis of impact on the permeability of the material by the plasticizer was assumed. [96]

Therefore, a casting for pure G-Polymer was tried, but the obtained film wasn`t analyzable, since the material tended to agglomerate towards the center of the glass support as shown in **Picture 4.1**, due to a strong surface tension of the solution.

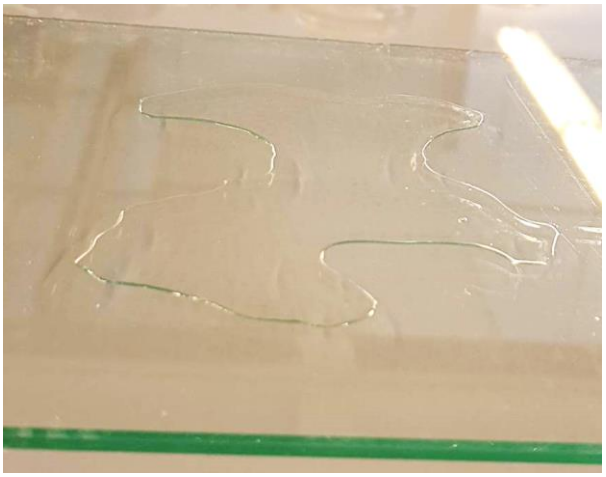

Picture 4.1 Pure Nichigo G-Polymer casted by solvent evaporation: it tends to agglomerate towards the surface center

4.2.7 X-Ray diffraction analysis

One strong hypothesis to explain the huge decrease of water permeability of blended films, was a change in crystallinity in the material, since the degree of crystallinity is strictly related to the permeation features. [82, 83] As explained in the **Section 2.2.8**, several film properties are directly proportional to the crystallinity degree. [97] The X-ray diffraction technique is the most reliable technique for determining the degree of crystallinity of the semi-crystalline polymer systems: the experiment for this work were run on a *virgin* M8630, a casted G-Polymer and a blended film M8630/G-Polymer in 70:30 ratio. **Figure 4.16** reported the spectra of the three samples.

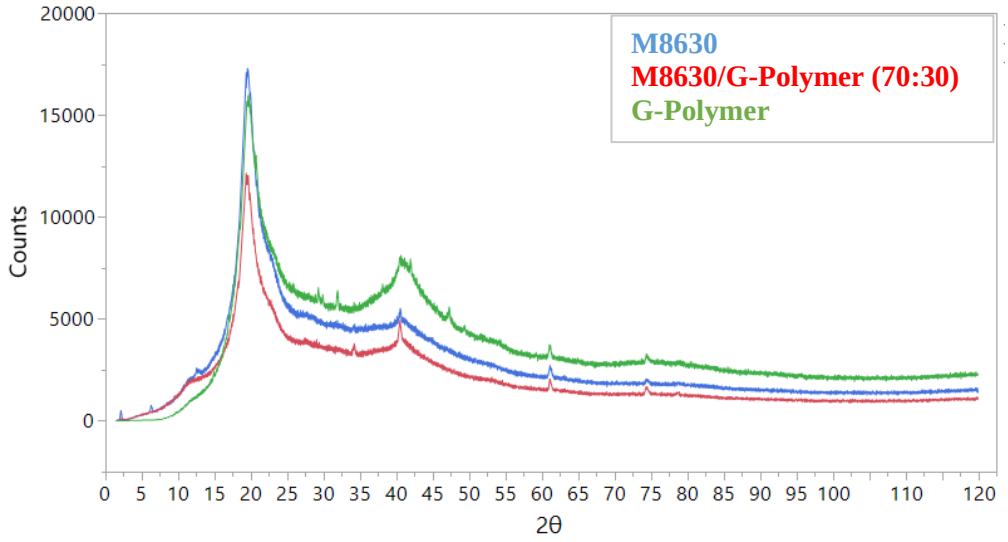

Figure 4.16 X-Ray diffraction spectra for M8630, G-Polymer and a blended film with 70:30 weight ratio M8630:G-Polymer

The degrees of crystallinity, DC (%),were calculated using the equation:

$$DC\ (\%) = \frac{Crystal\ derived\ scattering\ intensity}{Crystal\ derived\ scattering\ intensity + Noncrystal\ derived\ scattering\ intensity} x100$$

giving to the following results:

Table 4.3 Crystallinity degrees for the tested samples

Sample Name	DC (%)
M8630	23.9
M8630/G-Polymer (70:30)	21.3
G-Polymer	24.2

Therefore, looking into the results, the hypothesis of different degree of crystallinity for the materials was overcome: it`s possible to see some deviation, but considering the measurement error, usually around 3-4 %, the values are comparable, and no significant difference are detected.

4.2.8 Migration experiments

Over the water vapor permeability, the migration of a brightener molecule (FWA49) was monitored; in **Section 2.2.8** the method was broadly discussed. The films are placed between two permeation cells: one contains detergent with FWA49 specific concentration, while the other one is containing detergent without tracer molecule. The concentration of the brightener molecule passing from one side to the other, is monitored over time thanks to fluorometric analysis and give us a slope, strictly related to the permeation features to detergent.

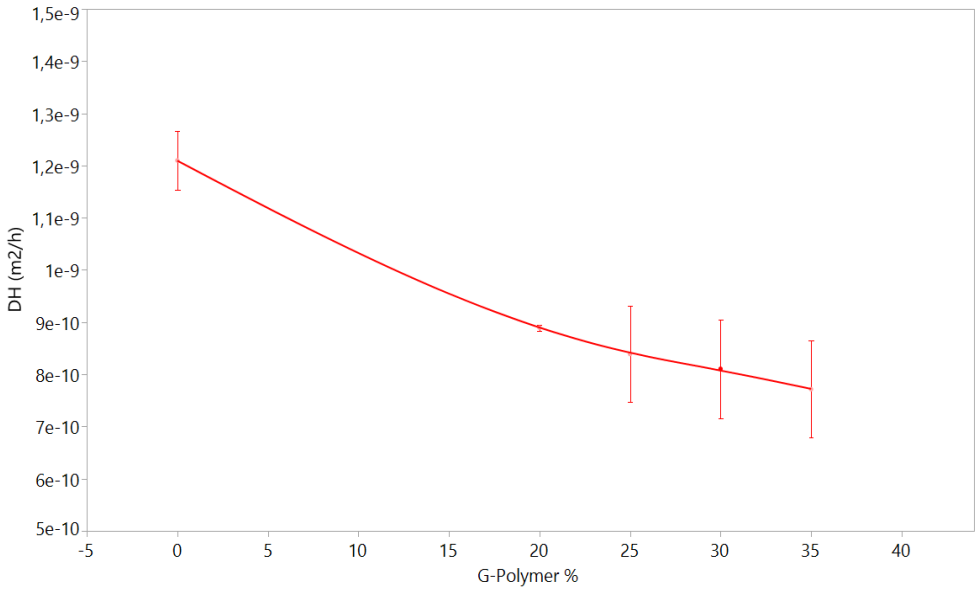

Figure 4.17 DH (Difference in Partition) results for Olympus virgin film (0%) and its blends with G-Polymer, charted vs G-Polymer percentage in weight: the bars indicate the standard deviation over the repetitions

The molecule studied in this test, is present in very low percentage inside the cleaning liquid contained in the water-soluble pouches to increase consumer whiteness perception.

In **Figure 4.17** *Olympus* blended and *virgin* films values for FWA49 molecule migration are graphed versus G-Polymer increasing percentage in the material.

Therefore, a barrier increases to the FWA49 molecule up to 1.6 times from the *virgin Olympus* to a film containing 35 % in weight of G-Polymer is observed: even if the improvement is not as high as for WVP, it can still give benefit accordingly to the purpose of the work.

4.2.9 Pouch dissolution (Beaker test)

A very important aspect of the work was to prove the processability of the new films to form pouches and to show comparable dissolution properties with respect to systems made by M8630 and *Olympus* .

Due to the not fast and nor easy capability to reach the 76 ± 4 μm thickness for the 3 films required for each pouch and the need of 3 repetitions for all specimen, single compartment pouches, called mono-pouch, were produced thanks to the simplified 1-up technique described in **Section 2.2.10**.

The results of the production were pouches with the aspect presented in **Picture 4.2**. The weight target was 20.0 g and the samples had a weight of 19.8 ± 1.1 g.

Picture 4.2 Mono-pouch sealed with 1-up method

Once established a good film processing and sealing, the samples were left aside for 2 weeks and then conditionated at 23 °C and 50% RH in a chamber for 24 hours before the test, thus allowing the equilibration of system film/detergent: after this time the pouches are ready for the *beaker test* (**Section 2.2.11**).

This experiment measures the conductivity of the water over 15 minutes of a beaker wherein is insert the pouch.

Figure 4.18 charts the Completion (%), defined as $\frac{Cond.(t)-\text{MIN}\,Cond.}{MAX\ Cond.-MIN\ Cond.}$ over 15 minutes, where Cond(t) is the

conductivity in time function and MIN and MAX Conductivities are the lower and higher value of the conductivity for a specific sample. The completion is a normalization of the conductivity values of the samples and facilitates the direct comparison of several pouches.

The completion charts reported are an average of 3 pouches per kind of film, meanwhile the liquid detergent contained in all the pouches is the same.

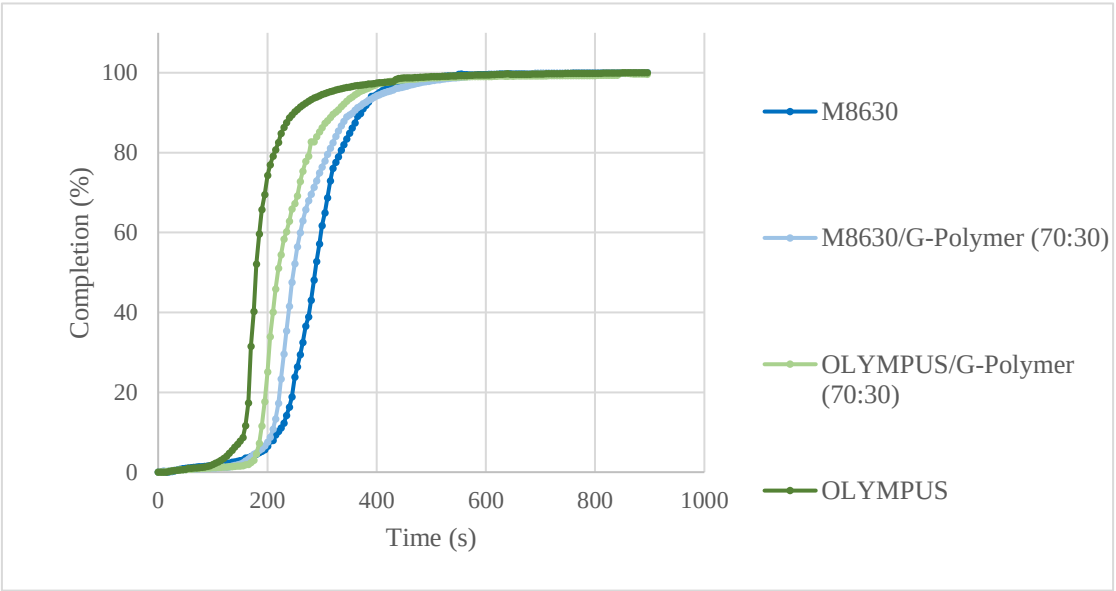

Figure 4.18 Completion (%) versus time (s) for 4 samples : 2 pouches made with virgin films and 2 pouches made with blended with 30 % in weight of G-Polymer

As expected, on the view of the results of the **Section 4.2.3**, the pouches formed with blended films have similar behaviors in terms of dissolution with respect to virgin ones. Even if the *virgin*

Olympus pouch dissolves slightly faster than the others, this experiment confirms again the no important impact on dissolution features related to the mixing with G-Polymer.

The blending with 30 % in weight of G-Polymer for both M8630 and *Olympus* have been chosen taking into account the higher cost of G-Polymer around 10 $/kg versus 3-4 $/kg of the polymer used in M8630/*Olympus* by the supplier MonoSol and the good enough results obtained for the barrier to water vapor (**Section 4.2.6**).

4.3 Conclusions

In this chapter a set of films consisting of M8630 or *Olympus* films blended with Nichigo G-Polymer was widely studied in several aspects.

Three fundamental properties for the final application were investigated: dissolution time, tensile properties and water vapor permeability (WVP).

After the blending, no significant deviation was found for both M8630 and *Olympus* system, regarding dissolution times: the higher discrepancy was about 5 seconds, not affecting the final application.

Tensile tests on the specimens before and after the contact with cleaning detergent and the solvents contained in it were performed: also from these experiments we can conclude that the features are similar for new materials and *virgin* ones.

On the other hand the most important result obtained was the drop of the water vapor permeability of the blended films with Nichigo G-Polymer. The miscible polymer and Maxwell theoretical models used to predict the blends permeability don't match with the empirical data, which show a decrease up to 5 times passing from ca $5.07 \cdot 10^{-6}$ g/Pa m day mean for not blended films to ca $1.12 \cdot 10^{-6}$ g/Pa m day for film mixed with a 35 % in weight of G-Polymer.

A change in crystallinity was the hypothesis assumed to justify this significant reduction in WVP, but the X-Ray diffraction analysis proved similar Degrees of Crystallinity (DC, %).

Those which are the most important properties are reported in **Figure 4.19**, a graph which charts Complete dissolution (s), Stress at 100 % Strain (MPa) and water vapor permeability (g/Pa m day) versus the G-Polymer percentage contained in the blended films.

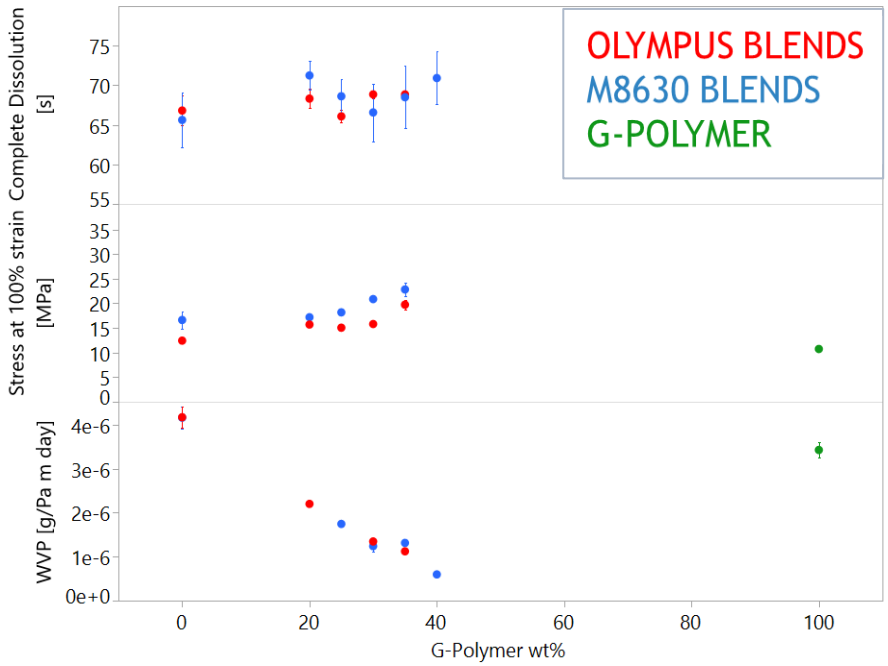

Figure 4.19 Summary of the three pillar properties for PVA film for water-soluble pouches for laundry

Another aspect studied was the interaction and compatibility with the laundry detergent and its most important solvent components. A gravimetric technique was used for it and the performances of the *virgin Olympus* and M8630 films and the blended films underline a higher swelling by glycerol interaction, but a complete compatibility of the new materials with detergent components as a whole.

Also the migration of a brightener molecule (FWA49) was investigated: in this case we observed a decrease of about 1.6 times passing from *virgin Olympus* with blended with 35 % G-Polymer one.

Last aspects examined were the film processability for the pouch forming and the pouch dissolution itself. Thanks to the 1-up technique, it was possible to form pouches; then the experiment called Beaker test, helped us to verifying, the good dissolution of the pouches produced with the new films.

5. Characterization of PVA Mowiol® 18-88 blended films

5.1 Introduction

In addition to study how G-Polymer is changing the properties of M8630 and *Olympus* films, the impact of G-Polymer on PVA Mowiol® 18-88 pure polymer is discussed in this chapter.

This PVA has a weight average Molecular weight ($\bar{M}_w$) of about 130,000 and a degree of hydrolysis of 86.7 – 88.7%. It was supplied by Sigma Aldrich in pellets form.

The aim of this chapter is to understand whether the G-Polymer is affecting the permeation features of a pure polymer, as well as did with the modification of *Olympus* (blend of a homopolymer and an anionically polymerized copolymer of PVA) and M8630 (mixture of PVA, chitosan and other components).

Also for these films, the target thickness was 76 ± 4 μm, directly comparable with the one of *virgin* films from plant.

For this set of blended films, just the Fluorescent Whitener Agent (FWA49) migration and water vapor permeability were investigated, because they are considered the core of the entire work.

5.2 Results and Discussion

5.2.1 Water vapor permeability studies

In this section, the water vapor permeability of PVA Mowiol® 18-88 blended with G-Polymer is discussed. As mentioned in **Section 2.2.6**, the method used for measuring the water barrier performances (Dry Cup Method) follows the ASTM E96-95 standard method. [79]

Figure 5.1 reports the data obtained for pure PVA Mowiol® 18-88 and its blends with G-Polymer.

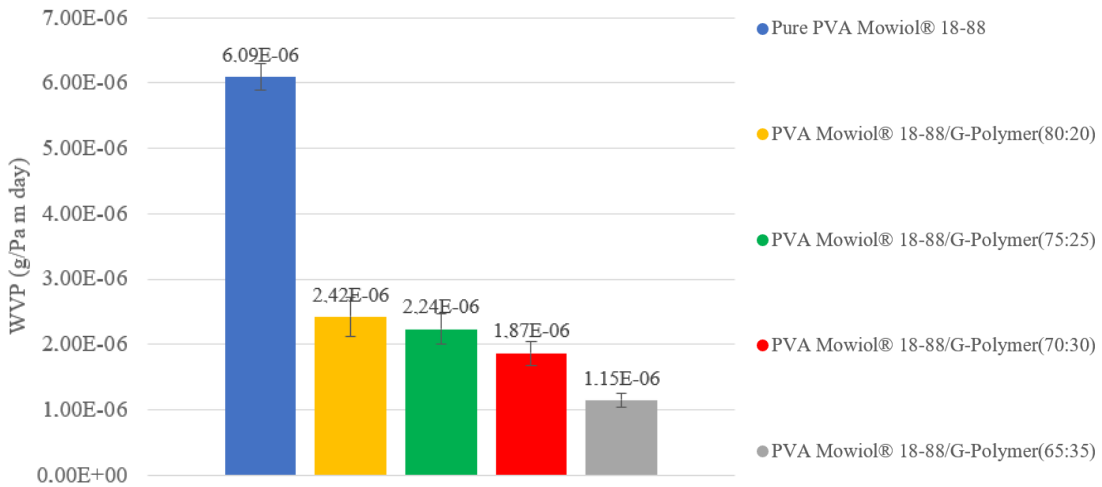

Figure 5.1 WVP (g/ Pa day m) of PVA Mowiol® 18-88 blended with G-Polymer

This chart shows a significant drop in water vapor permeability, passing from a mean value of $6.09 \cdot 10^{-6}$ (g/Pa m day) for pure PVA

Mowiol® 18-88 film to $1.15 \cdot 10^{-6}$ (g/Pa m day) for the blended film with 35 % in weight of G-Polymer. Therefore, these values confirm the same trend observed in M8630/*Olympus* blends.

A direct comparison with *Olympus* blended films was done and reported in **Figure 5.2**

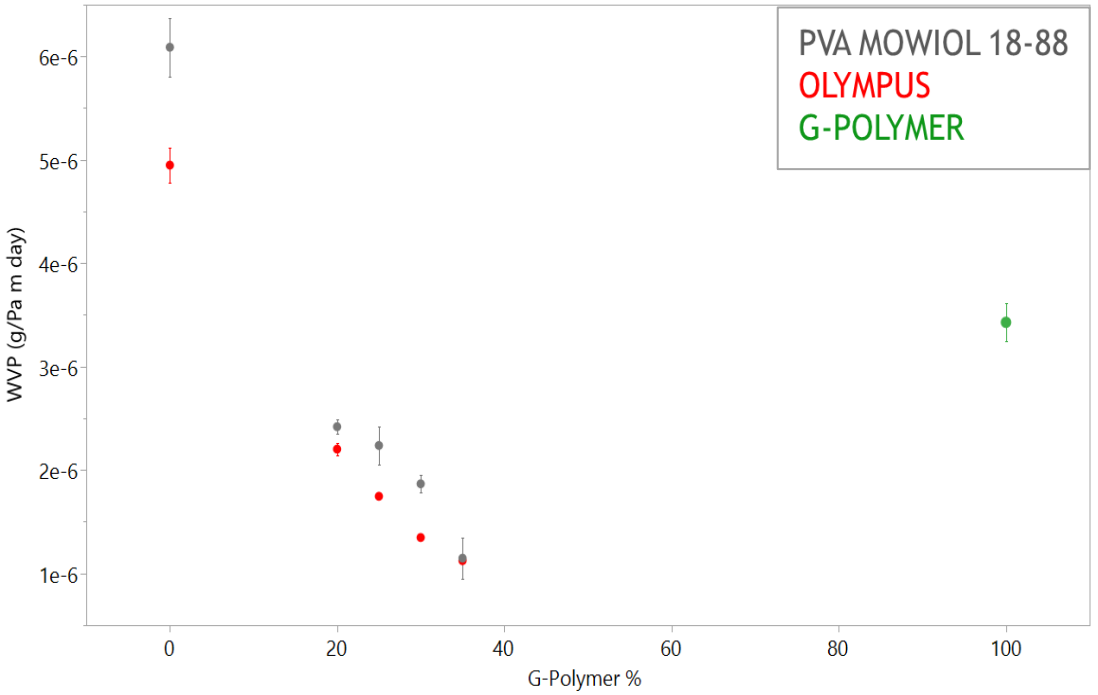

Figure 5.2 WVP (g/ Pa m day) comparison for PVA Mowiol® 18-88 and Olympus blends with G-Polymer

G-Polymer 0 % content indicates a *virgin* film from plant for *Olympus* and a pure PVA Mowiol® 18-88 film , meanwhile the 100 % gives the value for the pure G-Polymer film.

The bars for both **Figure 5.1** and **Figure 5.2** indicate the standard deviations for the mean values over three experiments. As can be seen in **Figure 5.2**, G-Polymer positively affects the water vapor permeability of PVA Mowiol® 18-88 film in a similar manner as did for *Olympus* film.

As done for previous blends, a model for miscible polymers (described in **Section 1.2.3**) was applied and the predicted values compared with the measured data.

The equation applied for predicting the permeability of miscible blends was

$$\ln P_b = \phi_1 \ln P_1 + \phi_2 \ln P_2 \qquad (5.1)$$

Where P_b, P_1 and P_2 are the permeability of the blend and the two unblended components respectively, and ϕ_1 and ϕ_2 are the respective volume fractions of components 1 and 2, [54, 55] in this case PVA Mowiol® 18-88 and G-Polymer.

For the calculation, the values of permeabilities considered for pure polymers were

$P_1 = 6.09 \cdot 10^{-06}$ [g/Pa m day] (see **Figure 5.1**)

$P_2 = 4.17 \cdot 10^{-06}$ [g/Pa m day] (G-Polymer film containing 20% of glycerol as plasticizer)

Table 5.1 Comparison of experimental data versus miscible polymers prediction models

Film	ϕ_1	ϕ_2	Empirical data WVP · 10^{06} [g/(Pa m day)]	Miscible Model WVP · 10^{06} [g/(Pa m day)]
PVA Mowiol® 18-88/G-Polymer (65:35)	0.65	0.35	1.15	5.34
PVA Mowiol® 18-88/G-Polymer (70:30)	0.70	0.30	1.86	5.44
PVA Mowiol® 18-88/G-Polymer (75:25)	0.75	0.25	2.24	5.54
PVA Mowiol® 18-88/G-Polymer (80:20)	0.80	0.20	2.42	5.65

As observed for M8630 and Olympus, the data contained in **Table 5.1** indicate that the model is not predicting correctly the empirical data.

As already mentioned (**Chapter 4**) the strongest hypothesis is the impact of the plasticizer (glycerol) on the permeation features of G-Polymer, [96] since the model proposed by Robeson [53, 54] claim a good prediction for values of pure polymers.

As discussed in **Section 4.2.6**, film casting for pure G-Polymer was found impossible to apply, due to the high surface tension between solution and glass surface (**Picture 4.1**).

Overall, the most important result is the significant increase in the barrier to water vapor up to 5 times observed in the PVA Mowiol® 18-88 blends with G-Polymer, which confirms the interaction between the two polymers, as seen for M8630 and *Olympus*.

5.2.2 Migration experiment

In the **Section 2.2.8** the method used for monitoring the migration of the Fluorescent Whitener Agent 49 (FWA49) was described in detail.

As mentioned before, this molecule is a brightener agent contained in a small amount in the cleaning liquid to enhance the white in the fabrics.

After several days monitoring and the due calculations, the value for difference in partition (DH) (m^2/h) of PVA Mowiol® 18-88 blended with G-Polymer are obtained and charted in **Figure 5.3**.

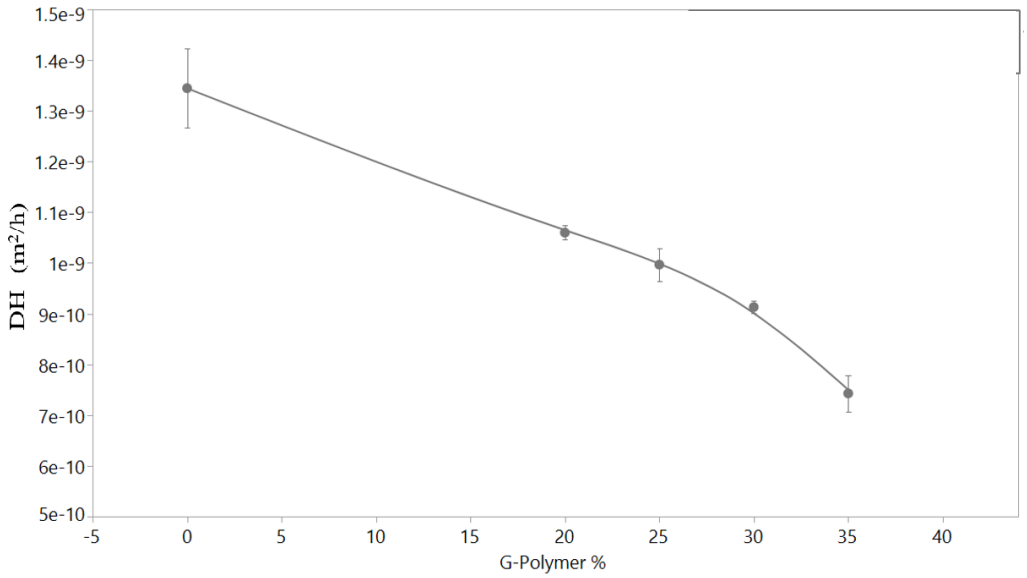

Figure 5.3 DH (difference in partition)results for PVA Mowiol® 18-88 film (0%) and its blends with G-Polymer, charted vs G-Polymer percentage in weight

The data obtained are closely comparable with the ones obtained for *Olympus* blends, and show a decrease of migration at brightener agent up to 1.7 times for the 35% G-Polymer blended with PVA Mowiol® 18-88, not as high as reported for water vapor permeability, but it is still an improvement towards the work target.

5.3 Conclusions

In this chapter, PVA Mowiol® 18-88 and its blends with Nichigo G-Polymer permeation features were studied. Thus, the barrier to water vapor and the migration to a brightener agent were examined.

Water vapor permeability showed a decrease up to 5 times for the blended film PVA Mowiol® 18-88/G-Polymer with 65:35 ratio, consistent with the results obtained for M8630 and *Olympus* blended with G-Polymer. This result proofs that Nichigo G-Polymer is also improving the water vapor barrier for films casted from pure polymer not only for commercially available mixtures (M8630 or *Olympus*).

Values obtained by applying the model for prediction of gas permeation for blends of miscible polymers proposed by Robeson [53, 54] show huge deviations with respect to experimental data, probably due to the addition of a plasticizer on G-Polymer; whose film permeability value was used in the calculation of model prediction. [96]

Migration of FWA49 molecule through the film over time was tracked, and DH decreased 1.6 times from pure PVA Mowiol® 18-88 film to a blend within 35 % in weight of G-Polymer.

6. General Conclusions and Future Works

6.1 General conclusions

The conclusions of this research are summarized as follows:

- The preparation and characterization of composite films of M8630 and micro crystalline cellulose particles with average size of 20 µm and 50 µm was carried out, optimizing the procedure to the system in terms of drying conditions and support of film casting.
- The dissolution times of the new composite films were studied, without noticing huge differences with respect to the M8630 virgin film features.
- Tensile tests underlined a significant drop in the mechanical properties of the composite films.
- Water vapor permeabilities on the filled films were studied and a decrease up to 1.6 times in comparison with the *virgin* M8630 was observed.
- PVA Mowiol® 18-88, M8630 film and *Olympus* film were blended with Nichigo G-Polymer to improve the barrier performances.
- Dissolution times of the blended films were confirmed to be comparable with *virgin* films M8630 and *Olympus*.
- Tensile tests were run on the blended films and no affection of the blend comparing with *virgin* films was recorded.

- The blended films showed full compatibility with detergent used in soluble unit dose for laundry.
- Water vapor barrier features on the blended films were monitored over time and an improving of up to 5 times was observed, in line with the work goal.
- Permeation of FWA49 brightener molecule was reported to decreases up to 1.6 times in relation with *virgin* films M8630, *Olympus* and PVA Mowiol® 18-88, confirming an increase in barrier properties.
- Crystallinity degrees of the virgin and blended films obtained by X-Ray diffraction analysis, reject the hypothesis of important differences in crystallinity of the G-Polymer versus M8630.

6.2 Future works

- The study of films in the range of blending with Nichigo G-Polymer 50-90 % in weight with M8630/*Olympus* could give a broader overview on the complete trends of the M8630/*Olympus* – G-Polymer system.
- A deep understanding of the mechanism implied in the huge permeation decreasing should be carried out. Solid state Nuclear Magnetic Resonance (NMR) analysis on the *virgin* films, pure Nichigo G-Polymer film and blended ones, could help to understand the structures of the materials and which effects can induce the permeability drop.

References

1. J. M. Hay, D. Lyon *Vinyl Alcohol: a Stable Gas Phase Species?* Nature, 1967. **216**: p. 790-791.
2. B. Capon, D. Rycroft, T. W. Watson, C. Zucco, *The Generation of Vinyl Alcohol in solution and Its Detection and Characterization by NMR Spectroscopy.* Journal of American Chemical Society, 1981. **103**: p. 1761-1765.
3. A. K. Cederstav, B. M. Novak, *Investigations into the Chemistry of Thermodynamically Unstable Species. The Direct Polymerization of Vinyl Alcohol, the Enolic Tautomer of Acetaldehyde.* Journal of American Chemical Society, 1994. **116**: p. 4013-4014.
4. W. Haehnel, W.O. Herrmann, Berichte der Deutschen Chemischen Gesellschaft, 1924. **8**: p. 400-439.
5. W.H. Montgomery, M. Sittig, *Water-Soluble Resins.* Van Nostrand Reihold, 1968.

6. C. K. Haweel, S. H. Ammar, *Preparation of Poly (vinyl alcohol) from Local Raw Materia.* Iraqi Journal of Chemical and Petroleum Engineering, 2008. **9**: p. 15-21.

7. Airvol®, *Poly(vinyl alcohol) Manual, Air Product and Chemicals, Inc.* 1990.

8. N. A. Peppas, *Turbidimetric studies of aqueous poly(vinyl alcohol) solutions.* Die Makromolekularre Chemie, 1975. **176**: p. 3433-3440.

9. N. A. Peppas, R. E. Benner, *Proposed method of intracordal injection and gelation of Poly (vinyl alcohol) solution in vocal cords: polymer considerations.* Journal of Biomaterials, 1980. **158**: p. 115-124.

10. J. G. Fatou, E. Riande, R. G. Valdecasas, *The crystallization of polymer–diluent mixtures.* Journal of Polymer Science Part B, 1976. **17**: p. 795-796.

11. F.F. Nord, M. Bier, S.N. Timasheff, *Investigations on proteins and polymers.* Journal of American Chemical Society, 1951. **1**: p. 289-293.

12. P. F. Luckham, S. Zhu, *On the Effects of Water Solvency towards Non-ionic Polymers.* Proceedings of The Royal Society A Mathematical Physical and Engineering Sciences 1982. **455**: p. 737-756.

13. C. Vasile, S. F. Patachia, V. Dumitrascu, *Thermoxidative degradation of vinyl alcohol/vinyl acetate copolymers. IV. Statistical copolymers.* Journal of Polymer Science: Polymer Chemistry 1983. **21**: p. 329-330.

14. C. Vasile, C. N. Caşcaval, P. Barbu, *Thermal degradation of vinyl alcohol/vinyl acetate copolymers. III. Study of the reaction products.* Journal of Polymer Science Part A, 1981. **19**: p. 907-916.

15. Research, Grand View, *Polyvinyl Alcohol (PVA) Market Size, Share & Trends Analysis Report By End Use (Paper, Food Packaging, Construction, Electronics).* 2019. **1**: p. 55-59.

16. F. Denome, S. Friedrich, R. Labeque, D. Lee, R. Rosmaniho, J. Shi, A. Verrall, *WO 2011/094470 A1*. 2011.

17. F. Denome, S. Friedrich, R. Labeque, D. Lee, R. Rosmaniho, J. Shi, A. Verrall, *WO 2011/094472 A1*. 2011.

18. R. Labeque, K. Van Elsen, L. Andrea, *WO 2014/089270 A1*. 2014.

19. A. Boutoille, F. Courchay, M. Moss,P. Sifnioti, *US 2009/0312220 A1*. 2009.

20. A. Verrall, S. Bening, K. Kugler, *US 2010/764226 B2*. 2010.

21. A.D. Massey-Brooke, M. Vaccaro, E. Robles,R.N. Somerville,M. Cuthbertson,M, Hatzopoulos, *WO 2016/094601 A1*. 2016.

22. M. Schmid, S.Sängerlaub, O. Miesbauer, V. Jost,J. Werthan, C. Stinga, D. Samain, C. Stramm, K. Noller, K. Müller, *Water Repellence and Oxygen and Water Vapor Barrier of PVOH-Coated Substrates before and after Surface Esterification.* Polymers, 2014. **6**: p. 2764-2783.

23. C.Cecutti, Z. Mouloungui, A. Gaset, *Synthesis of new diesters of 1,4:3,6-dianhydro-D-glucitol by esterification*

with fatty acid chlorides. Bioresourches Technology, 1988. **66**: p. 63-67.

24. N. O. V. Sonntag, J. R. TrowbridgeI, J. Krems, *Reactions of fatty acid chlorides. I. Preparation of fatty acid anhydrides.* Journal of American Oil Chemists` Society, 1954. **31**: p. 151-157.

25. S. Shaikh, A. Asrof, S.K, Hamad, E.Z. Al-Nafaa, M. Al-Jarallah, and B. Abu-Sharkh, *Synthesis, characterization, and solution properties of hydrophobically modified poly(vinyl alcohol).* Journal Applied Polymer Science, 1998. **70**: p. 2499-2506.

26. N.C. Stinga, *Utilisation de la chimie chromatogénique pour la conception et la réalisation de matériaux cellulosiques barrières à l'eau, aux graisses et aux gaz.* PhD Thesis, Universite Joseph Fourier, Grenoble France, 2008: p. 242-243.

27. M. Schmid, A. Benz, C. Stinga, D. Samain, K.P. Zeyer, *Fundamental investigations regarding barrier properties*

of grafted PVOH layers. Internal Journalm of Polymer Science, 2012. **2012**: p. 1-6.

28. Standardization, German Institute for, *DIN 53122-1 Testing of plastics and elastomer films, paper, board and other sheet materials - Determination of water vapour transmission* **1**.
29. F. Chang, T. Masaki, K. Kurachi, Y. Isobe, K. Onimura, T. Oishi, *Synthesis of polymer blends using waste pulp modified with alkyl ester groups.* Kobunshi Ronbunshu, 2007. **64**: p. 254-260.
30. U. Neumann, B. Wiege, S. Warwel, *Synthesis of hydrophobic starch esters by reaction of starch with various carboxylic acid imidazolides.* Starch-Staerke, 2002. **54**: p. 449-453.
31. L.E. Nielsen, *Models for the Permeability of Filled Polymer Systems.* Journal of Macromolecular Science, 1967. **A1**: p. 929-942.

32. R. K. Bharadwaj, *Modeling the Barrier Properties of Polymer-Layered Silicate Nanocomposites.* Macromolecules, 2001. **34**: p. 9189-9192.

33. C.H. Klute, *Diffusion of Small Molecules in Semicrystalline Polymers: Water in Polyethylene.* Journal Applied Polymer Science, 1959. **1**: p. 340-350.

34. V. C. Souza, M. G. N. Quadri *Organic-Inorganic Hybrid membranes in separation processes: a 10-year review.* Brazilian Journal of chemical engineering, 2013. **30**: p. 683-700.

35. A.S. Micheals, R.B. Parker jr, *Sorption and flow of gases in polyethylene.* Journal of Polymer Science 1959. **41**: p. 53-71.

36. G.L. Flynn, S.H. Yalkkowsky, T.J. Roseman, *Mass Transport Phenomena and Models: theretical concepts.* Journal of Pharmaceutical Sciences, 1974. **63**: p. 479-510.

37. S. Virtanen, J. Vartianen, H. Set, T. Tammelinb, S. Vuotic, *Modified nanofibrillated cellulose–polyvinyl alcohol films*

with improved mechanical performance. RSC Advances, 2014. **4**: p. 11343-11350.

38. P. Stenstad, M. Andresen, B. S. Tanem, P. Stenius, *Chemical surface modifications of microfibrillated cellulose*. Cellulose, 2008. **15**: p. 35-45.

39. E. H. Qua, P. R. Hornsby, H. S. Sharma, G. Lyons, R. D. McCall, *Preparation and Characterization of Poly(vinyl alcohol) Nanocomposites Made from Cellulose Nanofibers.* Journal Applied Polymer Science, 2009. **113**: p. 2238-2247.

40. S. Yoon, M. Park, H. Byun, *Mechanical and water barrier properties of starch/PVA composite films by adding nano-sized poly(methylmethacrylate-co-acrylamide) particles.* Carbohydrate Polymers, 2011. **87**: p. 676-686.

41. R. Bodmeier, J. Wang, H. Bhagwatwar, *Process and formulation variables in the preparation of wax microparticles by a melt dispersion technique. I. Oil-in-water technique for water-insoluble drugs.* Journal of Microencapsulation, 1992. **9**: p. 89-98.

42. T. Xiaozhi Tang, A. Sajid, *Recent advances in starch, polyvinyl alcohol based polymer blends, nanocomposites and their biodegradability.* Carbohydrate Polymers, 2001. **85**: p. 7-16.

43. K.H. Seob, K.H. Jun, L. Jun-Young, *Water vapor permeability, morphological properties, and optical properties of variably hydrolyzed poly(vinyl alcohol)/linear low-density polyethylene composite films.* Korean Journal Chemical Engineering, 2017. **34**: p. 539-546.

44. G. Gentile, M. Cocca, R. Avolio, M. E. Errico, M. Avella, *Effect of Microfibrillated Cellulose on Microstructure and Properties of Poly(vinyl alcohol) Foams.* Polymers, 2018. **10**: p. 813-824.

45. L. Sun-Young, D. J. Mohan, K. In-Aeh, D. Geum-Hyun, L. Soo, O.H. Seong, *Nanocellulose Reinforced PVA Composite Films: Effects of Acid Treatment and Filler Loading.* Fibers and Polymers, 2009. **10**: p. 77-82.

46. L. Berglund, *Cellulose-based nanocomposites.* Natural Fibres, Biopolymers and biocomposites, 2005: p. 807-832.

47. M. A. Hubbe, O. J. Rojas, L. A. Lucian, M. Sain, *Cellulosic Nanocomposites—A Review.* Bioresourches Technology, 2008. **3**: p. 929-980.

48. K. Syverud, P. Stenius, *Strength and barrier properties of MFC films.* Cellulose, 2009. **16**: p. 75-85.

49. M. Flieger, M. Kantorová, P. Řezanka, J. Votruba, *Biodegradable plastics from renewable sources.* Folia Microbiologica, 2003. **48**: p. 27-44.

50. C. Aulin, G. Salazar-Alvarez, T. Lindstrom, *High strength, flexible and transparent nanofibrillated cellulose–nanoclay biohybrid films with tunable oxygen and water vapor permeability.* Nanoscale, 2012. **4**: p. 6622-6628.

51. V. Favier, R. Dendievel, G. Canova, J. Y. Cavaille, P. Gilormini, *Simulation and modeling of three-dimensional percolating structures: Case of a latex matrix reinforced*

by a network of cellulose fibers. Acta Materiala, 1997. **45**: p. 1557-1565.

52. Kolarik, J., *Prediction of the Gas Permeability of Heterogeneous Polymer Blends.* Polymer Engineering and Science, 2000. **40**: p. 127-131.

53. L. M. Robeson, *Polymer blends in membrane transport Processes.* Industrial & Engineering Chemistry Research, 2010. **49**: p. 11859-11865.

54. A. E. Barnabeo, W. S. Creasy, L. M. Robeson, *Gas Permeability Characteristics of Nitrile-Containing Block and Random Copolymers.* Journal Polymeric Science, 1979. **13**: p. 151-158.

55. D.R. Paul, *Gas Transport in Homogeneous Multicomponent Polymers.* Journal of Membrane Science, 1984. **18**: p. 75-86.

56. P.G. De Gennes, P. Pincus, R.M. Velasco *Remarks on Polyelectrolyte conformation.* Journal de Physique, 1976. **37**: p. 1461-1473.

57. Y. Xianda, W. Anlai, C. Suqin, *Water-Vapor Permeability of Polyvinyl Alcohol Films.* Desalination, 1987. **62**: p. 293-297.

58. S. R. Sudhamania, M. S. Prasada, K. Udaya Sanka, *DSC and FTIR studies on Gellan and Polyvinyl alcohol (PVA) blend films.* Food Hydrocolloids, 2003. **17**: p. 245-250.

59. S. Jun-Feng, H. Zhen, L. Kai, F. Ling-Ling, L. Hong-Ru, *Mechanical Properties, Biodegradation and Water Vapor Permeability of Blend Films of Soy Protein Isolate and Poly(vinyl alcohol) Compatibilized by Glycerol.* Polymer Bullettin, 2007. **58**: p. 913-921.

60. R. K. Tubbs, T. K. Wu, *Polyvinyl Alcohol.* New York, John Wiley and Sons, 1973. **1**: p. 167-183.

61. N. Jelinska, M. Kalnins, V. Tupureina, A. Dzene, *Poly (Vinyl Alcohol)/Poly (Vinyl Acetate) Blend Films.* Scientific Journal of Riga Technical University Material Science and Applied Chemistry, 2010. **21**: p. 55-61.

62. A. H. Falqi, O. A. Bin-Dahman, M. Hussain, M. A. Al-Harthi, *Preparation of Miscible PVA/PEG Blends and*

Effect of Graphene Concentration on Thermal, Crystallization, Morphological, and Mechanical Properties of PVA/PEG (10 wt%) Blend. International Journal of Polymer Science, 2018. **2018**: p. 1-10.

63. E. Boswell, *WO 2018/187198*. 2018.
64. E. Boswell, *WO 2018/187200*. 2018.
65. E. Boswell, S. Mirle, V. Shanov, R. Malik, C. Mc Connel, *WO 2018/237212*. 2018.
66. T. Hodgon, D. Graham, M. Farrel, C. Kenneally, C. Williams, C. Zawaski, *WO 2019/006234*. 2019.
67. S. Mitsuo, S. Norihito, *US 2009/0286909*. 2009.
68. A. Siddiqui, N. Tamez De Carballero *WO 2013/90442*. 2013.
69. Gohsei, Nippon, 2008.
70. http://www.g-polymer.com/eng/suiyousei1/, *Nichigo G-Polymer™ Fundamental material properties-Water solubility.*
71. D. Edwards., D. Lee, *WO 2016/054459*. 2016.

72. L. Felton, *Mechanism of polymeric film formation.* Internal Journal Polymer of Pharmaceutics, 2013. **457**: p. 423-427.

73. J. Taylor , J.R.N. Taylor , M.F. Dutton, S. de Kock, *Identification of kafirin film casting solvents.* Food Chemistry, 2005. **90**: p. 401-408.

74. K. Kodre, S. Attarde, P. Yendhe, R. Patil, V. Barge *Differential Scanning Calorimetry: A Review.* Journal of Pharmaceutical Analysis, 2014: p. 11-22.

75. M.F.J. Pijpers, V.B. Mathot, *Optimisation of instrument response and resolution of standard – and high speed power compensation DSC.* Journal of Thermal Analysis and Calorimetry, 2008. **93**: p. 319-327.

76. P. S. Gill, S. R. Sauerbrunn, M. Reading, *Modulated differential scanning calorimetry*. Journal of Thermal Analysis and Calorimetry, 1903. **40**: p. 931-939.

77. M. Jackson, E. J. Magennis, *US 2014/0342964 A1*. 2014.

78. *ASTM D882 Standard Test Method for Tensile Properties of Thin Plastic Sheeting.* ASTM international, 2018.

79. *ASTM E96-95 Standard Test Method for Water Vapor Transmission of Materials.* ASTM international, 1995.

80. T. Morris, *Moisture permeability, diffusion and sorption in organic film-forming materials.* Journal of Applied Chemistry, 1951. **1**: p. 141-158.

81. E.L. Cussler, *Diffusion: Mass transfer in fluid systems.* Cambridge University Press, 2009. **1**: p. 25-26.

82. B. Goderis , P.G. Klein, S. Hill, *A comparative DSC, X-Ray and NMR study of the crystallinity of isomeric aliphatic polyamides.* Progress in Colloid and Polymer Science, 2005. **130**: p. 40-50.

83. A. K. Patel, R. Bajpai, J. M. Keller, *On the crystallinity of PVA/palm leaf biocomposite using DSC and XRD techniques.* Microsystem Technologies 2014. **20**: p. 41-49.

84. D. Edwards, *WO 2016/054459 A1*. 2016.

85. A. P. Verrall, S. E. Brown, R. A. Schroer, F. W. Denome, K. H. Combs, L, E. Miller, A. D. M. Brooker, *US 2008/0110370 A1*. 2008.

86. S. Hussein, N. Abbas Ali, H. I. Jaafer, *Barrier, Mechanical and Thermal of Polyvinyl Alchol/Microcrystalline Cellouse Composites in Packaging Application.* American Journal of Physics and Applications, 2017. **5**: p. 46-51.

87. S. Shamekh, K. Poutanen, P. Forssell, *Film Formation Properties of Potato Starch Hydrolysates.* Starch, 2002. **54**: p. 20-24.

88. MonoSol, *Standard Test Method for Solubility of MonoSol® Water Soluble Film when contained within a Plastic Holder.* MSTM 205, 2003.

89. L. W. Chan, S. H. Jin, P. W. Sia Heng, *Evaluation of Permeability and Mechanical Properties of Composite Poly (vinyl Alcohol) Films.* Chemical and Pharmaceutical Bulletin, 1999. **47**: p. 1412-1416.

90. K. Wang, W. Wang, R. Ye, A. Liu, J. Xiao, Y. Liu, Y. Zhao, *Mechanical properties and solubility in water of corn starch-collagen composite films: Effect of starch type and concentrations.* Food Chemirstry, 2016. **216**: p. 209-216.

91. L. Greenspan, *Humidity Fixed Points of Binary Saturated Aqueous Solutions.* Journal of Research of the National Bureau of Standards- A. Physics and Chemistry, 1976. **81**: p. 89-96.

92. A. Nyflott, C. Mericer, M. Minelli, E. Moons, L. Jarnstrom, M. Lestelius, M. Giacinti Baschetti, *The influence of moisture content on the polymer structure of Poly(vinyl alcohol) in dispersion barrier coatings and its effect on the mass transport of oxygen.* Journal of Coatings Technology and Research, 2017. **14**: p. 1345-1355.

93. S. Aid, A. Eddhahak, Z.Ortega, D. Froelich, A. Tcharkhtchi, *Experimental study of the miscibility of ABS/PC polymer blends and investigation of the processing effect.* Journal of Applied Polymer Science, 2017. **134**: p. 466-475.

94. N. Limpan, T. Prodpran, S. Benjakul, S. Praspran, *Influences of degree of hydrolysis and molecular weight of poly(vinyl alcohol)(PVA) on properties offish myofibrillar*

protein/PVA blendfilms. Food Hydrocolloids, 2012. **29**: p. 226-233.

95. P. C. Srinivasa, M. N. Ramesh, K. R. Kumar, R. N. Tharanathan, *Properties and sorption studies of chitosan–polyvinyl alcohol blend films.* Carbohydrate Polymers, 2003. **53**: p. 431-438.

96. G. Donhowe, O. Fennema, *The Effects of Plasticizer on Crystallinity, Permeability and Mechanical Properties of Methylcellulose Films.* Journal of Food Processing and Preservation, 1993. **17**: p. 247-257.

97. R. Gref, Q.T. Nguyen, P. Schaetzel, J. Neel *Transport Properties of Poly(vinyl alcohol) Membranes of Different Degrees of Crystallinity.* Journal of Applied Polymer Science, 1993. **49**: p. 209-218.

Appendices

Appendix A. Index of Figures, Pictures and Tables

Appendix B. Congress and Contributions

Congresses

Authors: G. Colace, J.A. Reina, M. Brandt, A. Martinez

Poster Presentation: Study of permeation on Poly(vinyl alcohol) membranes

Congress: 15th Doctoral Day at University Rovira i Virgili

Date: 23rd May 2018 **Place:** Tarragona, Spain

Authors: G. Colace, J.A. Reina, M. Brandt, A. Martinez

Poster Presentation: Study of permeation on Poly(vinyl alcohol) membranes

Congress: Euromembrane 2018

Dates: 9th – 13th July 2018 **Place:** Valencia, Spain

Authors: G. Colace, J.A. Reina, M. Brandt, A. Martinez

Poster Presentation: Study of permeation on Poly(vinyl alcohol) membranes

Congress: 21st Advanced Materials Congress

Dates: 3rd – 6th September 2018 **Place:** Stockholm, Sweden

Stay abroad

Organization: Procter & Gamble Services Company NV

Department: Soluble Unit Dose

Supervisors: Miguel Brandt and Alberto Martinez

City: Bruxelles **Country**: Belgium

Length: (18 months) October 2016-December 2016 / June 2018-September 2019)

Patent

Inventors: G. Colace, J.A. Reina, M. Brandt, A. Martinez

Field of the invention: Water-soluble unit dose article having a water-soluble film wherein the water-soluble film has a polymeric resin having a copolymer of Poly(vinyl alcohol) and butenediol and a second Poly(vinyl alcohol) polymer.

Application N°: EP19193970.1 **Year**: 2019